



Norwegian University of
Science and Technology

C02 Solar Assisted Heat Pump System for Water heating, Drying, and Cooling.

Oluwafemi Samuel Nana

Natural Gas Technology

Submission date: July 2017

Supervisor: Armin Hafner, EPT

Norwegian University of Science and Technology
Department of Energy and Process Engineering

Abstract

Solar energy is often considered as waste energy in the world as only few percentage of the solar energy reaching the earth being harnessed for use. With growing demand in heating and cooling demands around the world, it has become imperative that research be focused on how to make use of this waste energy. Heat pumps are considered better in meeting cooling and heating loads, a CO₂ as choice refrigerant. Not only those CO₂ have better thermodynamic properties, it is environmentally friendly as it does not contribute to ozone layer depletion with a global warming potential of 1.

With this study, theoretical analysis of integrated CO₂ heat pump has been carried out and experimental campaign has been able to justify the potentials of integrating a solar collector to a CO₂ heat pump with multiple loads (cooling and heating). A region with relative high solar radiation was selected and with the aid of a simulation tool, RHVAC, the corresponding cooling load required for residential purpose was determined. This cooling load served as reference load for the air evaporator. Improvising the solar collector with a glycol evaporator, additional heat was absorbed into the system, thereby increasing the heating capacity of the heat pump. The cooling load reference for the air evaporator ranges from 2.37 to 2.73 kW. A single transcritical heat pump was simulated in Pack calculation to predict the behavior of the system with only the air evaporator. Depending on the amount of heat supplied from glycol, an heat increase of twice the it's initial capacity was recorded.

The system parameters were varied to predict their influence on system performance. At 2.37 kW cooling load, the highest COP of 3.97 and 3.67 for heating and cooling at an evaporation temperature of 10°C with a high side pressure of 84 bar. At a cooling load of 2.73 kW, the highest obtainable COP for heating and Cooling were 4.04 and 3.55 respectively at an evaporation temperature of 10°C and high side pressure of 90 bar. The seasonal energy efficiency ratio (SEER) rating of the air evaporator was also performed. The performance of the system for drying applications was also carried out with a potential drying efficiency of 66% calculated. It was further discovered that integrating the dryer with the air evaporator at 2.73 kW cooling capacity, the drying efficiency increased to about 75%.

The performance of CO₂ heat pump was compared to alternative refrigerants, R134a and R410a. The CO₂ system had a better cooling performance than both refrigerants.

Preface

The content of this report presents the result of Master thesis carried out at the Norwegian University of Science and Technology (NTNU). Department of Energy and Process during a period spanning from January 2017 to June 2017. It is carried out in partial fulfillment for the award of a Master's Degree in Natural Gas Technology and it counts for 30 credits, one full academic semester.

The focus of the project was to carry out research as to how solar energy can be harnessed for application in a CO₂ heat pump. The bodywork of the project included carrying out experimental campaign on a heat pump rig, at NTNU. Analysis and presentation of the data recorded was also performed. Even though it was tasking, having a couple of useful hand around was quite helpful. I will then like to proceed to thank a host of people who helped in one way or the other to make this a success.

My first appreciation goes to my Academic supervisor, Professor Armin Hafner for those words of encouragement; he also contribute in no little measure his profound knowledge on the subject of heat pumps and refrigeration. I also extend my appreciation to my research advisor, Kryzstof Banasiak for contributing his immense knowledge of the test rig to the success of this project. My list of appreciation wouldn't be complete without mentioning Angle Alvarez, for always being at my beck and call whenever issues arise in the laboratory. Even though often times this is not quite convenient, he all the same offer this selfless service.

Am grateful to my parents Pastor and Deaconess Nana for always believing in me and help me achieve my long life dream of Master's degree.

Trondheim Norway
July, 2017
Oluwafemi Samuel Nana

TABLE OF CONTENTS

CHAPTER 1: INTRODUCTION	1
1.1 Background of study	1
1.2 Objectives	2
1.3 Outline of study	2
CHAPTER 2: LITERATURE REVIEW	4
2.1 Heating and cooling demand in building	4
2.1.1 Classification of heat pump load	4
2.1.2 Heat sources for integrated heat pump systems	5
2.2 Solar assisted heat pumps.....	8
2.2.1 Types of solar collector	8
2.2.2 Collector efficiency and losses	9
2.2.3 Types of Solar assisted heat pumps	11
2.2.4 Thermal applications of solar energy	13
2.3 Space cooling	15
2.4 Domestic water heaters	16
2.4.1 Hot water heat pump	16
2.4.2 Thermal storage of hot water	18
2.4.3 Previous studies on CO ₂ hot water heat pump	19
2.5 Drying	21
2.5.1 Domestic clothe dryer	22
2.5.2 Previous studies on heat pump dryers	24
2.6 Combined space cooling and hot water heat pump	26
2.6.1 Unitary air conditioner for cooling and heating	26
2.6.2 Previous studies on combine air conditioning and water heating	27
CHAPTER 3. THEORETICAL ANALYSIS	28
3.1 CO ₂ as a Working Fluid	28
3.1.1 Physical properties	28
3.1.2 Thermodynamics Properties	29
3.1.3 Transport properties	29
3.1.4 Safety	30
3.2 Main characteristics of CO ₂ heat pumps	30
3.3 Lorentz cycle	31
3.3.1 Performance indicators	33

3.3.1.1 Coefficient of performance	33
3.3.1.2 Volumetric cooling and heating capacity	34
3.3.2. Sensitivity analysis	34
3.3.2.1 Effect of optimum gas cooler pressure	34
3.3.2.2 Effect of gas cooler outlet temperature	35
3.3.2.3 Effect of Evaporation temperature	36
3.3.2.4 Effect of Refrigerant and water mass flow rate	36
3.3.2.5 Effect of superheat	37
3.3.2.6 Temperature Approach	37
3.3.3 Space Cooling	38
3.3.2.1 Performance indicator for space cooling	38
3.3.2.1 Include influence of air mass flow rate	38
3.4 Water heating	39
3.5 Drying cycle	41
3.5.1. Air drying cycle	41
3.5.2. Performance indicators for drying processes	42
3.5.2.1 Coefficient of performance (COP)	42
3.5.2.2 Specific moisture extraction rate (SMER)	43
3.5.2.3 Specific energy consumption (SEC)	43
3.5.2.4 Drying Efficiency	43
3.6 System Designs	45
3.6.1. Possible Solar-Gas cooler Configurations	45
3.6.2. Possible solar-evaporator configurations	47
3.6.3. System performance	49

CHAPTER 4. EXPERIMENTAL METHODS AND TEST FACILITY

4.1 Test facility	51
4.1.1 Compressor Unit	52
4.1.2 Gas cooler	53
4.1.3 Evaporators	55
4.2 Test procedure	56
4.2.1 Start-up procedure	56
4.2.2 During the experiment	57
4.2.3 End of experiment	57
4.2.4 Test Matrix	57
4.3 Instrumentation	58

4.3.1 Pressure	58
4.3.2 Temperature	58
4.3.3 Mass flow rate	58
4.4 Uncertainty of parameters	59
4.4.1 Compressor	59
4.4.2 Gas cooler	59
4.4.3 Evaporator	60
4.4.4 Coefficient of performance	60
CHAPTER 5. SIMULATIONS	
5.1 Design Conditions for space cooling	61
5.2 Energy consumption profiling	61
5.3 Heat pump modelling	62
CHAPTER 6. RESULTS AND DISCUSSIONS	
6.1 RHVAC results	66
6.2 PACK CALCULATION PRO results	67
6.3 Simulation results	70
6.4 Experiment results	72
6.4.1 Space cooling performance rating	74
6.4.2 Heat exchanger performance	75
6.5 Drying	76
6.6 Discussions	77
6.6.1 Influence of solar collector on heat pump performance	77
6.6.2 Impact of outlet temperature of gas cooler	77
6.6.3 Comparison of CO ₂ cycle to alternative refrigerants	78
6.6.4 Lorentz efficiency	79
6.6.5 Impact of air outlet temperature and relative humidity on dryer performance and efficiency	80
6.6.5.1 Effect of air temperature at dryer exit	80
6.6.5.2 Effect of relative humidity at the outlet of the dryer	80
6.6.6 Integration of the dryer with the air evaporator	81
CHAPTER 7. CONCLUSION FURTHER WORK	82
NOMENCLATURES	83
REFERENCES	84
APPENDIX	89

CHAPTER 1. INTRODUCTION

1.1 Background of Study

CO₂ heat pumps have been highlighted as the solution for present and future heat pump and refrigeration challenges associated with other heat pump systems. With emphasis on a greener world, which has led to the re-emergence of natural working fluids, previous studies have shown CO₂ heat pump systems to possess better system performance, safety, availability and with huge potentials. One of such potentials is the recovery and utilization of waste heat/energy in a heat pump systems with aim of improving system efficiency while also proving to be a useful application. The integrated systems typically consist of two or more different process cycles. The integration is such that it which comprises of a primary refrigeration cycle and another cycle which can be used for secondary applications. The secondary application can either be in a single, dual or multiple mode.

During the CO₂ heat pump process, a lot of heat accompanies the compression of the working fluid. This heat is removed from during gas cooling or condensation and is considered a waste. This waste heat can be harnessed. When harnessed, this recovered heat is put into useful work such as space heating, hot water heating, drying and other applications. This supplement the primary work being done and hence better energy efficiency of system is achieved. This will not only enhance the system performance, but also will lead to decrease in total energy demand, which hitherto has been supplemented by the successful conversion of the waste heat.

Previous studies have shown the potentials of reducing energy demand. One of such secondary processes that employs heat pumps for alternative applications is drying. Sequel to the use of heat pump systems, different drying processes such as sun drying, direct resistance heaters e.t.c. These applications have shown to either not to be so effective or costly. The sun drying process is highly dependent on the amount of solar radiation available, time of the day, location. Since this not equally distributed, it raises the question of efficiency. The direct resistance on the other is an energy intensive process and it is also costly. Bantle et. al (2016), reported a 70% reduction in energy demand from the simulation of a CO₂ heat pump system for drying applications. Ceylan et. al (2006), conducted an energy and exergy analysis timber dryer assisted heat pump. The study reported the potency of drying integrated heat pump, as initial moisture content of the poplar and pine timbers with 1.28 kg water/kg dry matter and 0.6 kg water/kg dry matter respectively was reduced to 0.15 kg water/kg. KloËcker et. al (2001) designed a drying heat pump with a 12kw capacity and experimentally recorded 65% energy savings compared to Passat type 132E direct heating mode. Sarkar et. al. (2006), modelled a transcritical CO₂ heat pump dryer and validated with experimental results while also establishing the important operating parameters such as dryer efficiency, recirculation air ratio, air mass flowrate and ambient temperature. KloËcker et. al (2002), established a relationship that showed that the energy saving potential increases with the Carnot efficiency of heat pump dryer.

Lorentzen 1994, introduced a novel approach of hot tap water heating. He proposed a transcritical Co₂ process simultaneous refrigeration and hot tap water production. This employs the sensible cooling for gas cooling and simultaneously hot water heating. Neskå et al. (1998), proposed that the application of CO₂ heat pump systems can reduce primary energy consumption with more than 75% compared to electrical heating. Stene 2007, highlighted the potential of CO₂ heat pump systems for domestic hot water sighting the annual heating demand

for domestic hot water (DHW) typically constitutes 50 to 85% of the total annual heating demand in the residence. Combining space cooling with water heating is a technology that most adaptable to geographical regions where the annual cooling load is large. For such regions, having a system that primarily cools residential building and also provides or supplement the hot water demand by residence is important. Heat pumps system that achieves this by using the heat rejected to provide this secondary application. Not only does it helps cuts energy cost but more importantly, it aids energy conservation and enhances better energy efficiency of the system.

1.2. Objectives

Improving the thermal performance and applications of heat pump systems have been an attractive research topic while tremendous of attempts have been conducted. The rejected heat from condensers in heat pump systems to ambient is considered wasted, and it counts very huge amount especially in countries where air conditioning is running most the day. Exploiting this heat in useful applications such as water heating, drying, and desalination could bring a lot of benefits. These systems usually operating by synthetic refrigerants such as R 134a which contributes to global warming and Ozone depletion. The best alternative of HFC refrigerants group is Carbon Dioxide (R744) since it is natural, and has competitive thermo-physical properties. In the meanwhile, integration of renewable energy resource with heat pump system is recommended, and can lead to increase the COP of the system and decrease the fuel energy consumption. For that, Carbon Dioxide Solar Assisted Heat Pump system for water heating, drying, and cooling is proposed. The system can provide the three application simultaneously or independently.

The objectives of the present study are highlighted as follows:

1. Theoretical analysis of integrated CO₂ heat pump systems, identification of key performance indicators
2. Experimental investigations of integrated CO₂ heat pump system to validate the theoretical results.
3. Discussion of results and comparing the results with system applying alternative working fluids.

1.3 Outline of study

The outline of study is described as follows:

Chapter 2 provides an overview of the possible heating and cooling demands in buildings. It also describes how the demands vary based on geographical location and the use of heat pump to meet these demands. The possible source of heat was reviewed including solar. A background review of useful literature important for the study were also examined. Three different loads (space cooling, hot water and drying) to be meet by the heat pump in study are discussed briefly.

Chapter 3 provides an insight into the properties of CO₂ as a working fluid, description of the main characteristics of CO₂ heat pumps. The Lorentz cycle is briefly discussed as the idea cycle that best describes the CO₂ heat pump operation and while its performance should be evaluated using Lorentz COP and efficiency. Performance indicators were established for the three different loads. Further theoretical analysis on system performance was carried out. A few system design options were also considered.

Chapter 4 gives a brief description the test rig, its components, instrumentation, test matrix and how the experimental campaign was carried out. Uncertainty of measured and derived parameters were evaluated.

Chapter 5 presents the reference basis on which the experiment was carried. Simulation tools were used to determine the space cooling load for a residence. This load was later interpreted to be the reference air evaporator capacity. An hourly profiling simulation tool was used to gain an insight of the SEER rating of space cooling heat pumps. This tool also estimated the performance of a single transcritical system with a single evaporator (air). A model to estimate and supplement experimental reading was also developed accordingly.

Chapter 6 provides the simulation and experimental results of the study and discussions.

Chapter 7 gives the conclusion of the study and provides an insight into possible further studies.

CHAPTER 2. LITERATURE REVIEW

2.1 Heating and cooling demand in buildings.

2.1.1 Classification of heat pump loads

Heat pumps can also be classified based on its applicability. There are two primary classes, cooling load and heating load as shown in Table 2.1 below. However, these processes both exist in the refrigeration and its configuration is solely based on applicability. When the primary function of the heat pump is to remove heat from a system or space, its application is found refrigeration and air conditioning. When the primary function of the heat pump is to add heat to a system or space, its application is found in space heating, e.t.c. This classification cuts across residential and industrial processes, however combination and integration of two or more of the applications is also possible.

Table 2.1: Classification of heat pump loads

Classification	Applications
Cooling load	Air conditioning Refrigeration
Heating load	Space heating Hot water heating Drying Desalination

Residential sector accounts for 48% of Heating and cooling consumption in the Italy with, only 29.4% of households have access to space cooling system. The most common air conditioning systems utilized are reversible HVAC systems which are applicable for summer and winter operations accordingly, found in 68.1% of homes with air conditioning according to report from GSE 2015. Recent data from Lapillonne et al (2014) shows that the demand for air conditioning has increased by about 100% in Italy from the year 2000 to 2011 and it is predicted that it will keep growing even as the production of Air conditioning keeps increasing.

In Europe, energy requirement for heating and cooling accounts for 50% of the total energy requirement, with residential sector representing 45% of the demand. Classifying by application as shown in the Figure 2.1 below, the average hot water demand in Europe is between 50 to 85%. The amount of energy required for space heating span across 35 to 75% of total demand. Process cooling with desalination as an example accounts for up to 48% while space cooling accounts for a high value of about 30% in Malta. [Eu.europa.eu]

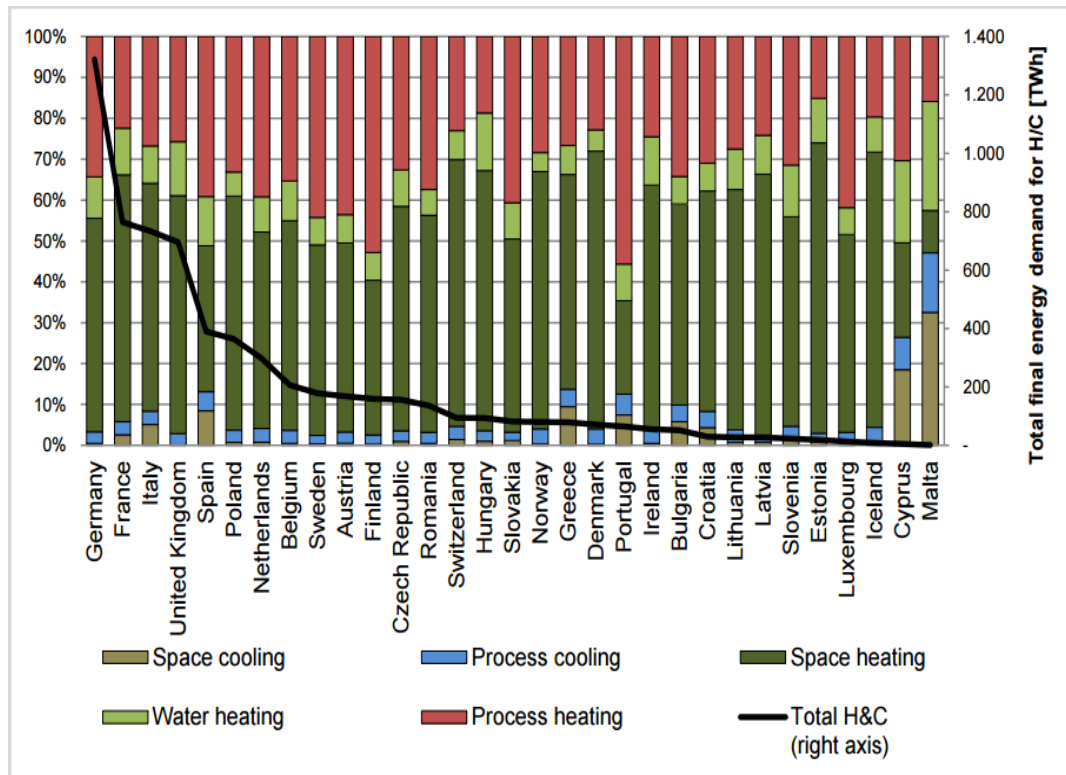


Figure 2.1: Applications of heating and cooling load by region [Ec.europe.eu]

2.1.2 Heat sources for integrated heat pump systems

An important parameter to be taken into consideration when designing a heat pump is the heat source. The absorption encapsulates the evaporation process and it occurs at constant temperature using latent heat.

The design of heat pump systems can be based on systems types. With reference to the gas cooler and evaporator design, the heat pump can be classified as direct or indirect systems. Examples of direct systems include air to air, water to water, air to water and brine to water, brine to air for the indirect systems. The air to air type of heat pump system utilizes air as the heat source and also as the medium of heat transmission from the refrigeration/air conditioning. The air to water type of heat pump systems utilizes water as the heat source and air as the medium of heat transmission away from the refrigeration/air conditioning space. An indirect system utilizes a secondary circuit to transmit heat from and to the air conditioning space. Examples of indirect systems include brine to air and brine to water heat pumps.

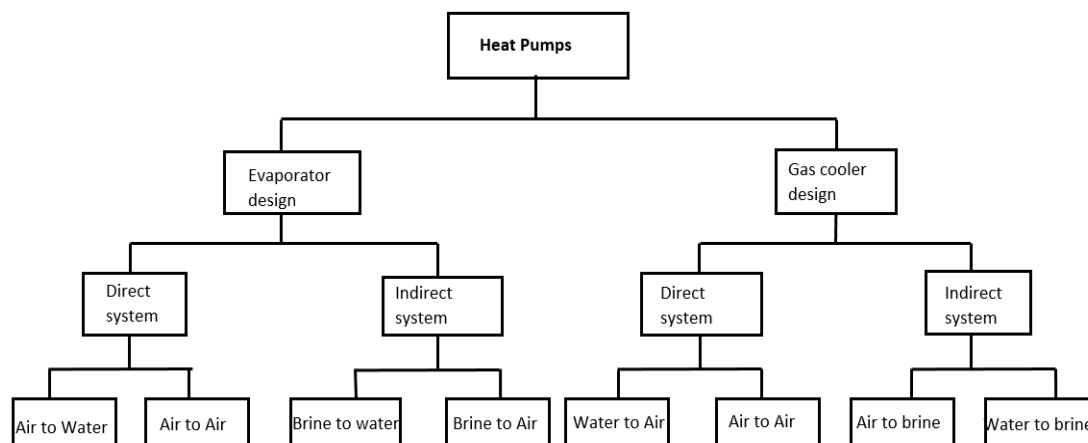


Figure 2.2: Classification of heat pumps based on design

Even with growing demand for cooling, heat accounts for 80% of the energy usage in residential buildings (Sarbu, I. and Sebarchievici, C., 2014.). It is imperative that renewable energy source be sourced for heat pumps. Examples of renewable heat source includes;

- Ambient air
- Ventilation air
- Solar
- Ground water
- Open water (lake, river)
- Grey water (waste water)
- Bedrock

- a. **Ambient air:** This is the most common source of heat for heat pump systems due to constant availability. It possesses a relatively low average source temperature. The major advantage of this heat source is its relatively low investment cost coupled with moderate potential energy saving. However, it does possess a few disadvantages which includes possible operational problems like defrosting of evaporator is required during winter operation. The performance on the system is also affected as the heating capacity of the heat pump decreases with decrease in the ambient temperature.
- b. **Ventilation air:** This is the air vented into the room does have the potentials of recovering heat from the exhaust air exiting the room. The waste heat recovered has the potential to serve as a heat source- Ventilation air though readily available, but due to its low air temperature possess low heating capacity and limited ventilation air flowrate. Heat pump utilizing waste heat as heat source often requires a heat recovery unit and an additional heat source.
- c. **Bedrock:** Bedrock is a potential heat source which makes use of the thermal energy buried deep down under the ground and it's often referred to as energy well. Its average source temperature is high and considerably stable. Although it attracts high investment costs and also requires proper ground conditions, large space for energy wells, its potentials for energy saving is quite high. An individual energy well can serve multiple residences.

- d. Solar:** Solar energy is a very high temperature source. Its applicability is highly dependent on variation in weather conditions, summer and winter. The amount of energy extractable depends on geographical location and the amount of irradiation also susceptible to time of day. At peak temperatures, the solar energy portends high energy saving potentials. It requires high investment cost.
- e. Open water:** Open water such as sea water, lakes, and rivers can also have potentials in serving as heat source. It has a relatively average source temperature at a relatively stable condition and depending on its availability, relatively high water flowrate can be applied generate a high heating capacity. However, its applicability hinges on location, as it can only supply residences close to the water body. It requires relatively high investment costs as it incorporates indirect systems design in its installation.
- f. Grey water:** Waste heat from waster waters from daily domestic use are potential heat source for heat pump systems. Large volume of hot water is utilized in daily activities from washing activities and showers. These waste-water has the potentials to provide stable, high temperature and quantity of energy. Although it incurs extra investment costs for equipment and treatment, it relative energy saving potential is high.
- g. Ground water:** Underground water body has the potential of being a high temperature source with stable supply. It requires good location and creates competition for land use. It requires good soil conditions for installation of equipment. It has a relatively high energy saving potential.

2.2 SOLAR ASSISTED HEAT PUMPS

In regions like Lombardy with relatively high temperature in summer, only 29.7 out of every 100 household has access to air conditioning. This shows that their massive potential for development of more air conditioning units even with the introduction of more efficient units.

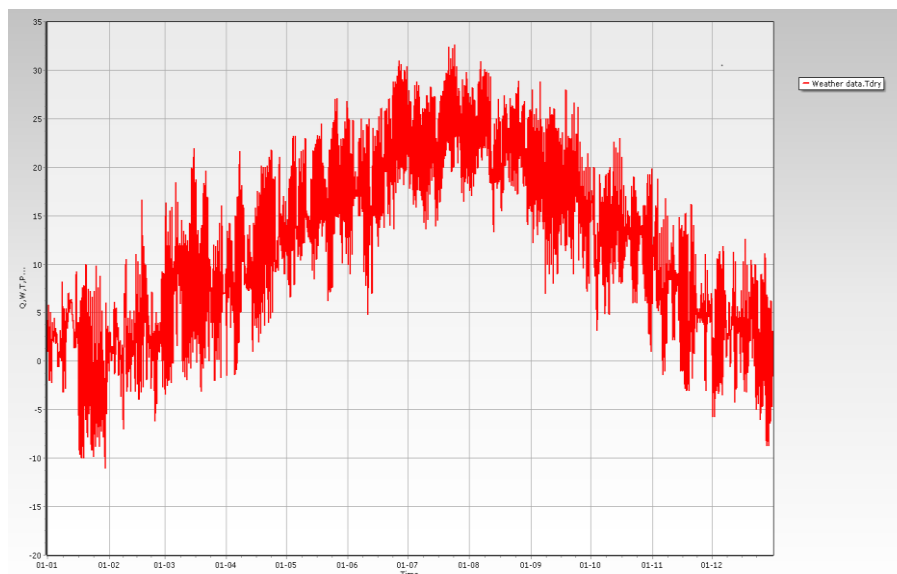


Figure 2.3: Temperature profile of a region in Italy

The amount of solar radiation penetrating into the earth space has increased dramatically due to climate change and this has resulted into increase in ambient temperature over the years. However, the amount of solar energy potentials compared to other forms of renewable energy is massive. Barber and Provey (2010), reported that with a potential of about 86,000TW, the global consumption represents less than 1% of the solar energy. A typical temperature of a region in Italy is shown in Figure 2.3 above.

2.2.1. Types of Solar collector

For solar energy to be harnessed, energy harvesting systems are required. Such systems include solar collectors, thermal storage tanks, heat exchangers and working fluid. Solar collectors are directly involved in transforming collected solar energy into heat. The principle of operation of solar collector is as follows; solar radiation is absorbed through the collector surface which transforms it into heat, which when transferred into a working fluid can be used for heating applications or stored in thermal storage prior to further usage. Solar collectors can be classified into the following subgroups;

- (i) Flat plate collector
- (ii) Point focusing collector
- (iii) Line concentrating collectors

Flat plate collector is the simplest type of solar collector and requires little maintenance. Its main distinction from other collectors is that it doesn't require sun tracking. Hence, it collects both beam and diffusion radiation. (Sukhatme and Sukhatme, 1996). The major parts of a flat plate collector include a tubing for transporting the working fluid in and out of the collector, an absorber plate for transformed solar energy into heat and glazing material which serves as a top cover. Though the choice of either or not use a glazing is optional, however when considered the most important parameter in the choice of glazing materials includes absorptivity, transmissivity and emissivity. It is desired that the glazing material, which is

topmost part of the solar collector, have very high transmissivity, very low absorptivity and emissivity values. Most common glazing materials used includes glass and plastic; however, plastic has a major disadvantage being low life span. (Bakari et al, 2014).

The absorber plate does the work of converting solar radiation into heat, which is then transmitted to the attached tubes for transporting the working fluids. The absorber is usually dark colored or covered with selective coatings, which has very high absorptivity value. A good absorber plate should be able to absorb large amount of solar energy while transmitting very amount of it back into the ambient. The flat plate collector is most suitable for low temperature applications below 80°C.

An adaptation to this is the evacuated tube collector which comprises of two tubes with vacuum in between them. The surface of the inner glass tube is coated to enhance high absorption of the solar radiation and prevent heat loss by emission. Coupled with the vacuum space in between the two tubes which prevents heat loss by convection, the evacuated tube collector yields better performance than the flat plate collector. (Islam and Sumathy, 2013).

Point focusing collector type of solar collector is suitable for high temperature applications. It entails sun tracking the sun on two or more axes and positioning the collector material(s) in such a way that the solar radiation reflected on the collector surface is focused at a single point. The fluid carrying medium is usually situated at this focal point and collects the heat. It has a very high collection efficiency. It can exist as two design forms as parabolic dish reflector, heliostat dish reflector. While the parabolic dish reflector utilizes a parabolic dish (made up of a single or multiple materials) to reflect the radiation on the focal point, the heliostat comprises of several flat mirrors known as heliostats which reflects its individual radiation on a focal point. (Sukhatme and Sukhatme, 1996).

Line concentrating collector is a type of collector is also suitable for high temperatures above 80°C. It entails tracking the sun on a single axis. It general consists of many parallel trough like reflective surface which reflects the solar radiation on a selectively coated long pipe which runs parallel across the connected troughs. The long pipe serves as the absorber transferring the heat into working fluid being transported to and from the trough lines. The absorber tube is often enclosed in glass tubing to minimize the loss due to convection. The reflective ability of the mirrors, absorptivity of the absorber determines the efficiency of collector. It is available in different design modules which includes parabolic trough, linear Fresnel, compound parabolic and cylindrical parabolic collectors. (Sukhatme and Sukhatme, 1996), (Desai and Bandyopadhyay, 2016), (Francipane et al, 2016).

2.2.2 Collector efficiency and losses

The amount of solar energy available is most dependent by four parameters namely; the amount of solar radiation hitting the surface of the collector, the total surface area of the collector, the absorptivity of the absorber plate and the transmissivity of the glazing material. The absorptivity and transmissivity factors determines the amount of solar energy penetrating and absorbed by the collector, they are assumed to be constant for a given absorber plate and glazing material. It is defined by the expression shown below;

$$Q_{avail} = A.I(\sigma_{ab}\tau_g) \quad \text{Equation 2.1}$$

Where A is the area of the collector and I is the solar insolation, the solar absorptivity of the absorber and the transmittivity of glass cover are represented as σ_{ab} , τ_g respectively.

However, due to losses associated with solar collectors, the useful solar energy gained under steady state operation is defined as follows;

$$Q_{useful} = A[I(\sigma_{ab}\tau_g) - U_{overall}(T_c - T_a)] \quad \text{Equation 2.2}$$

$$U_{overall} = U_{top} + U_{edge} + U_{bottom} \quad \text{Equation 2.3}$$

Where U_{top} , U_{edge} , U_{bottom} represents the respective losses associated with the top, edge and bottom of the collector.

The losses due to edge and bottom are often negligible due to assumption of proper insulation. Hence, only the impact of the top loss is considered (Samdarshi and Mullick, 1990.). The relation with relation to glass cover temperature can be simplified by introducing collector heat removal factor (F_R) and working fluid inlet temperature (T_i). The useful solar energy gain can be expressed using Hottel-Whillier-Bliss equation as follows;

$$Q_{useful} = F_R A [I(\sigma_{ab}\tau_g) - U_{overall}(T_i - T_a)] \quad \text{Equation 2.4}$$

The collector efficiency is defined as the ratio of the useful solar energy gained over the available and can be represented with the following equation;

$$\eta = \frac{F_R A [I(\sigma_{ab}\tau_g) - U_{overall}(T_i - T_a)]}{AI} \quad \text{Equation 2.5}$$

Losses associated with solar collectors; as it is with every other thermal system, solar collectors are also susceptible to losses during heat transfer. The amount of useful heat gained and collector efficiency is also defined by these losses. The solar collector is prone to losses due to top loss, edge loss and bottom loss, which are shown in Figure 2.4.

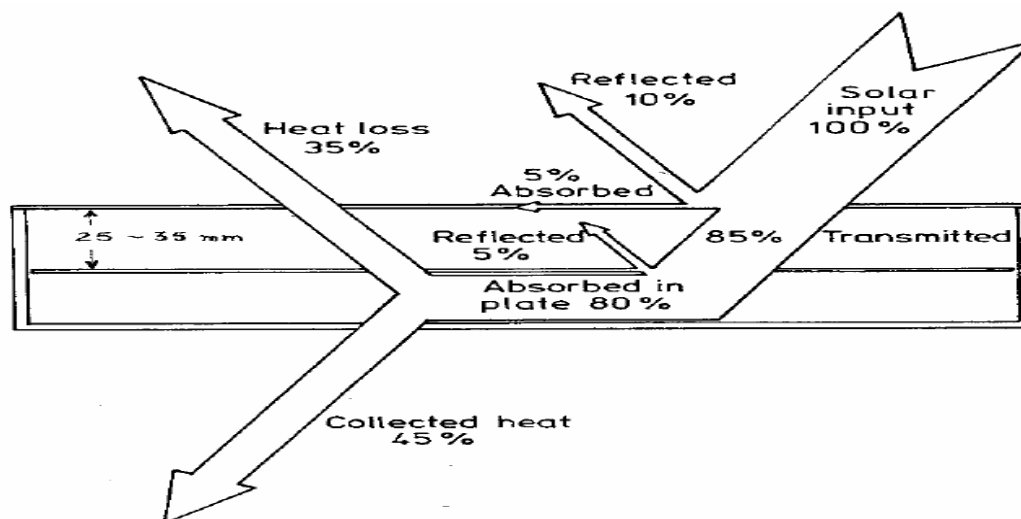


Figure 2.4: losses in solar collectors (Struckmann, 2008)

The under listed are means by which the flat plate solar collector under performs;

- a) **Loss due to radiation:** the amount of useful energy gain is affected by the amount of heat loss due to radiation. There are two ways in which this happens; heat loss

from the glazing material and heat loss from the absorber plate, which can be defined by their heat transfer coefficients respectively.

$$h_{r,ag} = \frac{\sigma(T_g^2 + T_a^2)(T_g + T_a)}{((1/E_g) - 1)} \quad \text{Equation 2.6}$$

$$h_{r,ag} = \frac{\sigma(T_g^2 + T_a^2)(T_g + T_a)}{((1/E_g) + (1/E_p) - 1)} \quad \text{Equation 2.7}$$

Where T_g, T_a represents the temperature of the glazing material and the absorber plate. Emissivity of the respective materials are represented as E_g and E_p .

The effect of this mode of heat loss can be minimized by using or selectively coating the absorber plate to enhance high absorptivity and low emissivity for both the absorber and the glazing material (bakari et al, 2014).

- b) Loss due to convection:** the most losses associated with solar collector are due to convection. It occurs on the top side of the collector between the glazing material and ambient, and between the absorber and the glazing material. This is often influenced by the ambient condition and the wind velocity. Losses due convection on the surface of the glazing material is greater significance. The heat transfer coefficient is expressed as shown below:

$$h_c = 5.7 + 3.8V_w$$

Where V_w is the wind velocity

The loss that occur between the glazing material and the absorber plate can be minimized by space evacuation between them. The loss coefficients are reduced by increasing the vacuum between the glazing material and the absorber plate (Agbo and Okoroigwe, 2007).

- c) Loss due to conduction:** this type of loss is often associated with the bottom an edge side of the collector. The effect of which can be mitigated by properly insulating the collector sides and bottom.

2.2.3. Types of Solar assisted heat pump (SAHP)

There are different types of solar assisted heat pumps with the two major types namely:

- a. Direct expansion and
- b. Indirect solar assisted heat pumps.

Direct expansion solar assisted heat pump systems (DX-SAHP) employ the use of solar collector which also doubles as the evaporator. Hence, for this type of system the collector replaces the conventional evaporator. The refrigerant is expanded into the solar collector where both solar energy absorption and evaporation occurs simultaneously. The refrigerant exits the collector-evaporator superheated. The performance of system improves significantly due to the elimination of indirect loop required for heat exchange in conventional SAHP. Usage of refrigerant instead of water or air as working fluid enhances longer solar collector life due to better heat transfer coefficients of refrigerants, elimination of corrosion problems associated with water is also achieved. The temperature of the collector is also reduced and the optimum temperature approach between 5-10°C is achieved. Large temperature difference between the collector and ambient undermines the performance of the system as potential solar energy will be lost to the ambient. Therefore, utilizing a refrigerant such as CO₂ with good thermos-

physical properties with engender high evaporation temperature, which in turn leads to better system performance.

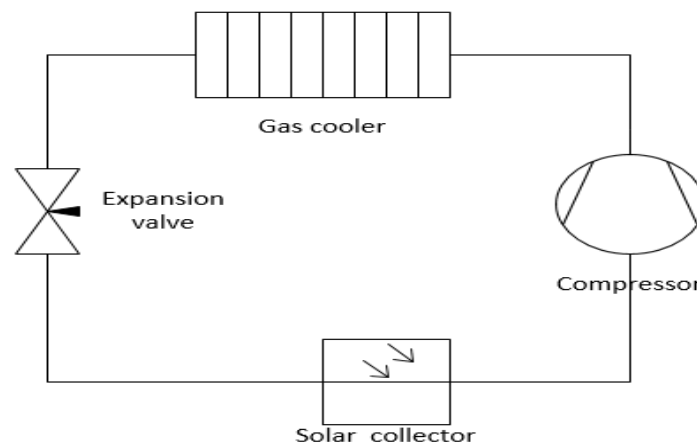


Figure 2.4: Direct expansion solar assisted heat pump

Xu et. al, (2005) previous studies demonstrated theoretically and experimentally direct expansion SAHP has very high efficiency on sunny days.

An indirect SAHP unlike direct system employs a separate heat exchanger loop to integrate the solar collector and the heat pump as separate units. The solar collector typically encompasses a collector loop with water or air in circulation. Indirect SAHP can be subjected to different configurations to optimize its application and performance. One of the problems associated with direct SAHP is installation which requires long supply and return lines between the rooftop solar collector and the indoor thermal storage where the heating process is needed. The indirect SAHP has a flexibility advantage, as the solar heat source can also be utilized (integrated) in a variety of applications. With a thermal storage, an indirect system can continue supplying heat even when there is a drop in solar radiation and the solar collector can no longer generate the required heat.

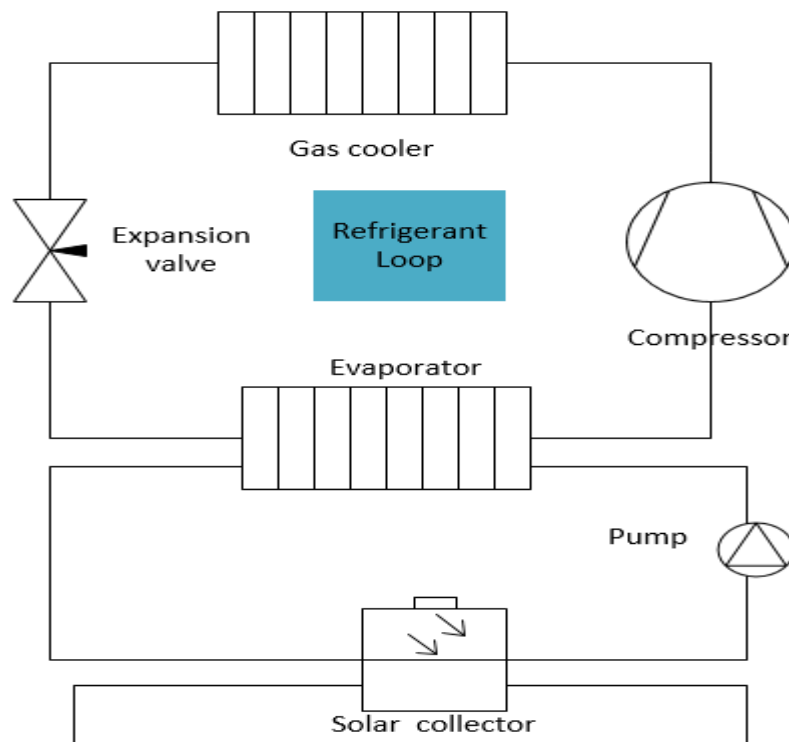


Figure 2.5: Indirect solar assisted heat pump

Several studies have proposed the use of unglazed or bare collector as the temperature on the collector is lower; a smaller temperature approach between the collector surface and ambient is achieved. Using a bare collector also enhances effective heat transfer between the ambient air and working fluid during periods when low solar radiation is available. Heat losses associated with glazed collector is minimized, a higher collector efficiency is achieved.

Although there are possibilities of mismatch in operation where there is a deviation in design conditions such as collector temperature, solar radiation. To mitigate this problem, a variable speed is proposed.

2.2.4 Thermal Applications of Solar energy

The application of solar energy as a heat source for heat pump applications has since gathered interest, most especially in space cooling systems. According to a paper presented by Hadorn (2012), different concepts are being implored in its application as heat source as shown in Figure 2.6.

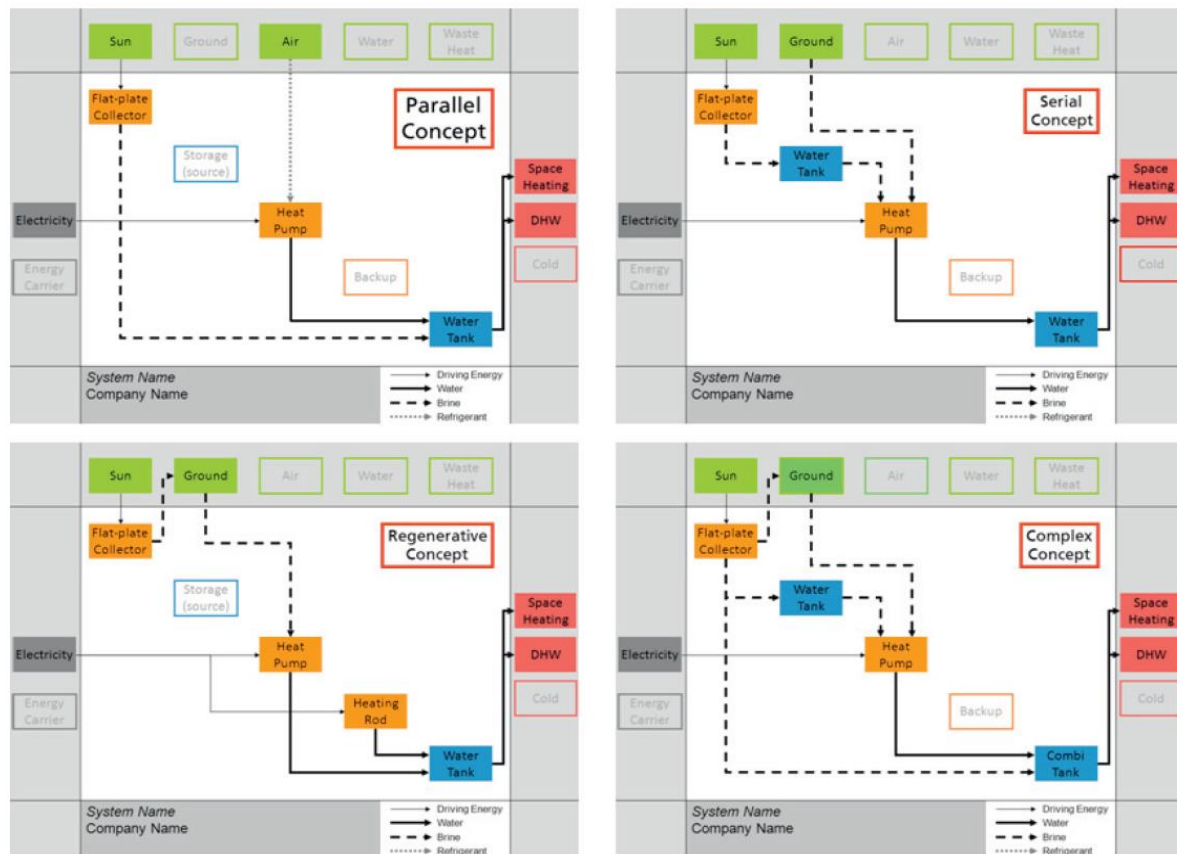


Figure 2.6: Thermal application of solar energy

In the parallel concept, the solar energy collected is applied in parallel with the heat rejection process of the heat pump. As water used as heat sink flows through the gas cooler or condenser for hot water heating in the collection tank, the heat is also sourced from solar collector to raise the hot water temperature.

Series concept describes the collection of solar energy in water and it used in combination other heat sources such ground, air, water and waste heat. The choice of secondary source depends on the locations. This leads to the implementation of two evaporators in series. The heating capacity of the system increases and more heat is extracted for heating applications.

Regenerative concept is quite a novel approach in the use of solar energy. Due to the depletion in the solar radiation because of time variation in the day, the amount of energy sourced from the solar collector also decreases. To compensate for this depletion, the solar collector is connected in series with another heat source which has a more stable and relatively high temperature. Therefore, the working fluid having extracted heat from solar collector then goes through the regenerative heat exchanger when extra heat is extracted.

Complex concept is a concept epitomizes the flexibility and different ways of harnessing solar energy to meet the energy requirement of a system and most importantly making it energy efficient. It is typically a combination of two or more concepts described above and is applicable in locations where solar radiation is high. Heat collected from the solar energy is utilized concurrently for various purposes, which includes hot water heating, thermal storage, and regenerative purposes.

2.3 Space cooling

The process of removing heat from confined environment is known as space cooling. There are different ways of achieving this. The earliest method of space cooling made use of ice that were harvested during the winter and kept for usage during the summer. This method makes use of water's large heat of vaporization and can be described as evaporative cooling. Other examples of evaporative cooling includes forced convection of air over wet materials. Nowadays, heat pump technology presents an alternative that is less laborious, faster, provides better performance and more efficiency. Most common equipment for space cooling are often referred to as air conditioners, taking into account the humidity alongside the temperature to give the required comfort. They also classified as air cooled and water cooled, with the air cooled type being the most common. Air conditioners are classified according to ASHRAE (Cooling, AHH, 2008) definitions as listed below:

- a) Unitary air conditioners and heat pump
- b) Room air conditioners
- c) Packaged terminal air conditioners

Unitary air conditioners and heat pumps are air conditioners that are factory-made assemblies that normally include an evaporator or cooling coil and a compressor/ condenser combination, and possibly provide heating as well. An air-source unitary heat pump normally includes an indoor conditioning coil, compressor(s), and an outdoor coil. It must provide heating and possibly cooling as well. A water-source heat pump rejects or extracts heat to and from a water loop instead of from ambient air. A unitary air conditioner or heat pump with more than one factory-made assembly (e.g., indoor and outdoor units) is commonly called a split system. Unitary equipment is divided into three general categories: residential, light commercial, and commercial. Residential equipment is single-phase unitary equipment with a cooling capacity of 65,000 Btu/h or less and is designed specifically for residential application.

Room air conditioners are encased assemblies designed primarily for mounting in a window or through a wall. They are designed to deliver cool or warm conditioned air to the room, either without ducts or with very short ducts (up to a maximum of about 48 in). Each unit includes a prime source of refrigeration and dehumidification and a means for circulating and filtering air; it

may also include a means for ventilating and/or exhausting and heating. The basic function of a room air conditioner is to provide comfort by cooling, dehumidifying, filtering or cleaning, and circulating the room air. It may also provide ventilation by introducing outdoor air into the room and/or exhausting room air to the outside. Room temperature may be controlled by an integral thermostat. The conditioner may provide heating by heat pump operation, electric resistance elements, or a combination of the two.

The Air-Conditioning and Refrigeration Institute (ARI) defines a packaged terminal air conditioner (PTAC) as a wall sleeve and a separate unencased combination of heating and cooling assemblies intended for mounting through the wall. A PTAC includes refrigeration components, separable outdoor louvers, forced ventilation, and heating by hot water, steam, or electric resistance. PTAC units with direct-fired gas heaters are also available from some manufacturers.

Cooling-only PTACs need not include heating elements. A packaged terminal heat pump (PTHP) is a heat pump version of a PTAC that provides heat with a reverse-cycle operating mode. A PTHP should provide a supplementary heat source, which can be hot water, steam, electric resistance, or another source. PTACs are designed primarily for commercial

installations to provide the total heating and cooling functions for a room or zone and are specifically for through-the-wall installation.

2.4 Domestic water heaters

Hot water heaters can be classified into three different categories namely; Electric resistance heater, solar hot water heater and heat pump hot water heater. Electric resistance hot water heater utilizes an electric element enclosed in a water tank for water heating. Although it is most common type of hot water heater due to ease of installation and its application for off-peak water heating. Even with its low cost, it is expensive in utilization as cost of electricity is relatively high.

The solar hot water heater is a more energy efficient heater; it can achieve a relatively high hot water temperature. However, this is dependent on location, climate and time. Although it has an initial high investment cost, but its low running and maintenance cost offsets this. There are also possible operation problems such as corrosion of the solar collector by water. However, it can be avoided by using an intermediate heat exchanger to connect a separate water loop to the solar collector heat loop. A separate circulation fluid is used for the absorption of solar energy from the collector. Heat pump hot water is the most energy efficient hot water heater. It has the potentials of utilizing or combining different heat sources. The daily average electricity use for water heating in heat pump, standard electric 50 gallon tank heater, flat plate solar collector 80 gallon tank and differential control pump is shown in Figure 2.7 below;

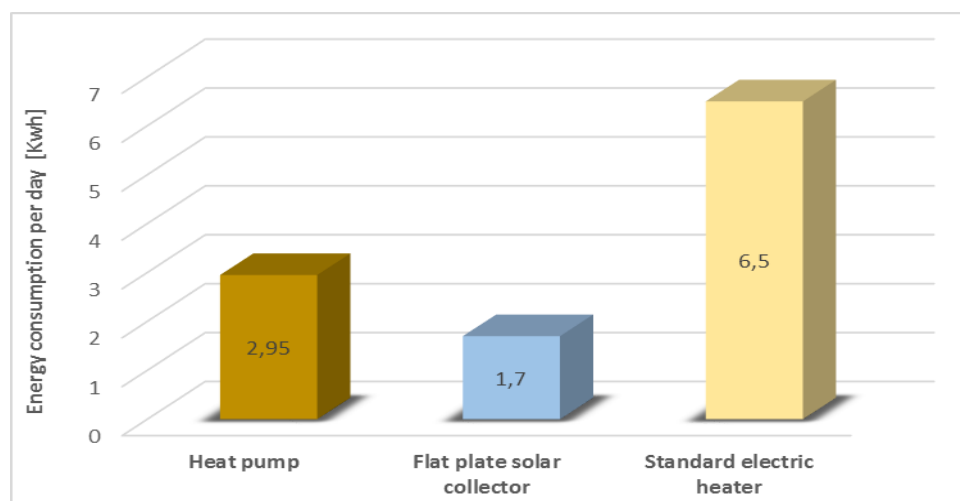


Figure 2.7: Energy consumption of potential hot water heaters (Source; homepower.com/articles)

2.4.1 Hot water heat pump

A conventional domestic heat pump hot water heater consists of two major loops; the refrigeration loop and the hot water loop. With the evaporator, the cooling capacity for space cooling is met while the gas cooler serves as the medium for heat sink for hot water production. The heat pump consists of the following components;

- Compressor
- Condenser/ Gas cooler configurations

- Expansion device
- Evaporator
- Low pressure receiver (not compulsory)
- Super heater (not compulsory)
- Sub cooler (not compulsory)
- De-super heater
- Pumps
- Hot water tank

The evaporator as component usually employs air source, the two-phase refrigerant absorbs heat from the air with the air serving as the primary heat source. The cooled air is channeled to the air handling unit for its application for space cooling. However, the primary heat source can be combined or integrated with other sources like ground heat exchanger for optimum performance. A saturated vapor is always desired at the exit of the evaporator. A super-heater is usually employed to achieve some amount of super heat. A hermetic scroll or reciprocating compressor is usually used for the compression process. The refrigerant leaves the compressor at high pressure and temperature. Due to very high temperature nature of the refrigerant latent heat is only experienced in the de-super heater, it is the component for the high temperatures hot water production. However, the sensible heat in the condenser can be used to preheat the water, this reduces the amount of heat required for the re-heating. The cold water enters the condenser for pre-heating within a temperature range of 5-10K. The hot water exiting the de-super heater after the reheating is collected in the storage tank. The heat exchange flow is usually counter-current for hot water.

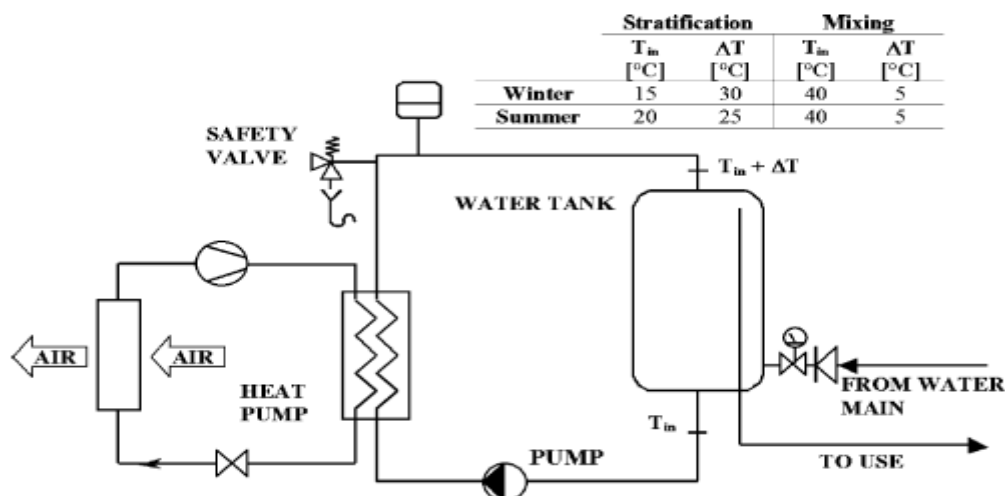


Figure 2.8: A representation of hot water heat pump (Cecchinato et al 2005)

The most common type of hot water heat pump is the air source heat pump. Other types of sources has been discussed in section 2.1.2 above. The heat pump have about two different configurations for water heating. The first configuration describes a system where the condenser is a part of the heat pump, the heat transfer to the cold water takes place in the condenser, and the hot water is conveyed to a separate vessel for storage. In the second configuration, the condenser is integrated with the storage vessel. The cold water is fed into the tank and the condenser carrying the hot temperature discharged refrigerant from the compressor is immersed in the cold water for hot water charging.

The type of condenser used determines the type of configuration to be used. The two applicable configurations are shown in Figure 2.9. A condenser that utilizes a coil tube heat exchanger is best fit for the second configuration. If a plate heat exchanger is used, the first configuration is used and a closed water loop is used for water circulating to and from the storage tank. In a counter flow direction, the water is pumped into the heat exchanger.

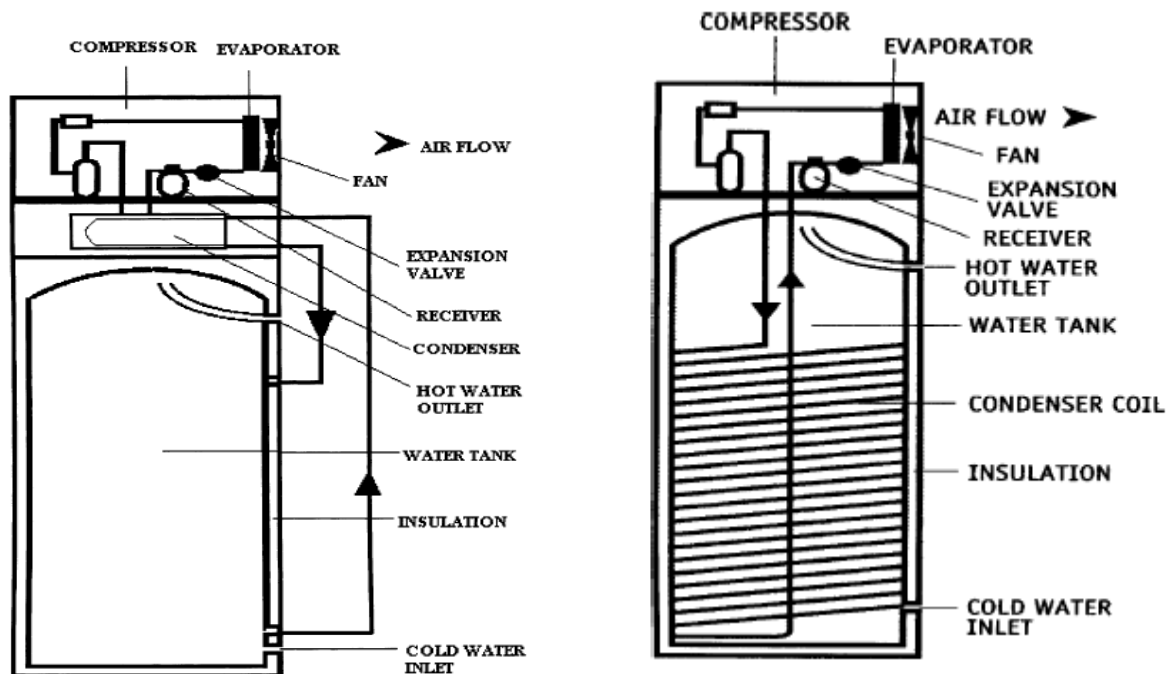


Figure 2.9: Configurations for hot water heat pump (Morrison et al, 2004)

A more efficient method for hot water heating is to use the condenser for pre-heating and de-super heater for the reheating. When only the condenser is enclosed in the storage tank, it is called a single coiled. When both condenser and de-super heater coils are enclosed in the storage tank, it is referred to as double-coiled. A better energy efficiency is achieved when the cold-water inlet at the condenser achieves a temperature lift of about 25-30°C. In the case of applying a condenser for hot water heating, a supplementary electric heating element immersed in the tank is usually available for peak load or reheating. The minimum temperature for storage of hot water is about 55°C to avoid bacteria growth.

There are two different approaches of a storage tank; single or double shell. Typical single shell hot water tanks have a volume capacity of up to 300 liters. In a single shell tank, the hot water is can be collected from the condenser or de-super heater. The double shell hot water on the other hand consist of two cylindrical vessels; primary and secondary. The primary vessel is usually with a higher volume capacity to the secondary vessel. Most hot water tanks are installed with the following accessories for optimum performance; shut-off valve, pressure reducing valve, check valve, safety valve, circulation pump, emptying valve pressure gauge and test valve.

2.4.2 Thermal storage of hot water

Thermal storage of hot water can be controlled based on their different operating modes as described in ASHRAE 2008, which can be adapted to hot water heat pump operation. Operating modes are usually defined by the variable parameters and the sequence in which they are operated. The underlisted modes are further discussed briefly.

- a) Charging with no load

- b) Charging storage while meeting loads
- c) Meeting load from discharging only
- d) Meeting loads from direct equipment operation and storage
- e) Meeting loads from direct equipment operation only

Charging with no load describes a scenario where the basic operation of the heat pump is to produce the hot water for storage. No hot water demand is covered directly from the heat pump operations while the heat pump operates at maximum capacity and constant flow supply to the storage. Hot water supply is therefore not limited to whether or not the heat pump is in operation even though the primary objective of the heat pump is to charge the storage. However, the storage tank must be well insulated to avoid exergy loss. A double shell hot water tank is most suited for this kind of operation.

Charging storage while meeting loads as an operation mode is quite different from that described above. The primary aim is meet demand while charging thermal storage simultaneously. The heat pump operates at maximum capacity; the flow supply ratio is dependent on the load. The hot water demand which is the priority when met, the excess hot water supply is diverted to the storage. This operating mode usually doesn't apply to residential buildings. Flows to both the load and the storage can be connected to the Mains supply using parallel or series piping configurations.

Meeting Load from discharging only, the total hot water demand is met directly from the thermal storage without the heat pump in operation. The hot water is typically produced and stored when the heat pump is in operating at peak period. The heat pump operates at a set conditions and steady state.

Meeting loads from direct equipment operation and storage, hot water demand can be met directly from the operation of the heat pump and simultaneously from the thermal. The heat pump in operation operates at a specific capacity and the supply hot water at constant temperature. This operating mode is very compatible for residential buildings with large hot water consumption. A control sequence should be in place to manage the distribution of the demands.

Meeting loads from direct equipment operation only is a simple operation as compared to the other modes. The hot water demand is met only from the operation of the heat pump, with no supply or flow from the thermal storage. This is most compatible for industrial and plant operations where continuous and large hot water is in demand.

2.4.3 Previous studies on CO₂ hot water heat pump

Neska et al (1998), carried out design and experimental analysis of a prototype of CO₂ heat pump hot water with a tap water inlet temperature of 6°C and hot water outlet temperature of 60°C. The air heat source system, which achieved a COP of 4.3 had a comparative advantage of energy consumption 75% lesser than electrical and gas fired system. The potential of the CO₂ system to deliver hot water at higher temperature unlike other conventional systems was highlighted.

Kim et al (2003), carried out study on the transient thermal behavior of a water heat system driven by a heat pump. The quasi steady state model includes variation of hot water temperatures and hot water reservoir size. The result of the study showed that smaller reservoir

favors larger transient performance degradation while larger reservoir size resulted in more heat loss during storage. Kim et al. 2005 performed a study to investigate the effect of internal heat exchanger on a transcritical CO₂ cycle with variables including secondary fluid temperatures at evaporator and gas cooler inlets. While evaluating the COP of the system with respect to length of the internal heat exchanger at different operating conditions, it was observed the COP increases with increasing length. The refrigerant mass flow rate decreases with increasing internal heat exchanger length while varying the discharge pressure. The compressor power also decreases accordingly.

Cheng and Gu (2005), carried out a study on the effect of high effectiveness of heat exchanger on system performance. Results showed that with high heat exchanger effectiveness at fixed ambient temperature and high side pressure. The study suggested that at low ambient temperature, compressor suction temperature and low high-pressure side, a high effectiveness should be considered.

Sakar et al (2005), simulated a CO₂ heat pump cycle for simultaneous cooling and heating applications. The system deliver secondary fluid heating at 73°C and results showed the optimal COP was achieved with system variables which includes compressor speed, heat source inlet temperature, compressor discharge pressure and the inlet temperature of the fluid to be heated. Yokoyama et al (2007), conducted a numerical simulation of CO₂ heat pump for a continuous water heating process. The study took into consideration the hourly change in hot water consumption and temperature distribution in the tank. The variation in the system's performance was also evaluated on an hourly and monthly basis as a result of changes in system parameters. High COP and system efficiency was obtained during the summer months while the system recorded low storage efficiency within the same time span.

Laipradit et al 2008, conducted a theoretical performance analysis of CO₂ hot water heat pump by modelling the transcritical process. The effects on the heat pump performance by the operating parameters such as the compressor rotational speed, the inlet water temperature at the gas cooler, the inlet air temperature at the evaporator and the mass flow rate ratio of water to refrigerant were presented. The study established a mass flow rate ratio of water and CO₂ between 1.2 and 2.2 as the most suitable value for hot water heating at temperatures above 60°C at 15–25°C ambient air temperature. For the following rated system capacities of a 4 kW compressor, a 10 kW gas cooler and a 6 kW evaporator, the COP is found to be between 2.0 and 3.0.

Test results and validation from the numerical studies carried out by Sakar et al 2009 showed that variation of the water flow rate has modest impact on the performance of the evaporator and gas cooler while the inlet temperature of the water at the gas cooler has a significant impact on the system performance. Sakar et al 2010 presented test results showing that COP increases by 0.6 per 1 kg/min compared to the gas cooler water mass flow rate, which has a COP increase of 0.4 for 1 kg/min. The effect of gas cooler water inlet temperature is more significant as COP decreases by 0.48 for given ranges compared to the evaporator water inlet temperature where COP increases 0.43 for given ranges.

Qi et al (2013), carried out an experimental investigation on optimum gas cooler pressure while studying the effect of refrigerant outlet temperature at varying ambient temperature. It was observed that optimum gas cooler pressure varies for different ambient temperature. Results also show that the COP decreases with increasing refrigerant outlet temperature of the gas

cooler. A correlation was developed for the relation between the gas cooler outlet temperature and the optimum gas cooler pressure, the correlation showed about 5% deviation only.

Cecchinato et al 2005 carried out a comparative analysis of system performance of R134a and CO₂ hot water heat pump systems. The results showed that the CO₂ system had a better COP at perfect water stratification compared R134a system while a lower performance was recorded for perfect mixing.

2.5 Drying

Drying is an essential and energy consumption process utilized in day-to-day activities and its application can be found in residential houses and industries. It entails the removal of the water content of a substance ranging from fruits, laundry and complex industrial processes. Drying employs the circulation of dry hot air around a substance with moisture in enclosed space, thereby making it lose its moisture content and absorbed water is evaporated into the ambient. Methods for drying include natural convection, sun drying and heat pump.

Heat pump dryer is quite similar in operation to conventional heat pumps. It comprises of two loops; heat pump and air circulation loop. It consists of primary components, which includes compressor, condenser, evaporator, expansion valve, pumps and air handling unit/ drying chamber. Heat pump dryer can classified as shown in Figure 2.10 below;

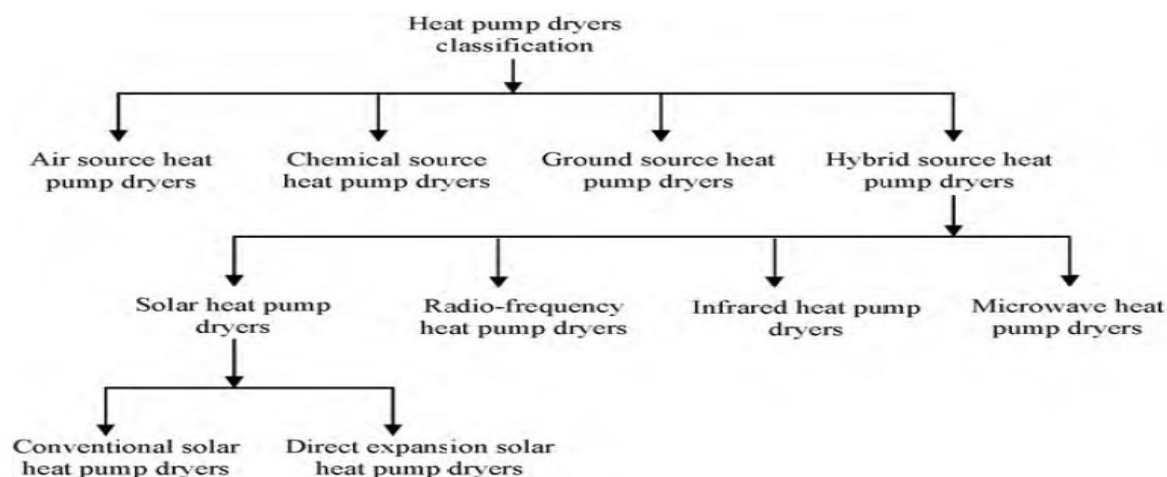


Figure 2.10: Classification of heat pump dryers (Daghigh et al, 2010)

Air source heat pump is the most common type. The circulation air is heated by the refrigerant latent heat rejection that occurs in the condenser. There are two types of air circulation namely, open loop circulation and closed loop circulation. In open loop circulation, the wet or humid air leaving the drying chamber is released into the ambient. However, in closed loop circulation the wet or humid air leaving the drying chamber is dehumidified and recirculated back into the condenser for reheating. For dehumidification of the moist air, the evaporator is used as shown in Figure 2.11. The moist air still carries enough energy to serve as heat source in evaporator. This way the system is better controlled, achieving energy efficiency unlike conventional dryer that vents the air into the ambient.

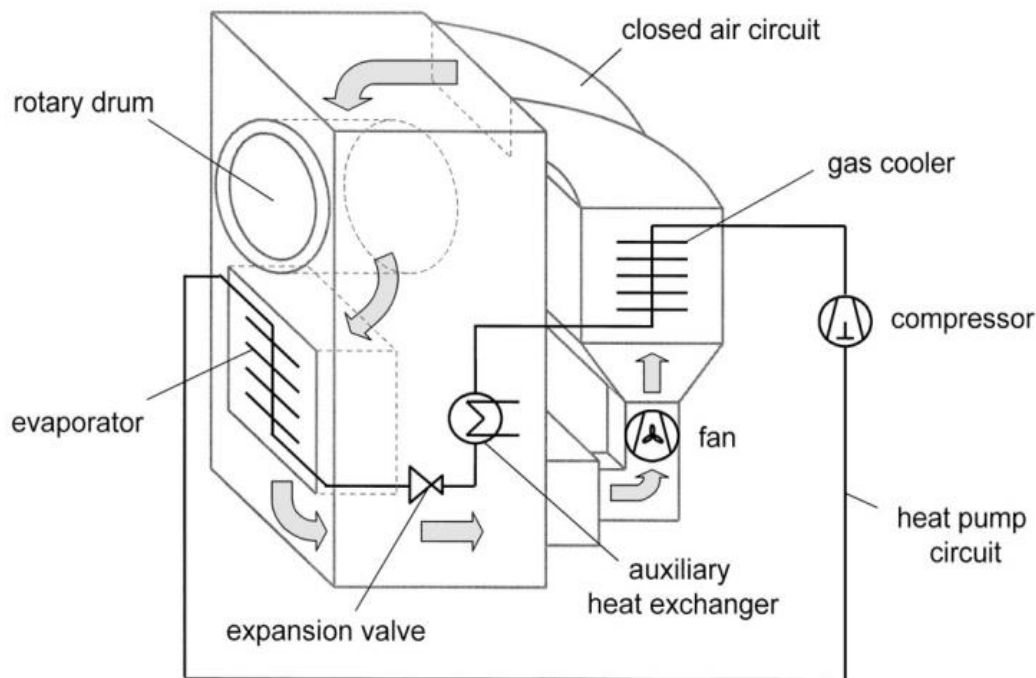


Figure 2.11: A prototype Heat pump dryer cycle (klocker et al, 2001)

Other heat sources has been discussed in section 2.1.2.....

2.5.1 Domestic Clothe dryer

Domestic Laundry application of heat pump dryer is the focus of this study. There are several factors that influences the performance of a cloth drying some of which includes type of material processing method and load bearing structure. Unlike other drying applications most of which employ continuous flow, domestic clothe employs batch processing. The structures for bearing the clothes could be a drum or a rectangular cabinet with internal drying racks. While a drying rack would provide better airflow, and prevent wear associated with the drum type, a drum container is more compact than a rack system. The drum system is most common if not the only loading structure in commercial production for residential purpose. To enhance the performance of the dryer, a spin mechanism is integrated with the drum. With this mechanism, better hot air circulation is achieved in the drum. The clothe dryer that employs this, is referred as domestic tumble clothe dryer. The different air circulation mechanism as shown in Figure 2.12. The first configuration depicts a scenario where exhaust air is vented, while the second configuration depicts the application of a dehumidifier for partial dehumidification of the exhaust air which is recirculated back into its primary process. The last configuration unlike the previous doesn't require a dehumidifier, it entails partial recirculation of the exhaust air to engender energy recovery.

Systems of Tumbler Drying

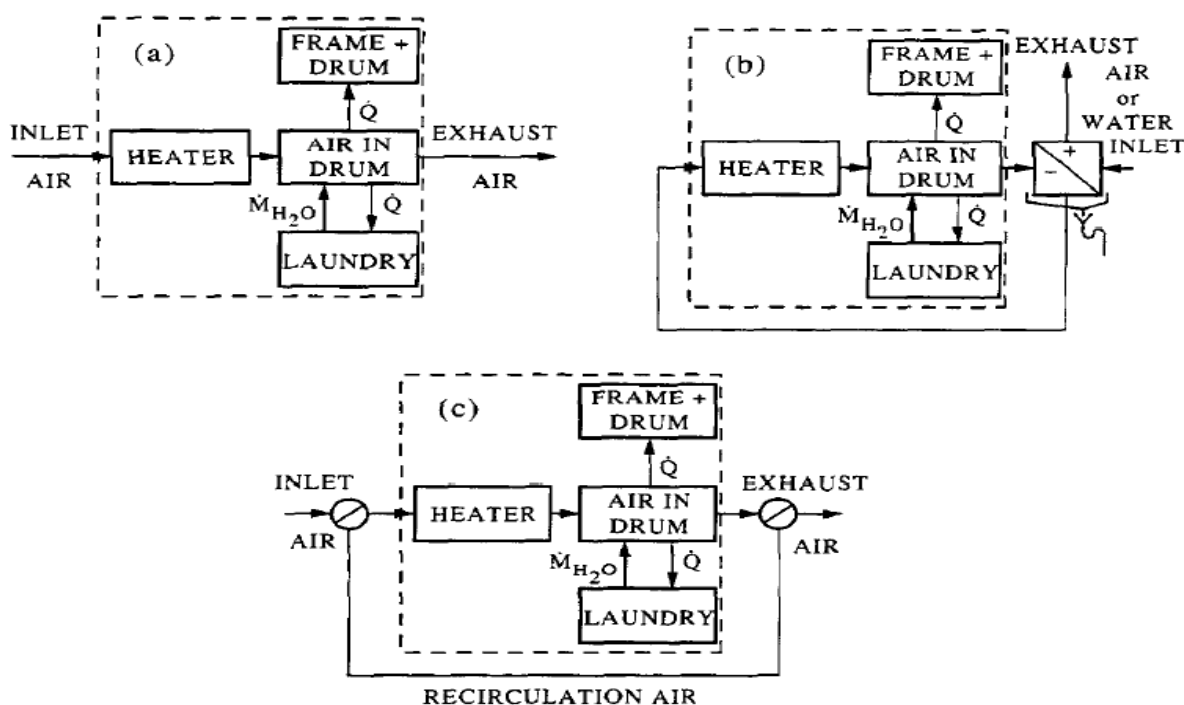


Figure 2.12: Types of tumble-drying system configurations (Conde, 1997)

The moisture absorption rate from the clothe by the dry air is influenced by the temperature and flowrate of the inlet dry air, the spin rate of the rotating drum and exhaust rate of the moist air. The heat pump condenser dryers are about 50% more energy efficient than the conventional condenser dryers. Other systems component integrations such as heat recovery heat exchangers, expanders help engender better system performance and energy efficiency.

The domestic clothe dryer are of two major types namely:

- The condenser cloth dryer
- Vented clothe dryer

The condenser dryer can be described as a cycle in which the moisture from the drying air from the exhaust of the dryer is condensed in a heat exchanger and collected. The condenser cloth dryers are of two types; electrical and heat pump depending on heat source which could either be an electric resistance element or a working fluid channeled through a condensing heat exchanger in heat pumps shown in Figure 2.13. Ambient air is heated in a condenser by a heat source. The hot dry air is fed into the drying chamber where it absorbs moisture from the clothes and become moist air which is discharged from the drying chamber. The moisture from the drying air is condensed in the evaporator, water collected and discharged. An intermediate heat exchanger might also be used for air dehumidification prior to recirculation as described in the closed loop air circulation type. The difference between the electric heater and heat exchanger in conventional condenser is their source of heat.

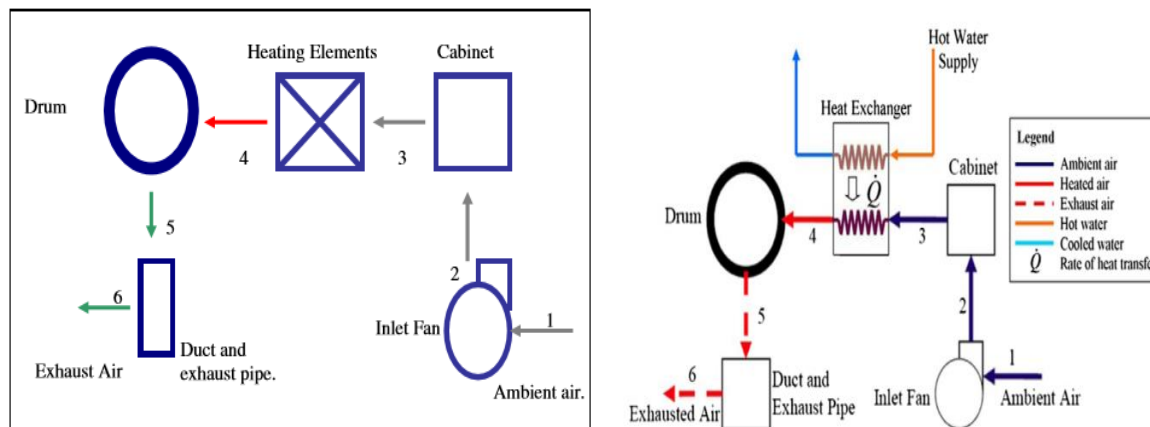


Figure 2.13: Electrical and heat exchanger types of Condenser dryer (Bansal et al., 2010)

The vented air dryers operate in a similar way as the condenser with the major difference being the condensation of the exhaust air, fresh air from ambient is heated and fed into the drying chamber and with moisture absorbed from the cloth, the moist air is vented through an exhaust. The vented air cloth dryer is quite simple in construction because of the lesser number of components required.

2.5.2 Previous studies on heat pump dryers

Previous studies on heat pump condenser type as highlighted as follows. Colak and Hepbasli (2008), carried out a review of heat pump drying, classifying the heat pumps on the type of heat source, applied products and also highlighted their respective performance indicator. Schmidt et al, conducted study on the compatibility of transcritical CO₂ process to the air dehumidification process of heat pump dryer. Comparing the performance to that of a subcritical R134a process, the CO₂ process gave a better COP offsetting its larger throttling losses with better compressor performance and heat transfer during air heating process. KloEcker et al (2002). Later designed and carried out experimental investigation of a 12kw heating capacity batch type dryer with CO₂ as the working fluid. Comparing the results of the experiments, the prototype recorded a 65% energy saving potential over a Passat type 132, which utilizes electric resistance for air heating.

The thermodynamic properties of CO₂ influenced its performance. Braun et al (2002) simulated model for both conventional air vented dryer and heat pump air cycle tumble clothe dryer using a reversed Brayton cycle, the results of which showed the impact of the air heat pump components responsible for its better performance of about 40% over a conventional air vented dryer. The significance and effect of high efficiencies of an expander, compressor and heat recovery heat exchanger effect on the MER were also established.

Ameen and Bari (2004), made a feasibility study of cloth drying using the heat rejected in split type domestic air conditioner in humid tropics. The test featured drying rates of 0.424kg/h, 0.319kg/h and 0.139kg/h for heat pump assisted dryer, commercial clothe dryer and natural indoor drying. The result of their investigation showed the air conditioner rejected heat dryer be around 77% and 30% faster than commercial dryer and natural indoor drying respectively. While the energy consumption for the commercial dryer was 1.909kWh/kg, the air conditioner rejected heat dryer has none since the heat utilized can be described to be waste for the air conditioner's operation.

Ambarita et al (2017), carried out a study on the performance of R22 heat pump dryer and residential air conditioner (RAC) for cloth drying in a designed 1m³ volume chamber. With three weights cloth ranging from 3.00 kg to 6.3 kg, the heat pump dryer had a faster drying time with an average of 1.047 kg/h than the RAC assisted dryers 0.822 kg/h. The RAC assisted dryer had only one source of energy consumption in auxiliary fan as compared to heat pumps auxiliary fan energy consumption and excess energy rejected from the condenser in form of heat, hence a better average SMER of 2.492 kg/kWh as against heat pump dryers 1.492 kg/kWh was achieved.

Deng and Han (2004), performed an experimental study of 6.4 kW cooling capacity of a split type direct expansion RAC for a 30m² room in Hong Kong. The rejected waste heat was for clothing drying in a rectangular chamber with hanging bars, the performance was better than an electrical tumble dryer for the same drying load. With an initial cloth weight of 2.98 kg, within a drying duration of 90 minutes the RAC assisted dryer achieved a dry weight of about 1.68 kg. The energy consumption of RAC assisted dryer is around 20 Wh for additional condenser fan usage as against 1569 Wh electricity consumption for the electrical tumble washing and drying.

Bansal et al (2010), designed a household heat pump clothes tumbler dryer with shorter drying times and lower moisture extractions rate than an electrically heated household tumble dryer at the same power input. The performance of the heat pump was influenced with by the mass flow rate and the temperature of water heat source in the heat exchanger. Increasing the inlet water temperature from 66 deg to 86 deg, the drying time decreases drastically by 41 minutes while the relation is not same for MER. The maximum MER was achieved at around 80 deg, above this temperature the MER decreases. This same trend is obtainable for the water mass flow rate for the dryer, with the maximum MER achieved at 0.1 kg/s.

Van Mil and Bolman 1986, postulated that a decreasing trend in hot air temperature from the start towards the end of the drying operation improves significantly the drying efficiency of clothe dryers. Lemaire et al 1987, experimentally conducted and evaluated the effect of varying drying system parameters such as inlet air temperature, recirculation rate, load ratio and drum speed to derive an optimal cost functions.

Conde (1997), reported a 20% energy recovery potential for a tumble dryer utilizing a heat recovery heat exchanger for the energy required for dry air heating with two years back time for investment cost incurred. Deans (2001), simulated a model of the total mass and energy balances for a domestic tumbler dryer evaluating the effect of fabric type, energy recovery potentials from the exhaust stream by recirculation and sensitivity of dryer's performance to operating condition. The results from the experimental validation of the simulation showed that about 63% of the energy supplied to dryer was utilized for moisture evaporation from the clothes. While sensitivity analysis inferred that mass of the cloth and power input into the dryer are main factors as SEC decreases with increasing power input and vice versa for air mass flow rate. The drying times for cotton, nylon and wool like fabric were estimated to be 147, 142, 150 minutes respectively with the power consumption following similar trend. The exhausted moist air accounted for about 16% of the energy loss thereby providing a potential avenue for energy recovery.

Bengtsson et al (2014), performed a model simulation to examine the effect of compressor cylinder volume and total heat transfer of the condenser on drying time and power consumption

of a closed type heat pump tumble dryer. The results of simulation which shows that increasing the cylinder volume of the compressor by upto 50% effects a decrease in drying by upto 14% and is validated with experimental set up.

Bansal et al (2010), carried out the modelling and experimental evaluation of water heat source for the condenser of the household tumbler dryer while also utilizing a waste heat recovery heat exchanger. The result presented a lower MER with up to 10% energy efficiency and about 10% faster drying time compared to the conventional electrical dryer. Yamankaradeniz et al (2016), carried out a performance analysis of a recirculating heat pump drier. Experimentally evaluating the impact of by-pass air ratio, the system performance factors values (SMER and COP) decrease after an optimal value of 40% of by-pass air ratio.

2.6 COMBINED SPACE COOLING AND HOT WATER HEAT PUMP

The heat pump has many advantages over a host of individual cooling and heating appliances, with the major one being its bivalent nature of operation, which combines both cooling and heating processes. One of the ways both space cooling and heating can be achieved is by integrating the individual heat pumps, which performs different operation. The return air from the evaporator of the space cooling heat pump is integrated as a heat source for the hot water heat pump using a heat recovery heat exchanger. However, these two different operations can be combined in a single heat pump unit. Residential water heating system generally require high heating capacity from the heat source. The potential of using a unitary air conditioner for simultaneous cooling and heating was reported in ASHRAE 2008 (Cooling, A.H.H., 2008).

2.6.1 Unitary air conditioner for cooling and heating

In typical unitary air conditioners for cooling process only, a desuperheater is used to perform heat rejection. However, the desuperheater is replaced with a condenser for combined cooling and water heating. This type of operating conditions offers better energy efficiency and saves space when compared with an externally air cooled condenser. A typical unitary space-cooling machine with integrated condenser coil is shown in Figure 2.13 below.

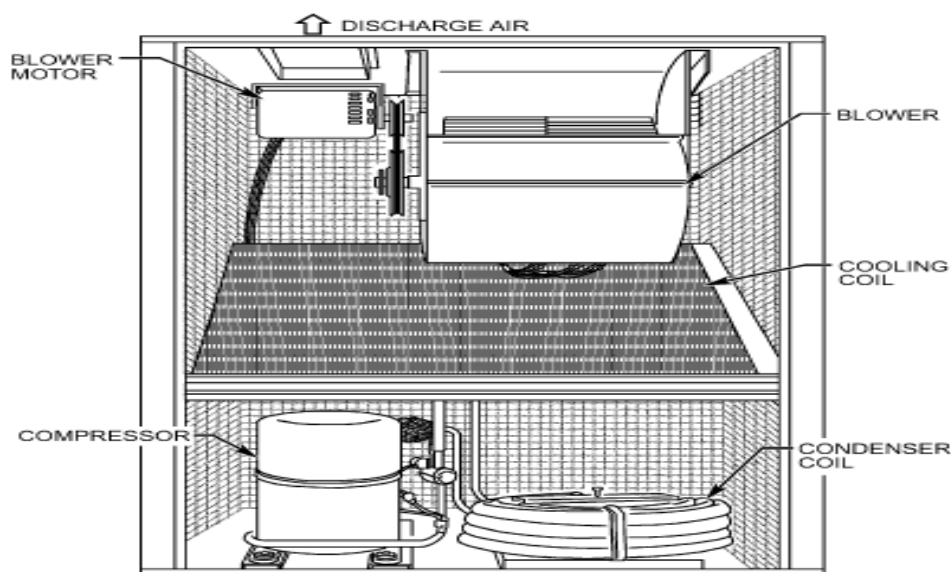


Figure 2.13: a typical unitary air conditioner (Cooling, A.H.H., 2008)

Dudley et, al. (1991) patented a variable speed heat pump for combined hot water heating and space cooling. The invention employs two condensers, water-cooled and outdoor air cooled

connected in series. Two methods for heat rejection are full condensing mode and desuperheating mode. The control mechanism of the system was such that a specified cooling load and hot water load, heat rejection is performed in the full condensing and the excess heat from the compressed refrigerant is channeled to the outdoor air condenser. At peak cooling load and low hot water demand, the desuperheating mode is activated and the outdoor air condenser carries out the bulk of the heat rejection.

Harmon and you (2007) also made an invention for space cooling and water heating. Even though the invention is similar to that of Dudley's, it employed a different control mechanism for varying load capacities. The first heat exchanger, which is water-cooled condenser, is used for water heating at a set point temperature of about 60deg. The second heat exchanger, which is air-cooled condenser, is used to achieve low return temperature of the refrigerant back to the evaporator. The water and air-cooled condensers are connected in parallel. The control mechanism with respect to the variation in the loads is such that when the hot water load is met, then a bypass valve is activated to channel the refrigerant to the outdoor air condenser thereby bypassing the water cooler condenser.

2.6.2 Previous studies on combined air conditioning and water heating

Ritcher et al (2003) presented the first experimental air-to-air CO₂ combined heat pump. Matching its cooling capacity with that of a commercially available R410A heat pump at operating indoor and outdoor temperatures of 26.5°C and 35° respectively. Even though the CO₂ system's performance resulted in a lesser heating COP compared to the referenced R410a system, but performed better at lower outdoor temperatures.

Ji et al (2003) incorporated a water heater to the outdoor unit of a split type air conditioner. Test campaigns were carried out and the results showed that a higher COP of 4.02 was recorded for the dual operation as against 2.91 for air conditioning purpose alone. Techarungpaisan et al (2007) simulated a steady state model of a split type air conditioner with integrated water heater. The results of the simulation was validated with experimental campaigns.

Bryne et al (2009) carried out a comparative system performance. The design and simulation of a heat pump for simultaneous heating and cooling using R407C and CO₂ as refrigerant. While results showed that R407C had higher first law COP and second law efficiency compared to the CO₂ in both heating with ambient temperature range of -15°C to 15°C and dual mode with ambient temperature of 20°C, the CO₂ had higher first law COP and second law efficiency at cooling mode with ambient of 25°C.

CHAPTER 3. THEORETICAL ANALYSIS

3.1 CO₂ as a Working Fluid

The choice of working fluid in refrigeration cycles is guided by the properties it possess. Hence, the importance of refrigerant properties cannot be overemphasized. These attributes helps to determine the system design parameters for a refrigeration system. When compared with other refrigerants, CO₂ possess numerous advantages. Some of the general properties of CO₂ compared with other refrigerants are highlighted in Table 2.1 below. CO₂ properties can further be subdivided and discussed under the following categories:

- i. Physical properties
- ii. Thermodynamic properties
- iii. Transport properties
- iv. Safety

Table 3.1: Comparison of CO₂ properties with other refrigerants (Belman-folres et al, 2014)

Numerical assignment	Boiling point, K (at 0.1MPa)	Critical temperature, K	Critical pressure, MPa	Volumetric heat capacity, kJ/m ³	Density, Kg/m ³ (at 20°C and 0.1MPa)	Safety group	ODW/GWP
R-134a	246.85	374.2	4.12	2868	4.336	1	0/1 300
R-290	231	369.8	4.31	3907	1.865	2	0/3
R-744(CO ₂)	194.6	304.1	7.38	22545	1.839	1	0/1
R-22	232.4	369.1	4.98	4356	3.651	1	0.05/1 700
R-717	239.8	406.1	11.42	4382	0.716	2	0/0
R-410A	325.85	343.3	4.85	6753	3.062	1	0/1 740
R-407C	229.35	359.2	4.70	4029	3.639	1	0/1 610

1. Security group: negligible toxicity, non-flammable.
2. Safety group: toxic, flammable, or both

3.1.1 Physical properties

Carbon dioxide is a colorless, odorless gas. The triple point of carbon dioxide is about 5.11bar at -56.6C and it exists in three phases namely solid, liquid and gas at this thermodynamic condition. The critical point of CO₂ is 73.8 bar at 31.1C and at this state where CO₂ cease to exist in two phase. At temperatures and pressures above the critical point, CO₂ assumes a super critical state of supercritical fluid. Supercritical CO₂ exhibits both the characteristics of liquid and gas at this condition. Refrigeration cycle's operation above this point is known as super-critical, while subcritical is achieved below this point. In situations as it is common that refrigeration cycles are designed to operate both in supercritical and subcritical conditions, such a cycle is referred to trans- critical. Carbon dioxide cannot exist in liquid state at pressures below 1 bar and -78.5C and this boundary is defined as sublimation point. CO₂ is available and abundant in nature. At standard conditions it is about 1.67 times denser than air. It is soluble in water, in ethanol and in acetone.

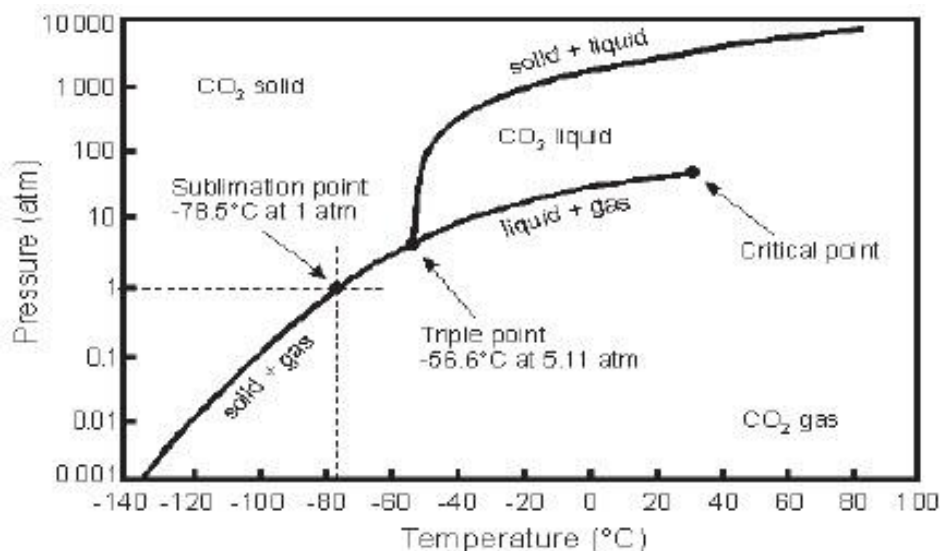


Figure 3.1: Physical properties of CO₂ (globalccsinstitute)

3.1.2 Thermodynamics Properties

These are the properties that describes the relationship of temperature and heat with energy and work with regards to the performance of the system. Other properties aside the physical properties that defines CO₂ as a refrigerant includes the normal boiling point, boiling point curve, molecular weight, volumetric refrigeration capacity. CO₂ has low critical temperature, high triple point pressure and high operating pressures. It has a low critical temperature compared to other conventional refrigerants. With a critical temperature of 31.1 C, the practical upper level for condensation is 28C. CO₂ has a high triple point pressure of 5.18 bar and below this pressure, CO₂ solidifies. This is can also be a disadvantage as this limits the suction pressure and corresponding evaporation temperature. The suction temperature is limited between the ranges of -32C to -53C, even though it provides some benefits of maintaining a positive pressure within these temperature ranges.

Although the high pressure comes with challenge of special system design requirement at high temperatures, however a higher pressure is beneficial for low side operation (Taylor, 2002). High operating pressure also results in high specific volumetric capacity, low need for stroke volume in the compressor and within pressure ranges of 30 to 120 bar, higher compressor efficiency is achieved due to low compressor pressure ratios (Nekså et al, 2010). CO₂ also has a low Dt/Dp over a given saturation range. This helps increase the efficiency of CO₂ systems.

3.1.3 Transport properties

The transport properties describes the heat transfer potentials and pressure drop of a working fluid in refrigeration systems. They include density, specific heat capacity, viscosity, surface tension and thermal conductivity. With a density of 1.98 kg/m³, carbon dioxide is a denser gas than air. The density of the refrigerant influences pressure drop throughout the refrigeration cycle and the compressor capacity. Density of CO₂ varies rapidly with temperature near the critical point and has a low density ratio compared to other refrigerants. With a high vapor density, high volumetric refrigeration capacity (VRC) is obtained. CO₂ possess better characteristics than most HFCs and other conventional refrigerants, however NH₃ possess better characteristics to CO₂. However, CO₂ possess low viscosity compared to NH₃ which is

quite beneficial (Lorentzen and Pettersen, 1993). In the liquid phase, CO₂ has low viscosity and surface tension compared to other refrigerants. The negative impact of high viscosity and surface tension is that it promotes pressure drop and hence leads to reduction in system capacity. Low viscosity promotes heat transfer by increasing velocity of fluid flow (Kim et al, 2004).

Surface tension property of refrigerants influences nucleate boiling and two-phase flow characteristics. Heat transfer is negatively affected by nucleate boiling due to superheating and formation of vapor bubbles. Hence, a small surface tension is required for effective heat transfer due to low nucleate boiling. CO₂ has a low surface tension compared to other refrigerants within the same evaporation temperature range (Kim et al, 2004). CO₂ has relatively high thermal conductivity and high specific heat capacity. These properties helps engender high and efficient heat transfer.

3.1.4 Safety

The safety of refrigerants is discussed in terms of ozone depletion potentials (ODP) and global warming potential (GWP). ODP is a phenomenon that describes the relative amount of degradation a substance it can cause to ozone layer while GWP describes the amount a gas contributes to global warming. Unlike HFCs, CO₂ has no ozone depletion potential and global warming potential of 1. This gives a relative advantage over HFCs and other conventional refrigerants. More also, CO₂ does not contribute to smog formation.

3.2 MAIN CHARACTERISTICS OF CO₂ HEAT PUMPS

The major components are evaporator, compressor, gas coolers, throttling device. The processes involved in heat pump operations are characterized as highlighted below:

- Isobaric
- Non-adiabatic
- Isobaric
- Isothermal

CO₂ refrigeration systems have two operation characteristics which is usually described by the region where heat release occurs in the normal boiling curve as shown in the Figure 2.2 below. This defines the type of refrigeration cycle in operation. There are two types of cycle that can be described based on these characteristics namely:

- i. Subcritical cycle
- ii. Trans-critical cycle

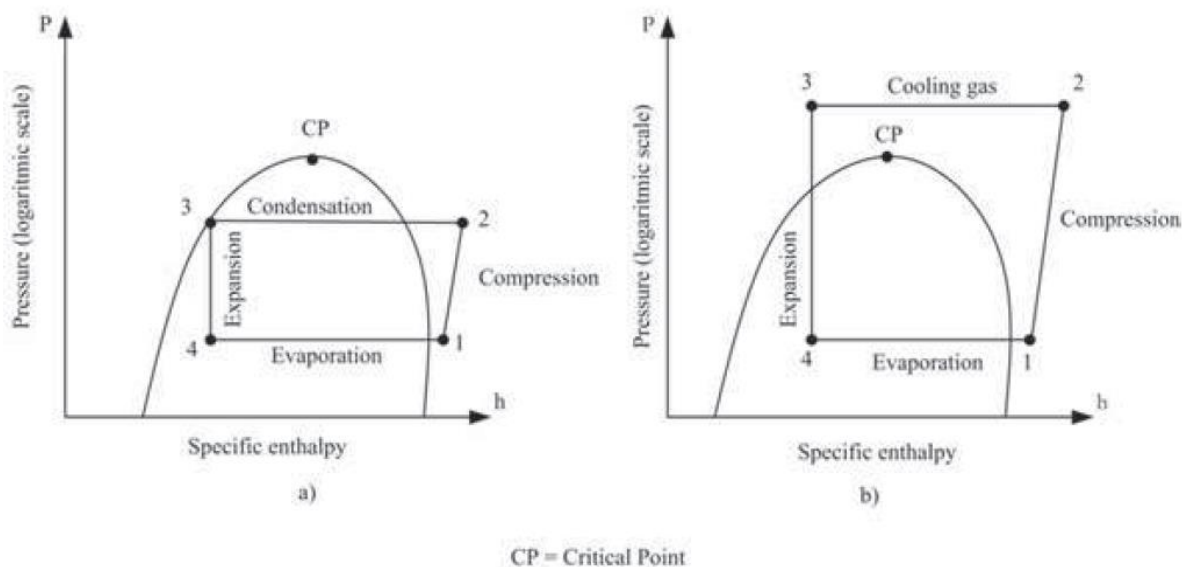


Figure 3.2: Subcritical and Transcritical cycle (Belman-folres et al, 2014)

As seen from the Log P-h diagram, when the region of heat release is below the critical point (critical pressure), the cycle is described as subcritical cycle while heat release above the critical point is known as transcritical cycle.

In Subcritical cycle, heat absorption occurs by evaporation of the refrigerant at low pressure, and heat rejection takes place by condensing the high pressure refrigerant both below critical point. There is transformation of the refrigerant from its two phase to saturated vapor state in evaporator and from superheated vapor to two phase. Some degree of superheat is required before compression. However, use of CO₂ in a subcritical cycle is confined within some boundary limits. Its operability is limited within temperature range of minimum -55°C for evaporation and a maximum 30°C with corresponding pressures below critical pressure of 73.8. CO₂ can be used as a secondary fluid as well as in cascade fluid. A typical example of this is a CO₂-NH₃ cascade refrigeration (Belman-folres et al, 2014). However, most CO₂ heat pump operates in transcritical cycle unlike conventional heat pumps which operates in subcritical cycle. The CO₂ transcritical process can hence be described by Lorentzen cycle as against Carnot cycle used in conventional heat pumps.

3.3 LORENTZ CYCLE

Lorentzen introduced the application of CO₂ for air conditioning, which was utilized car. The Lorentzen cycle has some distinct components from the conventional cycle, which include the positioning of the receiver after the evaporator and the introduction of intermediate heat exchanger for superheating and sub-cooling.

The positioning of the receiver enables the sufficient supply of CO₂ while also mitigating against the flooding of the compressor, which could result in liquid slugging by retaining the liquid fraction of the refrigerant at the exit of the evaporator. It also helps to moderate refrigerant supply depending on the variations in the system's capacity or operations. The intermediate heat exchanger is able to sub-cool the refrigerant at gas cooler and reduce the large expansion loss associated with CO₂ systems. The superheating at the suction line of the compressor ensures complete vaporization of the refrigerant. Sub-cooling and superheating

increases the cooling capacity. During sub-cooling, the state of the refrigerant is shifted from point b to c as seen on the p-h diagram in Figure 3.3. The liquid fraction of the refrigerant also increases at the evaporator inlet which enhances better evaporator performance. On this superheating side, this is achieved by shifting the state of the refrigerant, which is saturated or flooded at point e to superheated state f. Even though superheating decreases the density of the refrigerant and could influence the cooling effect negatively, it is however increases the discharge temperature of the compressor. The higher the discharge temperature of the refrigerant, the higher the potentials of matching it with high hot water return temperatures demand. The enthalpy difference between the evaporator outlet to compressor suction is equal to the amount of enthalpy difference for sub-cooling in the internal heat exchanger.

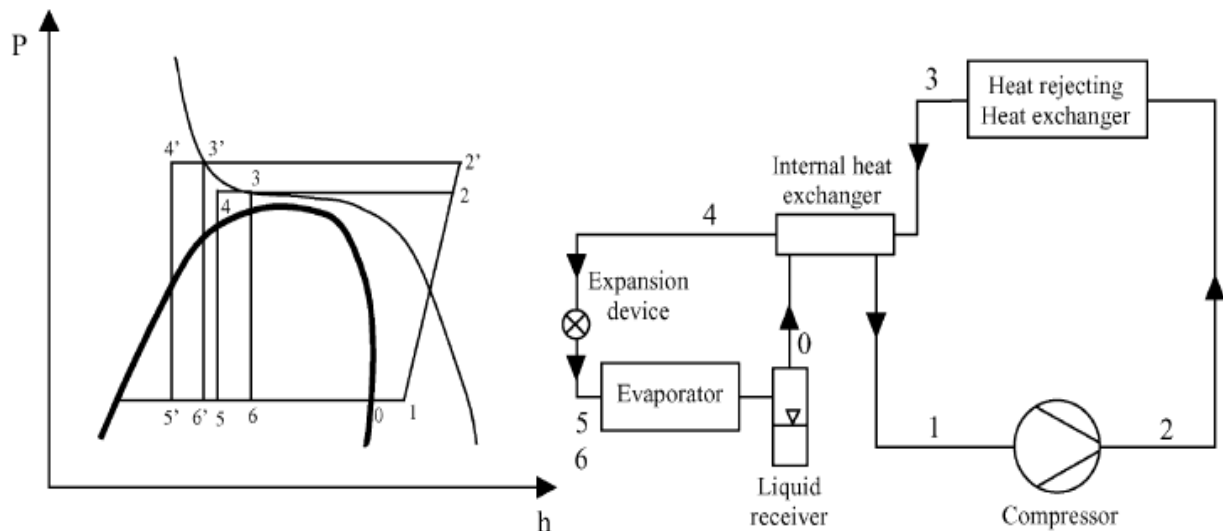


Figure 3.3: Process flow of transcritical CO₂ cycle and the corresponding t-s diagram

In a transcritical cycle, an evaporator still serves the heat absorption function, but heat rejection occurs through sensible cooling in gas cooler and not through condensation at high pressure within the supercritical region. The pressure ratio is higher in transcritical cycle compared to subcritical cycle and this is due to its high pressure and is often accompanied with large expansion loss. The superheated vapor is compressed to deliver high temperature. Energy consumption in transcritical systems is relatively low in cold climates or season, while efficiency is reduced in hot climates or season. The distinctions between the processes in transcritical Lorentz cycle and conventional cycles are highlighted in Table 3.2

Table 3.2: Comparison of Lorentz cycle to a conventional heat pump cycle

Lorentz cycle	Conventional
Irreversible non-adiabatic compression	Isentropic compression
Non-isobaric, non-isothermal heat rejection	Isobaric heat rejection
Non isenthalpic expansion	Isenthalpic expansion
Non-isobaric, non-isothermal heat absorption	Isobaric heat absorption

With the assumption of no loss in the heat pump cycle, the performance of a conventional system, which absorbs and reject heat at constant temperatures during cooling and heating processes, is often defined by Carnot COP as:

$$COP_{carnot,heating} = \frac{T_{room}}{T_{room} - T_{amb}} \quad \text{Equation 3.1}$$

$$COP_{carnot,cooling} = \frac{T_{room}}{T_{amb}-T_{room}} \quad \text{Equation 3.2}$$

The efficiency of a Carnot cycle is defined as the ratio of the real COP of the heat pump systems. It compares the actual performance of a heat pump to that of an ideal Carnot process with cycle losses taken into consideration and it is represented as;

$$\eta_{carnot} = \frac{COP_{actual}}{COP_{carnot}} \quad \text{Equation 3.3}$$

For a transcritical process, while heat absorption takes place at constant evaporation temperature, the heat rejection takes place at gliding temperature. Hence, the performance of the cycle is better defined by Lorentz coefficient of performance ($COP_{lorentz}$) as proposed by Neskå. It expressed using the state points as shown below:

$$COP_{lorentz,heating} = \frac{T_2-T_3}{(T_2-T_3)-(T_0)*\ln(T_2/T_3)} \quad \text{Equation 3.5}$$

$$COP_{lorentz,cooling} = \frac{(T_0)*\ln(T_2/T_3)}{(T_2-T_3)-(T_0)*\ln(T_2/T_3)} \quad \text{Equation 3.6}$$

Where,

$$T_0 = \left(\frac{T_1-T_4}{\ln(T_1/T_4)} \right) \quad \text{Equation 3.7}$$

The practical transcritical process can be relatively compared to the ideal process using Lorentz cycle efficiency, defined as;

$$\eta_{lorentz} = \frac{COP_{actual}}{COP_{lorentz}} \quad \text{Equation 3.8}$$

3.3.1 Performance indicators

3.3.1.1 Coefficient of performance

Coefficient of performance of a heat pump is a parameter that indicates the efficiency of a heat pump. It evaluates the amount power required to generate the cooling/heating capacity from the system. It is the basics for most comparisons of different heat pump's performance. The $COP_{cooling}$ is the ratio of the cooling effect generated by the evaporator to the amount of power input from the compressor while the $COP_{heating}$ is the ratio of the useful heat generated from the gas cooler to the compressor power input. It is expressed as follows:

$$COP_{cooling} = \frac{Q_{evap}}{W_{comp}} \quad \text{Equation 3.9}$$

$$COP_{heating} = \frac{Q_{gc}}{W_{comp}} \quad \text{Equation 3.10}$$

For integrated heat pumps where both the cooling and the heating effect of the heat pump is harnessed, a combined COP is used to evaluate the performance of the system and it is defined as shown below.

$$COP_{combined} = COP_{cooling} + COP_{heating} \quad \text{Equation 3.11}$$

3.3.1.2 Volumetric cooling and heating capacity

Volumetric cooling capacity (VCC) is the volumetric amount of heat removed from a space due to the ability of the refrigerant to absorb the heat in the evaporator. The heat removed is usually carried by a secondary fluid. It is defined as the product of the gas density of the refrigerant and specific enthalpy of evaporation (enthalpy difference at the inlet and outlet of the evaporator).

$$VCC = \rho \cdot (h_1 - h_4) \quad \text{Equation 3.12}$$

While volumetric heating capacity (VHC) can be defined as the volumetric amount of heat the gas cooler is able to dissipate from the gas cooler and supplied to a secondary fluid. It is defined as the product of refrigerant density and specific enthalpy of condensation (enthalpy difference between the inlet and the outlet of the gas cooler).

$$VHC = \rho \cdot (h_2 - h_3) \quad \text{Equation 3.13}$$

3.3.2 Sensitivity analysis

There are several system parameters in trans-critical CO₂ process that influences performance. To properly evaluate and enumerate their influence, a sensitivity analysis was carried out. Some of the parameters considered includes the following. A combined COP was also evaluated for concurrent operation of cooling and hot water heating.

- Optimum gas cooler pressure
- Gas cooler outlet temperature
- Evaporation temperature
- Refrigerant mass flow rate
- Water mass flow rate
- Amount of superheat
- Temperature approach

3.3.2.1 Effect of optimum gas cooler pressure

The optimum gas cooler pressure is the optimum gas cooler pressure with the highest COP. The cooling and heating capacity of the heat pump increases with the increasing gas cooler pressure and the COP also increases. The compressor work also increases but not so rapidly when compared to the cooling and heating capacity. At some point, the compressor work input increases more rapidly than the cooling and heating capacity with increasing pressure and this affects the COP negatively.

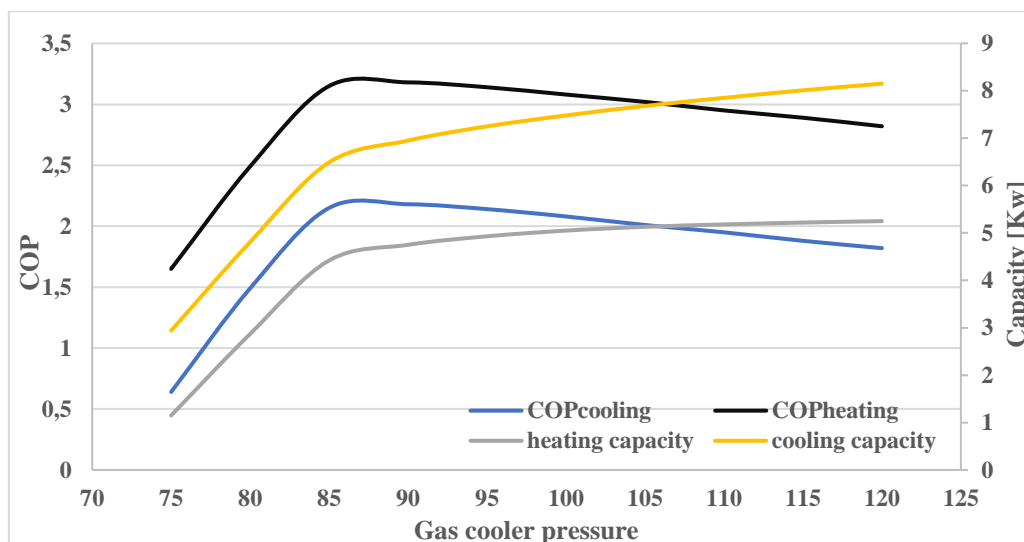


Figure 3.4: Coefficient of performance in relation to the gas cooler pressure.

As seen in Figure 3.4 above, the gas cooler outlet and outlet temperature were set at 35 and 0.15 respectively. A 5K temperature was estimated between CO₂ and the secondary fluid used as heat sink. The highest COP of about 3.20 was achieved at a gas cooler pressure between 85 and 90 bar. With a maximum gas cooler pressure of 120 bar, the cooling and heating capacity of 5.25 and 8.15 kW was obtained respectively. The cause for the rapid increase in the compressor work input is due to the drop in the isentropic efficiency above the optimum gas cooler pressure.

3.3.2.2 Effect of gas cooler outlet temperature

The outlet gas cooler temperature is an important parameter when designing heat pump systems for water heating. The water inlet temperature and the temperature approach often determine it. A small pinch is usually envisaged. A low gas cooler temperature increases the capacity of the heat exchangers. The gliding temperature of CO₂ gives an advantage for good temperature match between the refrigerant and the process stream. The effect of varying gas cooler outlet temperature is analyzed for both heating and cooling capacities as shown in Figure 3.5. At different evaporation temperatures, ranging from -5 to 10°C and an optimum gas cooler pressure of 90 bar, the gas cooler temperature was varied between 30 and 35°C.

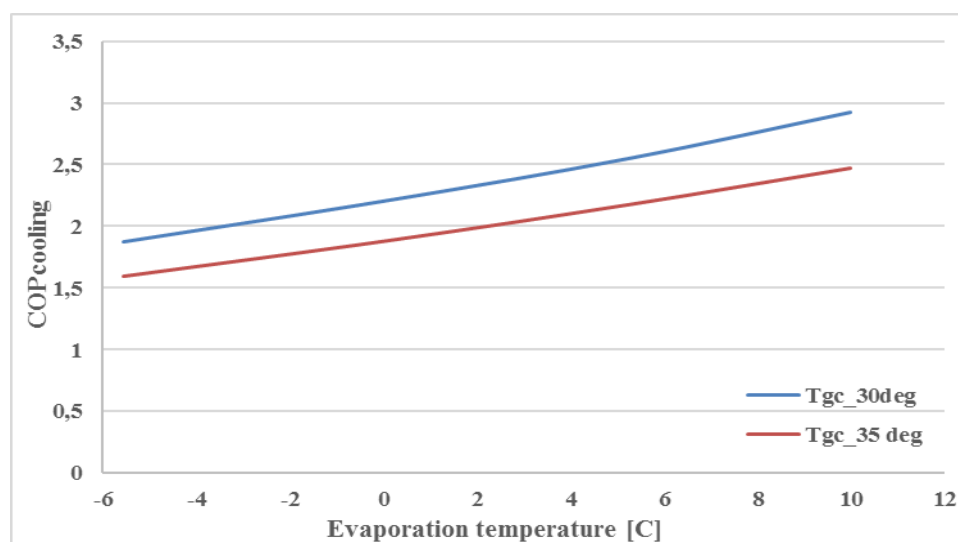


Figure 3.5: Coefficient of performance in relation to the gas cooler outlet temperature

As observed, the coefficient of performance for the cooling process increases with increasing evaporation. A high gas cooler exit temperature also enhances a better evaporator performance.

3.3.2.3 Effect of Evaporation temperature

The effect of evaporation temperature on the cooling capacity is analyzed. The evaporation temperature is varied with gas cooler pressure with a fixed gas cooler outlet temperature of 20C and is rated with COP_{cooling}.

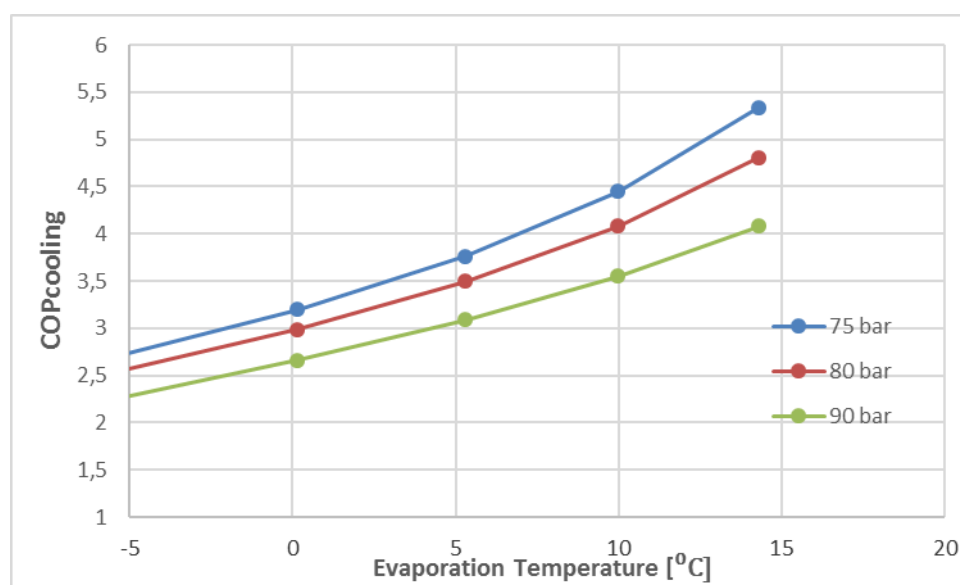


Figure 3.6: Coefficient of performance for different evaporation temperatures

A similar trend can be observed for the three gas cooler pressures, the COP_{cooling} increases with increasing evaporation temperature as shown in Figure 3.6. At a specific pressure, increasing the evaporation temperature leads to reduction in the compressor pressure ratio. The optimum COP_{cooling} was obtained at lower gas cooler pressure. The reduction in the COP with increasing pressure is due to the increase in throttling loss and reduction in the cooling capacity. The cooling capacity increases more rapidly than the required compressor power.

3.3.2.4 Effect of Refrigerant and water mass flow rate

Although the mass flow rate of the refrigerant in a transcritical cycle is not an independent variable as it depends on the parameters listed above. In an increase in refrigerant mass flow rate leads to increase in the system's heating and cooling capacity and vice versa. Increased refrigerant mass flow rate engenders higher heat transfer coefficients in both in the gas cooler and evaporator and also a higher COP. Superheating the refrigerant at suction lowers the mass flow rate and leads to reduction in delivered capacity due to decrease in its density at the suction. An increase in the gas cooler pressure also leads to decrease in the refrigerant mass flow rate.

The mass flow rate of water as heat sink is also an important parameter. Increasing the mass flow rate of water leads to increase in heating capacity in the gas cooler due to increase in the waterside heat transfer coefficients although this might impact negative on the water temperature at the outlet of the gas cooler by decreasing it.

3.3.2.5 Effect of superheat

As highlighted in Lorentzen work, the impact of internal heat exchanger on the performance of gas cooler was validated. The effect of superheat at the evaporator and suction of compressor. At a gas cooler pressure of 80 bar, a gas cooler outlet temperature of 35C at the refrigerant side. Increasing the amount of superheat increases the refrigerant temperature at compressor discharge line as seen in Figure 3.6.

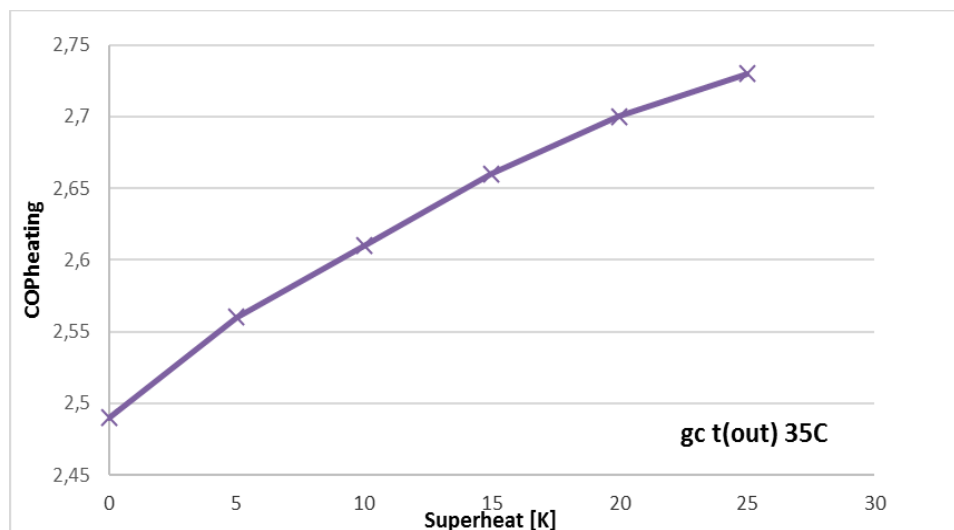


Figure 3.6: Effect of superheat on coefficient of performance

The discharge enthalpy consequently increases, causing an increase in the driving force due to increase in the temperature range. The first 5K superheat gave an increase of about 2.8% of COPheating and this decreases subsequently with each 5K increase. A maximum COPheating increase of about 10% was obtained for the overall superheat range (0-25) K. Apart from its influence on discharge temperature, the specific volume also increases.

3.3.2.6 Temperature Approach

Temperature approach of both the primary and the secondary fluid is an important parameter in system design as it is a determining driving force for heat transfer. Lower temperature approach enhances better heat transfer, increased heating/cooling capacity and high COP.

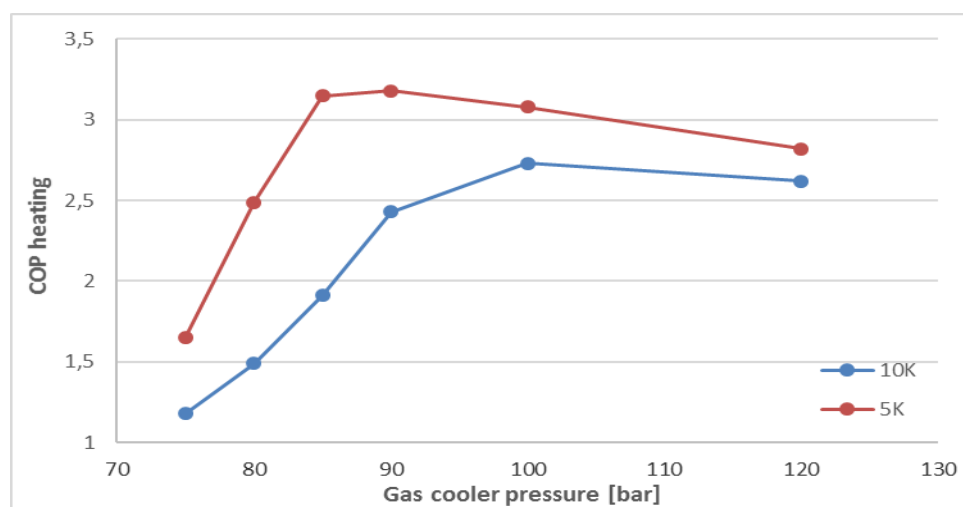


Figure 3.7: Impact of temperature approach on system performance

With an assumed water inlet temperature of 30C, two different temperature approach of 5 and 10K between the refrigerant and water which resulted in gas cooler outlet temperatures of 35 and 40C respectively as shown in Figure 3.7. The lower temperature approach of 5K showed higher COPheating compared to the 10K approach across a wide range of gas cooler pressure. At a maximum gas cooler pressure, both approaches showed similar trend of decreasing COP. A similar trend is expected for the COPcooling. Plate heat exchangers have potentials of achieving lower temperature approaches.

3.3.2 Space Cooling

Space cooling is required due to heat gains in residential buildings, which leads to increase in temperature and humidity often way-off the comfort zone. The sources of these heat sources can be either internal or external and can be in form of sensible or latent heat. Internal heat gains have their sources ranging from lightings, equipment and activities of the occupants. External heat gains infers the heat gain indoor of a building with the source being external. The major source of external heat gain is solar radiation. Its mode of penetration includes infiltration, through the walls, roofs, door and Glass.

Quantitatively, the amount of heat removed from space is equal to the amount of cooling provided by the air conditioning equipment. The amount of cooling required in space is dependent on the outdoor temperature in a specified climate. An example of this relationship is given in Table xxx below;

Table 3.3: Cooling load by region

Climate (city)	Peak Outdoor temperature	Peak Cooling load
Trondheim	32°C	2.73 kW
Milan	28°C	1.5 kW
Niamey	37°C	3.45 kW

For a set point indoor temperature, increase in outdoor temperature results in increased required cooling load. While also increasing the set point indoor temperature leads to reduction in cooling load required.

3.3.2.1 Performance indicator for space cooling

To determine the energy efficiency of a space-cooling heat pump, a terminology known as Seasonal energy efficiency ratio (SEER) is defined. SEER is the ratio of the total cooling load provided by the heat pump in a cooling season to the total energy input within the same season. A high SEER depicts a high efficiency. The instantaneous energy efficiency of the system can also be established by energy efficiency ratio (EER) which is defined as the ratio cooling capacity of the system to the energy input into the system. While SEER covers different temperature ranges, EER covers an individual indoor and outdoor temperature. SEER and EER can be related to the COP of a system using the following equations 3.14 and 3.15.

$$SEER = \frac{EER}{0.87} \quad \text{Equation 3.14}$$

$$EER = 3.413 \times COP \quad \text{Equation 3.15}$$

3.3.2.2 Include influence of air mass flow rate

The mass flow rate of air into the conditioned space is also an important parameter to consider in design and control of space cooling systems. Its impact can be either positive or negative. Increasing the mass flow rate of air a preset temperature condition increases the cooling

capacity of the evaporator while decreasing the mass flow rate does otherwise. The speed of the fan is to be adjusted to meet the desired operating conditions.

3.4 WATER HEATING

Hot water demand in residential homes are usually expressed as a function of the number of dwellers and the required supply temperature and tapping temperature. Using a regression model of the effect of number of occupants on consumption developed by Defra (2008), the daily volumetric hot water consumption can be expressed as follows:

$$V_{hotwater} = 40 + 28N \quad \text{Equation 3.16}$$

Where N is the number of occupants (maximum of 5)

For a residential building with four individual, the volumetric hot water consumption using the equation above can be estimated as 152 liters per day. Typical hot water temperature at different tapping sites are listed in the table 3.4 below:

Table 3.4: Applications and temperature ranges for hot water

Application	Temperature, °C
Safety showers and eyewashes	16 to 35
Hot service without mixing valves	40
Nursing homes and hospitals	40 to 46
General purpose	49 to 60
Laundry service	71
Kitchen sanitization	82

Residential energy consumption from hot water usage vary from home to home which depends on the volume and the temperature of the water at the tapping sites. However, it can be classified using the different tapping profiles according to the EU energy labelling scheme shown in Appendix xxx. Matching the heating capacity of the gas cooler with sample profiles (M&L), a hot water-drying load ratio can be estimated as shown in Figure 3.8. When the hot water demand is met, the remaining heat capacity is channeled into clothe drying.

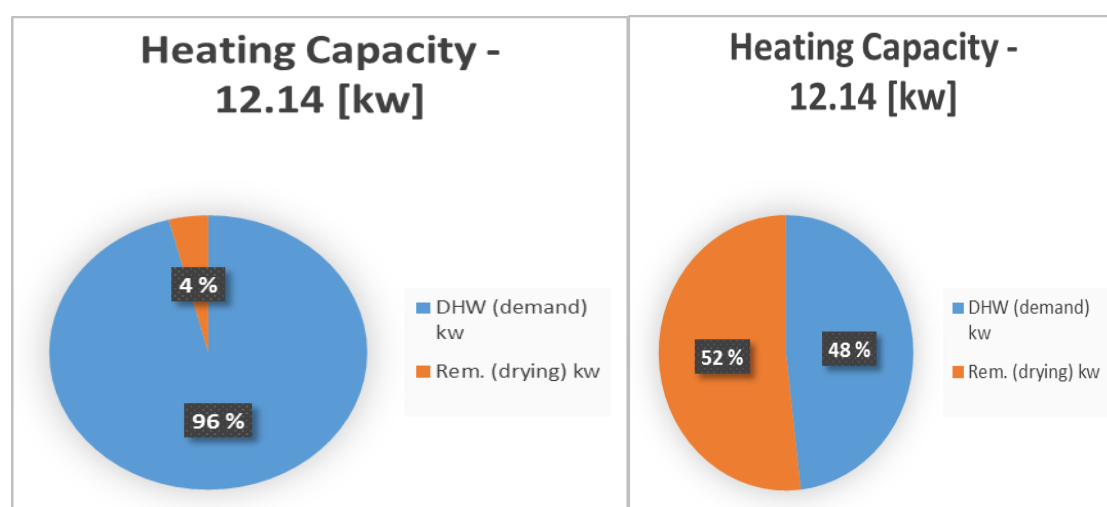


Figure 3.8: A pictorial representation of heat capacity distribution

Another important parameter to be considered in the water heating process is the storage. The process of feeding the storage tank with hot water is known as Charging. It is time dependent operation, which is referred to as charging period and it represents the amount of time taken to meet the energy demand for a specified volume of hot water consumption. The energy demand is equal to the amount of hot water load met by the heating capacity of the gas cooler. The charging period of a hot water storage can be expressed using equation 3.17:

$$\tau = \frac{V_{hotwater} \cdot \rho \cdot C_p \cdot (T_{tank} - T_{cold,in})}{Q_{gc}} \quad \text{Equation 3.17}$$

Where $V_{hotwater}$, ρ , C_p represents volume of hot water, density of water and specific heat capacity respectively. The temperatures of the water inlet and in the tank are represented as T_{tank} , $T_{cold,in}$ respectively.

With the set point temperature of hot water been achieved at the outlet of the gas cooler and the mass flow rate ratio set accordingly for the hot water storage and air heating, the heated water is fed into the storage. The charging of the thermal storage is dependent on the mass flow rate of the hot water to the storage, heating capacity of the gas cooler, the fluid properties of water, volume of storage tank, temperatures of water at inlet and outlet of gas cooler.

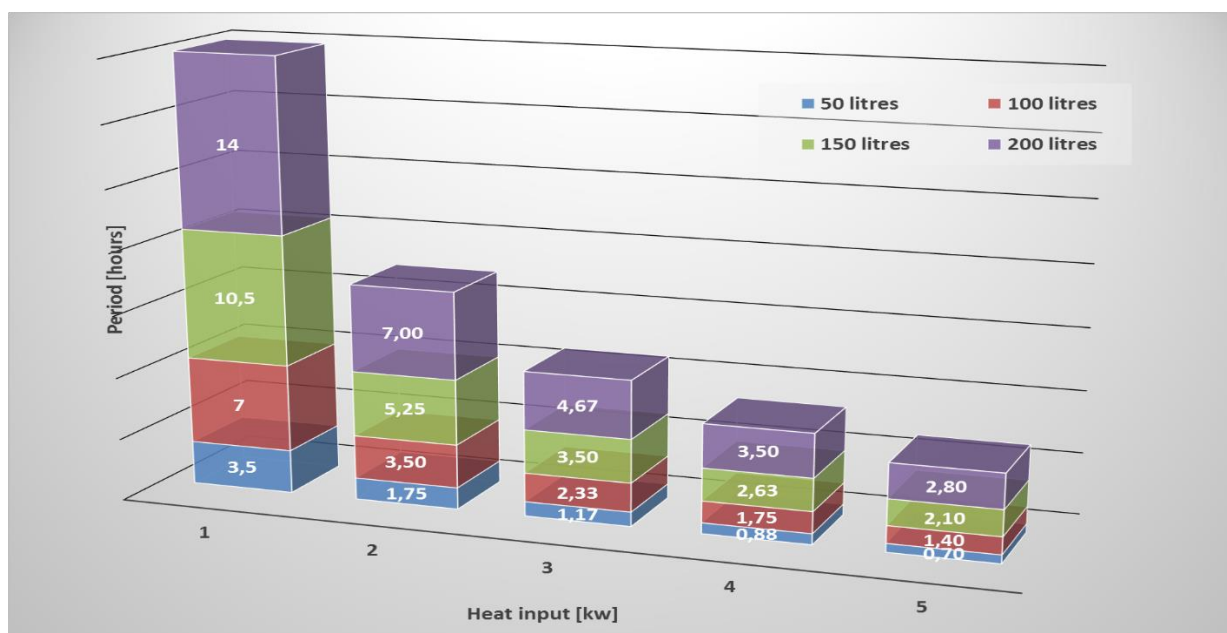


Figure 3.9: A plot of heat input versus charging period

As observed in Figure 3.9, For a heating capacities ranging from 1 to 5 kW and storage volume range of 50 to 200 liters, the water inlet temperature of 10°C and supply temperature of 70°C were assumed. Large storage volumes contribute to longer charging period while higher heating capacity results in lower charging period. At hot water storage of the same volume, doubling the heat capacity results in double charging period.

As with every thermal storage system, hot water systems are also subjected to heat loss. These losses can either be within between the storage tank, piping system and ambient. The heat loss between the tank and ambient is determined using equation 3.18.

$$Q_{loss} = \frac{Surface.Area_{tank} \cdot (T_{tank,in} - T_{ambient})}{R} \quad \text{Equation 3.18}$$

3.5 DRYING CYCLE

3.5.1 Air drying cycle

The air-drying cycle is different cycle from the heat pump cycle. Even though integrated to be known as heat pump dryer, unlike the conventional heat pump cycle, it takes into consideration the humidity alongside the temperature. Air-drying process for clothes typically operates at standard atmospheric pressure which is relatively constant throughout the process. The air-drying cycle under review utilizes a closed loop circulation. Even though the air circulation and heat absorption is similar for both CO₂ and HFCs heat pumps, however its performance is influenced by that of the heat pump cycle. The air-drying cycle is often represented in psychometric and mollier diagrams. An h-x diagram of the drying air cycle is shown in Figure 3.10 below.

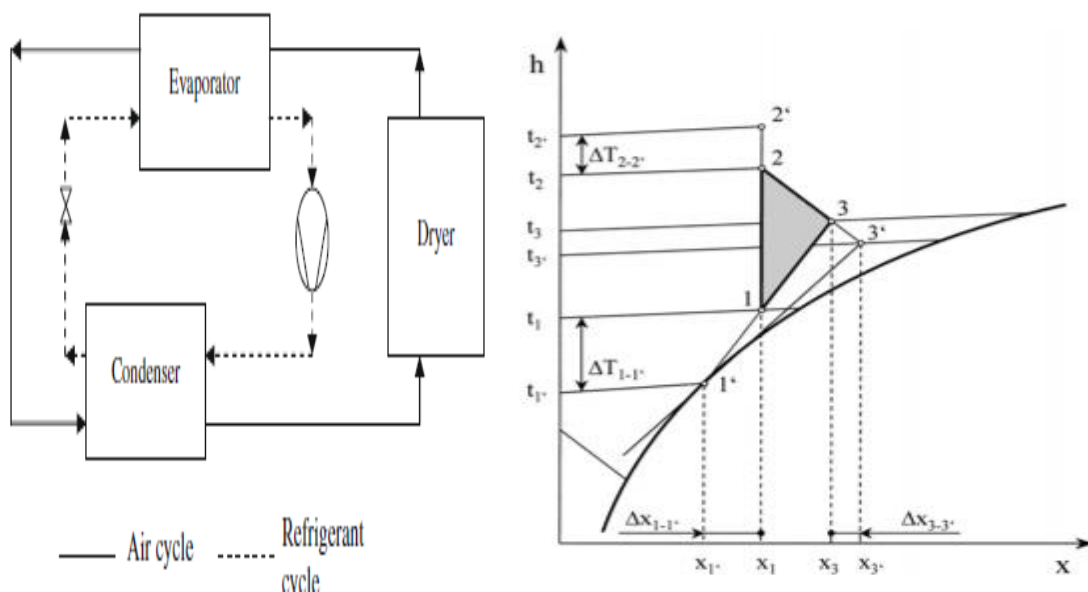


Figure 3.10: A drying process with corresponding h-x diagram (Klockner et al, 2000)

There are three main processes involved in the air drying cycle namely;

- Process 1-2 : heating of the air in condenser or gas cooler, as it the case for CO₂ heat pumps
- Process 2-3: adiabatic humidification of the drying air by cloth moisture in the drying chamber
- Process 3-1: dehumidification and condensation of absorbed moisture from the drying air.

The drying air enters absorbs heat from heat source medium, which is usually the heat sink side of the heat pump cycle at a constant absolute humidity and its temperature rises from t to t_2 . Its relative humidity is high at condenser inlet and low at the condenser outlet. The hot dry air at t_2 fed into the drying chamber evaporates moistures from the clothes and the drying air moisture content from x_2 to x_3 . The drying air which is now moist, exits the drum humidified at high humidity and low temperature t_3 . The moisture content, which is condensed in an evaporator as the temperature is reduced from t_3 to t_1 are removed through an exhaust. A t-h diagram of drying cycle in a CO₂ and R134a heat pump is depicted in Figure 3.11 below.

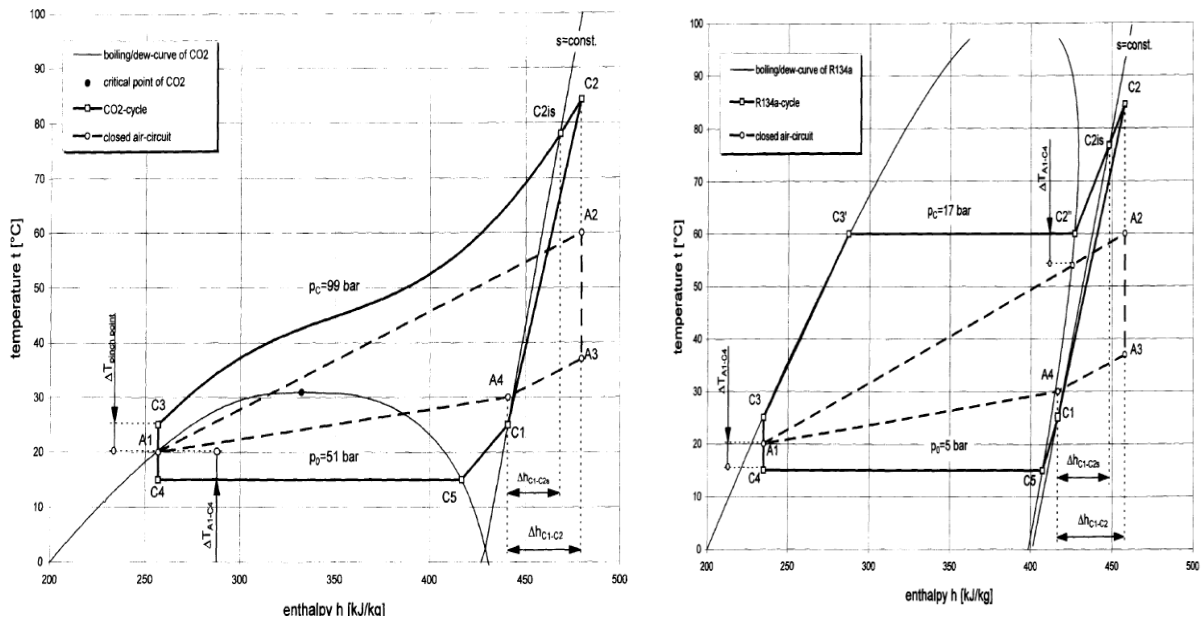


Figure 3.11: A temperature- enthalpy diagram of CO2 and R134a cycle (Schmidt et al, 1998)

At a high drying air inlet temperature and lower humidity, the drying rate is faster due higher heat content and more moisture is evaporated from clothes. The gliding temperature of CO2 provides a better temperature match between it and the air as compared to that R134a. A good temperature match is needed for effective heat transfer. Hence, more exergy losses accompanies the air heating process in the R134a cycle compared to that of the CO2 cycle.

3.5.2 Performance indicators for drying processes

Performance indicators are tools for measuring how efficient the system operates and enable to make comparative systems under the same operating conditions. The performance of air-drying cycle is evaluated using the following parameters:

- Coefficient of performance (COP)
- Specific moisture extraction rate (SMER)
- Specific energy consumption

3.5.2.1 Coefficient of performance (COP)

Coefficient of performance of a drying system is a parameter used to evaluate the proportion of heat output harnessed for air heating from the condenser/gas-cooler to the total power input. It represents how close the performance of the cycle is to an ideal cycle. It is represented in equation 3.19.

$$COP_{heating} = \frac{Q_{gc}}{P_{tot}} \quad \text{Equation 3.19}$$

The amount of heat delivered by the condenser or gas cooler for air heating can be evaluated using the expression below;

$$Q_{gc} = \dot{m}_{CO2} * (h_2 - h_3) \quad \text{Equation 3.20}$$

The total power input into the heat pump for the drying process include the power requirement for compressor, fans and pumps.

$$P_{tot} = P_{comp} + P_{fan} + P_{pump} \quad \text{Equation 3.21}$$

For this study, only the power required by the compressor to deliver the required amount heat for drying the air at high temperature. Hence, the COP of the heat pump is utilized. It can also be described using the enthalpy variations in the heat pump cycle as highlighted in a previous section. The power required for the rotational operation of the drum is also not considered. The implication of high COP is low relative running cost.

3.5.2.2 Specific moisture extraction rate (SMER)

The specific moisture extraction rate (SMER) is a performance parameter that describes the performance of both the heat pump and the drying chamber. It is the ratio of the amount of water evaporated from the cloth to the amount of energy consumed by the heat pump system. It describes the degree of performance of the system in converting the available energy to useful work. Considering only the compressor work, SMER is represented by the expression below:

$$SMER_{cp} = \left(\frac{x_{A1} - x_{A3}}{h_{r1} - h_{r2}} \right) * \frac{\dot{m}_A}{\dot{m}_r} \quad \text{Equation 3.22}$$

Where $\left(\frac{\dot{m}_A}{\dot{m}_r} \right)$ is the mass flow ratio of air to the refrigerant, which is derived from energy balance and is expressed in the equation 3.23 below;

$$\dot{m}_A \cdot (h_{A2} - h_{A1}) = \dot{m}_r \cdot (h_{r2} - h_{r3}) \quad \text{Equation 3.23}$$

$$\frac{\dot{m}_A}{\dot{m}_r} = \frac{h_{r2} - h_{r3}}{h_{A2} - h_{A1}} \quad \text{Equation 3.24}$$

Previous reports suggested heat pump dryers to have SMER values to be within the range of 1.0 to 4.0 as compared to 0.72 to 1.2 range, 0.12 to 1.28 range for vacuum drying and hot air drying respectively. However, higher SMER are obtainable for heat pump dryers. A high SMER also signifies a low running cost and faster drying time.

3.5.2.3 Specific energy consumption (SEC)

Specific energy consumption is a parameter used to define the amount of energy used to remove a specified amount of water. Typical energy consuming equipment include compressor, fan and pumps. It is the reciprocal of the specific moisture extraction rate. If only the power input to the compressor is considered, SEC can be expressed as follows:

$$SEC_{cp} = \frac{1}{SMER_{cp}} \quad \text{Equation 3.25}$$

$$SEC_{cp} = \frac{1}{\left(\frac{x_{A1} - x_{A3}}{h_{r1} - h_{r2}} \right) * \frac{\dot{m}_A}{\dot{m}_r}} \quad \text{Equation 3.26}$$

Where subscript cp represents the compressor

A high SEC implies high-energy requirement and high running cost will be incurred for the heat pump dryer. When used comparatively, a system with low SEC is more energy efficient.

3.3.2.4 Drying Efficiency

Drying efficiency is phenomenon that describes the ratio of energy used to evaporate moisture from the cloth to the total energy consumed. It can be evaluated using the temperature values at specified nodes in the dryer to evaluate its performance. It signifies the deviation of the real

drying process from the best possible process in terms of energy consumption. It can be expressed as follows:

$$\eta_d = \left(\frac{T_{d,in} - T_{d,out}}{T_{d,in} - T_{d,sat}} \right) \quad \text{Equation 3.27}$$

Heat pump dryers can have drying efficiency up to about 95% as compared to a maximum of 40% and 60% for hot air and vacuum drying respectively. Although, this is not the most accurate way to measure the performance of the dryer and gives the reason for the introduction of SMER.

3.6 SYSTEM DESIGNS

The system design for the Solar assisted integrated CO₂ heat pumps first considered the alternative integration of the solar appliance to a heat pump system. Different ways by which this can be achieved includes solar energy as power source, energy source for heat pump evaporator, heat source for water heating. Solar energy can be harnessed in photovoltaic cells and with the aid of an inverter, it used to power the compressor of the heat pump. This offsets the electrical input from the electricity grid and also the cost of electricity. A battery system is put in place to save excess power during low solar exposure period. The only disadvantage of this is that such configuration is that the initial investment cost can be very high.

The alternative use is its application as solar evaporator in the low pressure side to be able to deliver large heat capacity at the high pressure side. For cooling operations, the solar evaporator serves as a secondary heat source to the primary air evaporator which is designed to meet a specified cooling load. Depending on the system variables, the cooling capacity is rationed between the air heat source and solar source. However, the system will experience low heating capacity and productivity during periods of low solar irradiation.

The last design explored involves the integration of the solar collector with heat rejection side of the heat pump. The heating load is supplemented by the heating capacity provided by the solar collector. The water is first preheated in the solar collector at low temperatures and then reheated in the brazed plate heat exchanger. An intermediate gas cooler is used for air heating process. With thermal storage included, a continuous solar collector is not required and this take care of the problem low solar radiation might pose. The mass flow rate of water is adjusted to match the heating capacity. This design is considered appropriate for reasons to be highlighted in the next subsection.

3.6.1 Possible Solar-Gas cooler Configurations

There are different ways the solar collector can be integrated with the high-pressure side of the heat pump. The reason for this integration is supplement the heating capacity of the gas cooler and enable it meet the required heating load. A few possible configurations as shown in Figure 3.21 are discussed as follows.

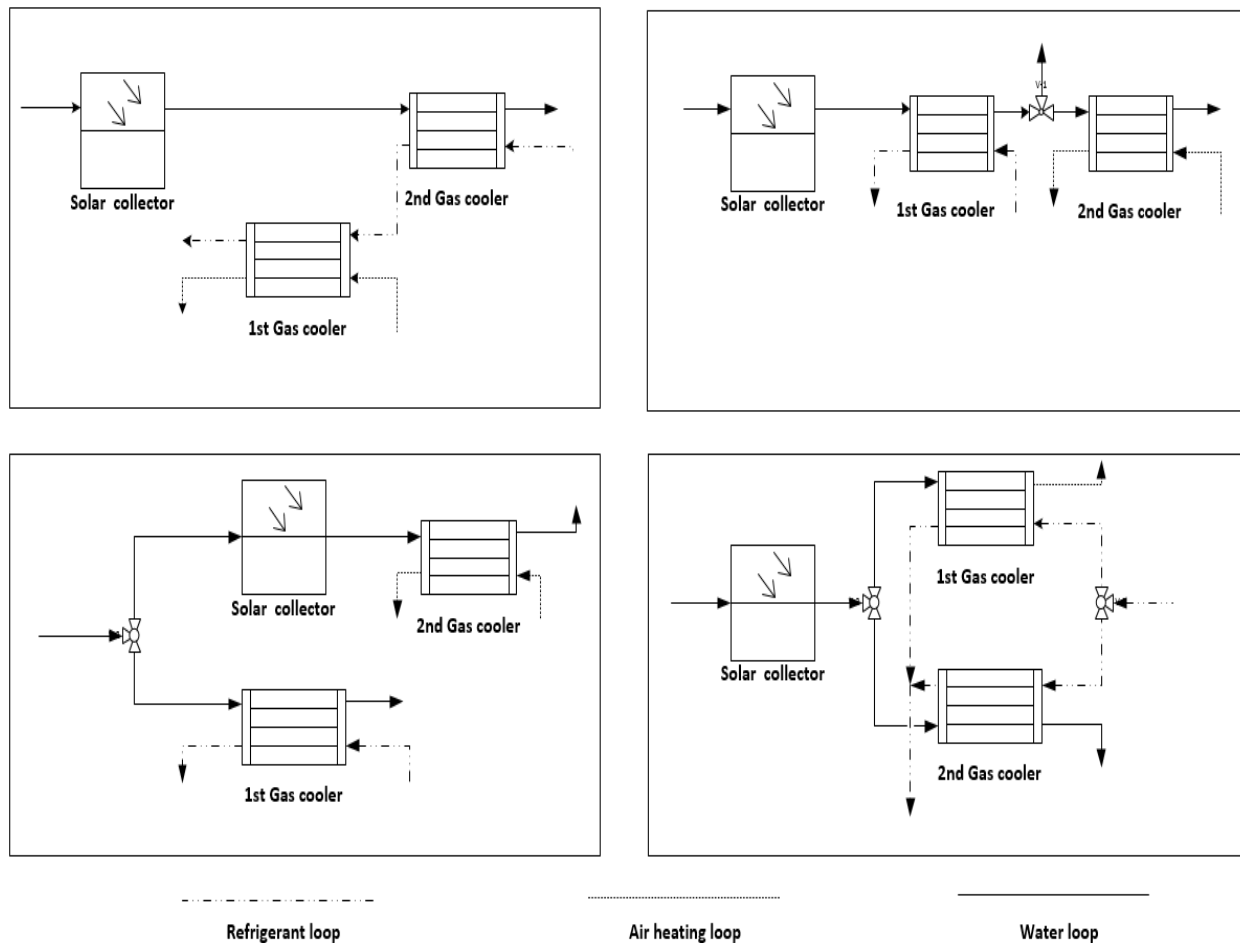


Figure 3.12: Solar collector integrations to the gas coolers

In the first configuration, the solar collector is in series with the second gas coolers. The solar collector preheats the water, the first gas cooler is used for clothe drying and the second gas cooler is used to reheat the water. The ratio of the hot water load distribution is based on the amount of load requirement fulfilled by the solar collector. The heat capacity ratio between the first and the second gas cooler is dependent on the priority and control capacity is dependent on the flow rates of the secondary. The air and water exit the gas coolers at different temperatures. The disadvantage of this configuration is that it is not appropriate for secondary fluids to be supplied at same temperature (high). This configuration results in low temperature of refrigerant at the outlet of the first gas cooler which consequently results low temperature of the secondary fluid temperature.

For the Second configuration, the solar collector is connected in series with a single gas cooler. Water, which is the secondary fluid, is first heated in the solar collector and the rest of the load is met in the main gas cooler of the heat pump. To adapt this configuration to air heating application, the main gas cooler supplies both the thermal storage and an intermediate heat exchanger connected for air heating. This supply is made using a three-way valve at the outlet of the main gas cooler. This way, the secondary fluid is able to supply the same temperature (high) for simultaneous water and air heating. Depending on the load ratio for the different applications, the three-way valve regulates the mass flow rates of the secondary fluid respectively. The collector and the main gas coolers should have geometry large enough to handle the volumetric flow rate of the secondary fluid for efficient performance.

In third configuration, the solar collector is connected in parallel with a single gas cooler. The solar collector provides the heating capacity required for the air heating process while the gas cooler is used to provide the water heating capacity. Water is considered to be the best fit fluid for both the solar collector and gas cooler. Using a water loop in the solar collector against using direct air supply is due to higher thermal conductivity of water compared to air. The major advantage of this system is that the operations of the gas cooler and the solar collector are not related and as such, the processes can be controlled independently. The constraint of this configuration is that the hot air load is limited by the heating capacity provided by the solar collector and this capacity is always delivered at low temperature. A low air temperature for drying will result in longer drying time. The gas cooler covers the hot water load for thermal storage.

Fourth configuration describes the integration of the solar collector in series with the two gas coolers. The gas coolers are connected in parallel. This type of configuration favors the use of only one secondary fluid and enables the capacity variation of the gas coolers. The secondary is first heated in the solar collector and then the flow at the exit is split in to the two gas coolers for further heating. The refrigerant flow at the discharge line of the compressor is also split in two gas cooler. The mass flow rate ratio is the capacity control mechanism of the gas coolers, which is dependent on the heat load requirements. High temperatures are obtainable for the secondary fluid for simultaneous water and air heating. Using water as a secondary fluid, an extra heat exchanger is needed for the air heating process.

3.6.2 Possible solar-evaporator configurations

In this system design, it is desired that some solar energy is integrated with the low pressure side of the heat pump. Since the air evaporator is constrained by the cooling load, an extra heat source is needed to also be able to deliver hot water and drying simultaneously. As it is with the gas coolers, there are also a couple of possible integration configuration as highlighted below.

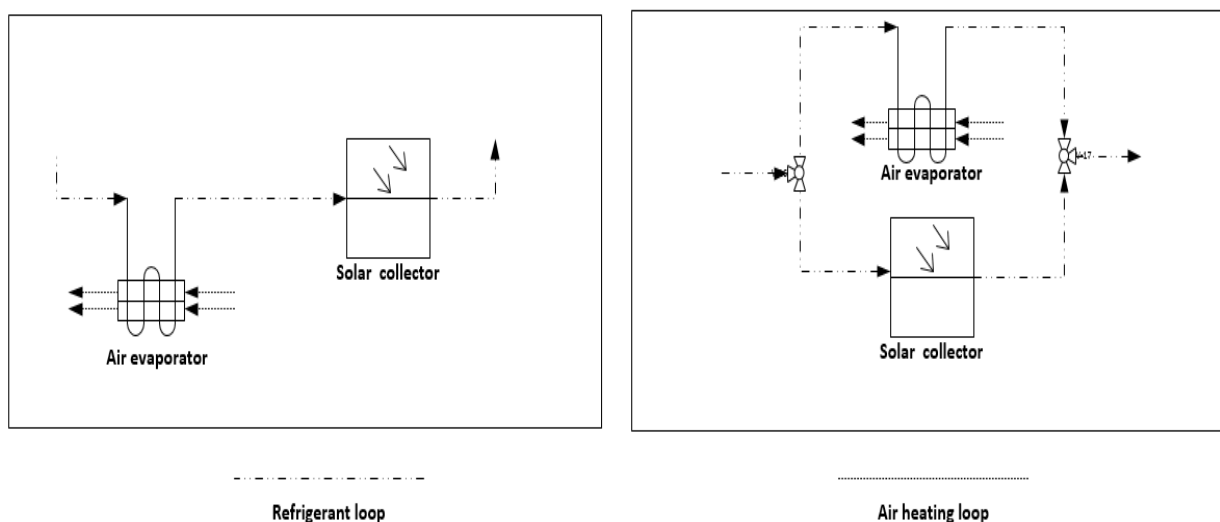


Figure 3.13: Solar collector integrations to the evaporators

In the first configuration, the solar collector is integrated in series with the air evaporator. There is only one possible positioning for the solar collector (evaporator) is after the air evaporator and outlet of the collector is directly connected to the compressor suction line. Having the solar collector before the air evaporator will cause operation problems due to negative temperature profile, as the solar collector absorbs heat at temperature higher than ambient. The refrigerant

is first heated in the air evaporator to meet the cooling load. The refrigerant thereafter absorbs the heat from solar collector. This might create operational problems while trying to meet the both the cooling load and heating load at the same time. The operating conditions of the solar collector is dependent on the performance of the air evaporator. There is possible temperature cross if the same flow rate, which delivered the heating capacity at the high-pressure side, is allowed through both the air evaporator and solar collector consecutively in situations where there is low solar insolation.

In the second configuration, the solar collector is integrated in parallel in parallel with the air evaporator. The refrigerant flow out of the gas cooler is split into two. The separate flows are fed into the air evaporator and the solar collector. With separate flows, the two components are independent of each other and capacity control can be carried out independently.

The final system design showing the integration of solar collector with both the low and high-pressure side of the heat pump is shown in Figure 3.14.

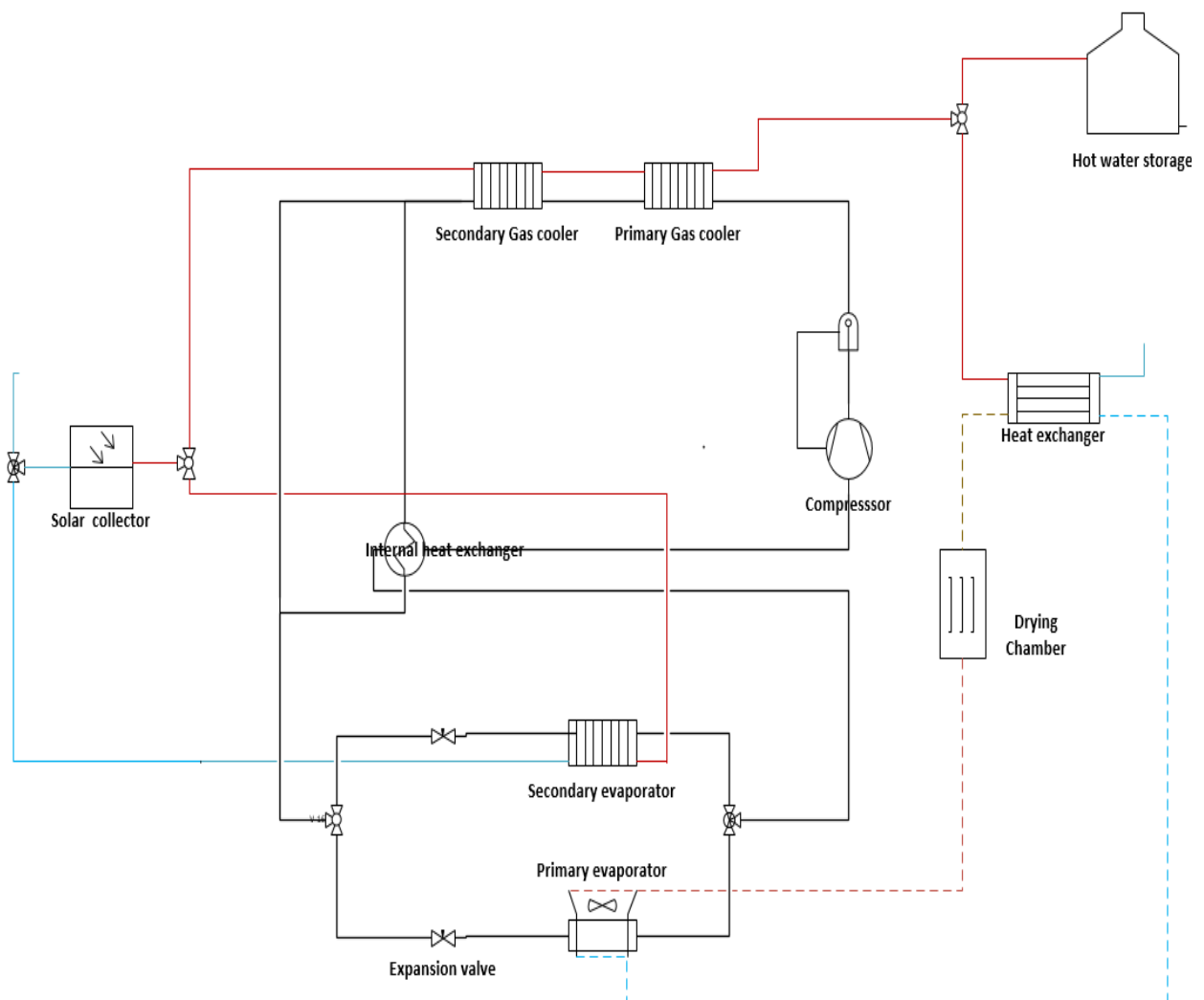


Figure 3.14: Layout of proposed integrated heat pump system

3.6.3 System performance

Consider the a real performance assessment of the heat rejecting side of the heat pump at different outlet temperature of the hot water while also meeting a specified cooling load at the low-pressure side. This is expressed using temperature-enthalpy (t-h) diagram. In this analysis, it is assumed that the solar collector pre-heats the water to a temperature within close proximity of that ambient air. The temperature of the fluid used in solar absorption is usually 5-10K above the ambient, but since this also depends on the efficiency of the collector and the properties of the fluid used, it is safe to make this assumption. At a water pre-heated to 28°C by the solar collector and a water outlet temperature of 60°C from the gas cooler and an assumed minimum temperature approach of 2K between the inflowing water and counter current refrigerant. A (t-h) diagram of the water heating process is presented accordingly in Figure 3.15.

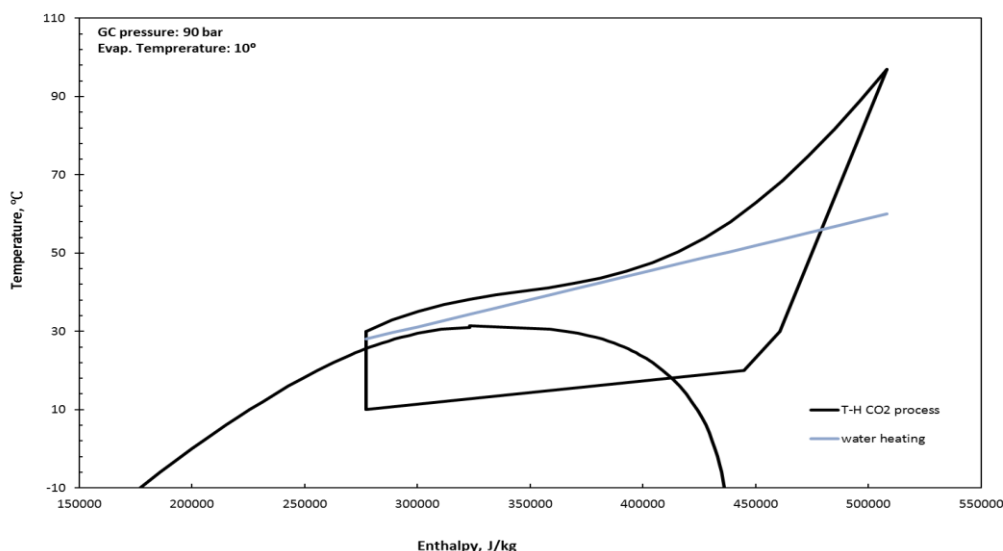


Figure 3.15: A temperature- enthalpy diagram of the heat rejection process in CO2 process

The pinch can be seen to occur at the point where the S-shape of the CO2 cycle sway back towards the linear hot water line. The pinch is influenced is inlet and outlet temperatures of both the primary and secondary fluids. A lower inlet water temperature gives larger pinch while higher outlet water temperature results in a smaller pinch point.

Considering variation of system parameters, the performance of the water heating gas cooler is evaluated. The gas cooler pressure was increased from 85 to 95 bar while also varying the outlet temperature of CO2 and inlet temperature of the water into gas cooler using the combinations 30/28°C, 28/25°C and 25/20°C.

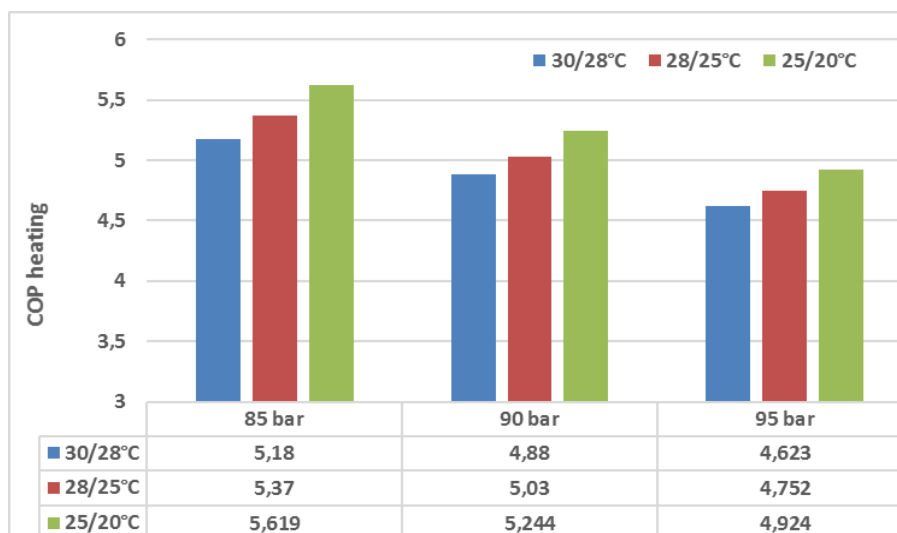


Figure 3.16: Coefficient of performance in relation to the gas cooler temperature approach

The COP heating of the gas cooler of 5.18 decreases to 4.623 by varying the gas cooler pressure from 85 to 95 bar at 30/28^oC combination temperatures. A similar trend is observed for the other temperature combinations. However, the COP heating increases with decreasing temperature combinations across an increasing gas cooler pressure.

Heating water for drying process in some cases can be constrained by the kind of clothing material to be dried. This in turn gives rise to heating the drying air at low temperature to avoid shrinkage of the cloth. The impact of this is considered for the same heating capacity delivered by the heat pump at the same operating. The outlet temperature of water in the gas cooler is set at 40^oC for the same gas cooler pressure range and temperature combinations. It can be seen clearly from the results as presented in Figure 3.17 that the in order for the water as heat sink to accommodate the potential heating capacity from the gas cooler of the heat pump, its operating parameters has to change. Therefore results shows that to achieve a lower exit temperature of the water heat sink out of the gas cooler, the flow rate of the water has to be increased.

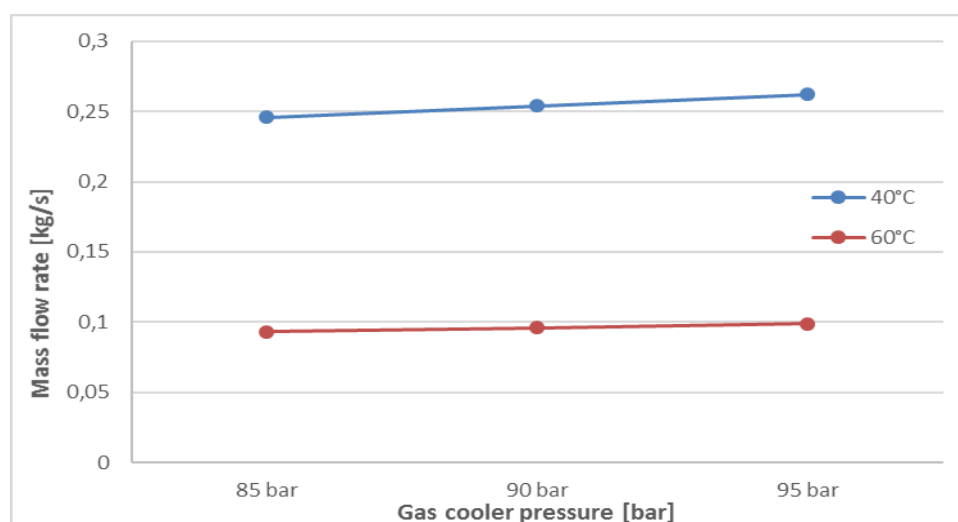


Figure 3.17: Variation of the mass flow rate with exit temperature

CHAPTER 4. EXPERIMENTAL METHODS AND TEST FACILITY

4.1 TEST FACILITY

The experimental facility used for this study was a previously constructed test rig for ejector experiments. The rig was modified to meet the configuration options discussed previous section. The ejectors were replaced with two expansion valves, one needle valve and a pneumatic valve. The pneumatic valve was not easy to control so it was set on the PID to operate at pressure above the operating high side pressure and this makes it in active. The rest of the components were kept as they are and a simplified process flow is presented in Figure 4.1.

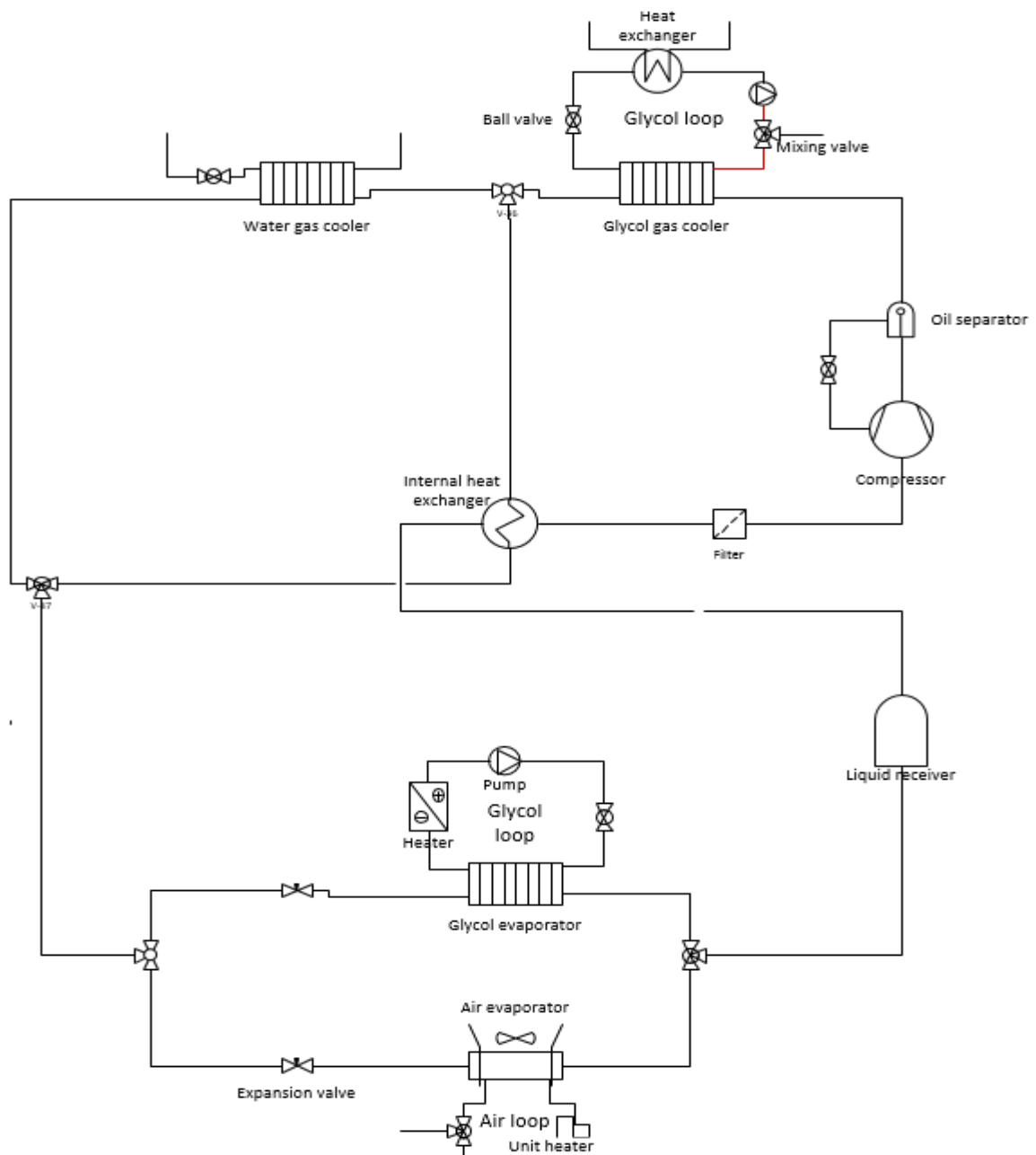


Figure 4.1: PFD of test rig

The rig consist of five loops: the main refrigerant closed loop, the glycol loop evaporator, closed air loop, open water gas cooler flow and glycol gas cooler loop. The serial connection

of the gas coolers enables for easy control of the gas cooler outlet temperature. The evaporators (air and glycol) was connected in parallel to stimulate the ambient conditions and the capacities of the evaporator.

The test rig consist of the following primary components;

- Semi hermetic reciprocating compressor
- Brazed plate heat exchangers
 - Glycol gas cooler
 - Water gas cooler
 - Glycol evaporator
- Micro channel louvered air evaporator
- Intermediate heat exchanger
- Throttling valves
- Low pressure receiver
- Electric heaters
- Fans
- Safety valves

4.1.1 Compressor Unit.

The compressor utilized for this experimental process is a dorin CD 380H model of CD200 semi hermetic compressor series. It has a heating capacity of 11kW at evaporation temperature of 10°C, gas cooler out temperature of 35°C at gas cooler pressure of 90 bar. The specifications of the compressor are given in the table below;

Table 4.1: Compressor specifications

Number of Cylinders	2	
Bore	28	Mm
Stroke	28	Mm
Displacement @ 50 Hz	3,00	
Displacement @ 60 Hz	3,60	
Suction valve (socket welding)	10	
Suction valve (butt welding)	14	
Discharge valve (socket welding)	10	
Discharge valve (butt welding)	14	
Oil charge	1,3	
Net weight	77	

The compressor has been in use for quite some time now and it is susceptible to drop in performance during experimental conducts. A pictorial representation of the compressor is presented in Figure 4.2.

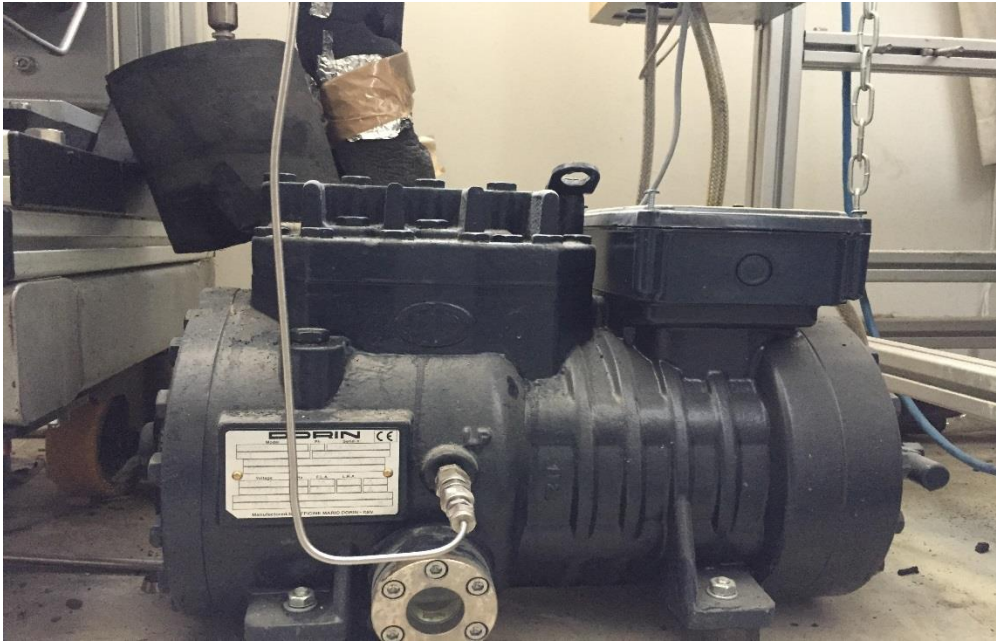


Figure 4.2: Dorin compressor unit

The compressor is fitted accessories as shown in the schematic of the compressor is shown in Figure 4.3.

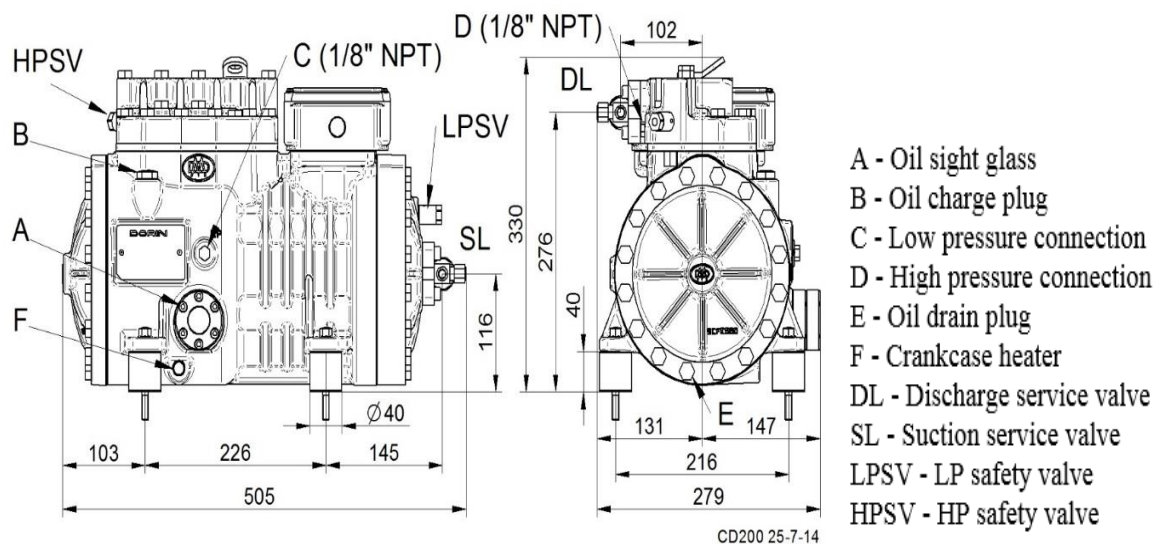


Figure 4.3: A schematic of the compressor unit with accessories

4.1.2 Gas cooler (Brazen Plate Heat exchangers)

Three of the heat exchangers used in this setup are from Kaori, manufacturer of brazed plate heat exchangers. Their specialized K040C series CO₂ heat exchanger is a perfect fit for this experimental setup, both as gas cooler and evaporator. The K040C series which is characterized by 60-70% lower pressure drop and 10% better heat capacity than multiple tube heat exchangers, is about 1/3rd the space and weight of multiple tubes heat exchangers. A sample of the Kaori brazed plate heat exchanger is shown in Figure 4.4 below:



Figure 4.4: Kaori brazed plate heat exchanger for gas cooling

Made of stainless steel SUS316 (standard) and brazed with copper, K040C series has a maximum working pressure 200 bar and operating temperature range of -195 to 150°C which makes it suitable for this experiment since heat rejected from the compressor is at very high temperature. The fluid flow direction in this heat exchanger is counter current. The specification for both the gas cooler and evaporators are given in Table 4.3 below.

Table 4.3: Kaori brazed plates heat exchangers classification

	Kaori model	Water storage volume (litres/day)	L (mm)	W (mm)	H (mm)	Weight (kg)	Heat transfer area (m ²)	Total volume (litres)
Glycol gas cooler	K040C*20	770-860	314	76	53	4.54	0.347	0.561
Water gas cooler	K040C*12	410-500	314	76	37	3.52	0.193	0.325
Glycol evaporator	K040C*12	410-500	314	76	37	3.52	0.193	0.325

The glycol and gas cooler heat exchangers were connected in series, with the glycol gas cooler connected to the compressor discharge line. The glycol heat exchanger is able to handle large heat transfer due to its larger heat transfer area and hence used for the reheating of the water. An extra heat exchanger was installed to cool the outlet hot glycol with the water from the main supply. With this, the glycol is recirculated for gas cooling.

4.1.3 Evaporators

The evaporators were connected in parallel, this to allow for variation of refrigeration load. For this experiment, the glycol evaporator represents the solar collector. The heat that is sourced from the glycol evaporator represents the useful heat the solar evaporator contributes to the system. The rest of the heat is from the air source evaporator. The amount of heat contributed through the air source evaporator is determined by the required cooling capacity for the air conditioning. In a multiple evaporator system, individual evaporators are better controlled with fluctuations in loads. With a parallel configuration, the low side pressure is maintained and it is easier to control individual evaporators unlike series configuration there is alternation of the pressure level and the evaporating temperature likewise. The air evaporator used in this experimental campaign is a micro channel louvered heat exchanger shown in Figure 4.5

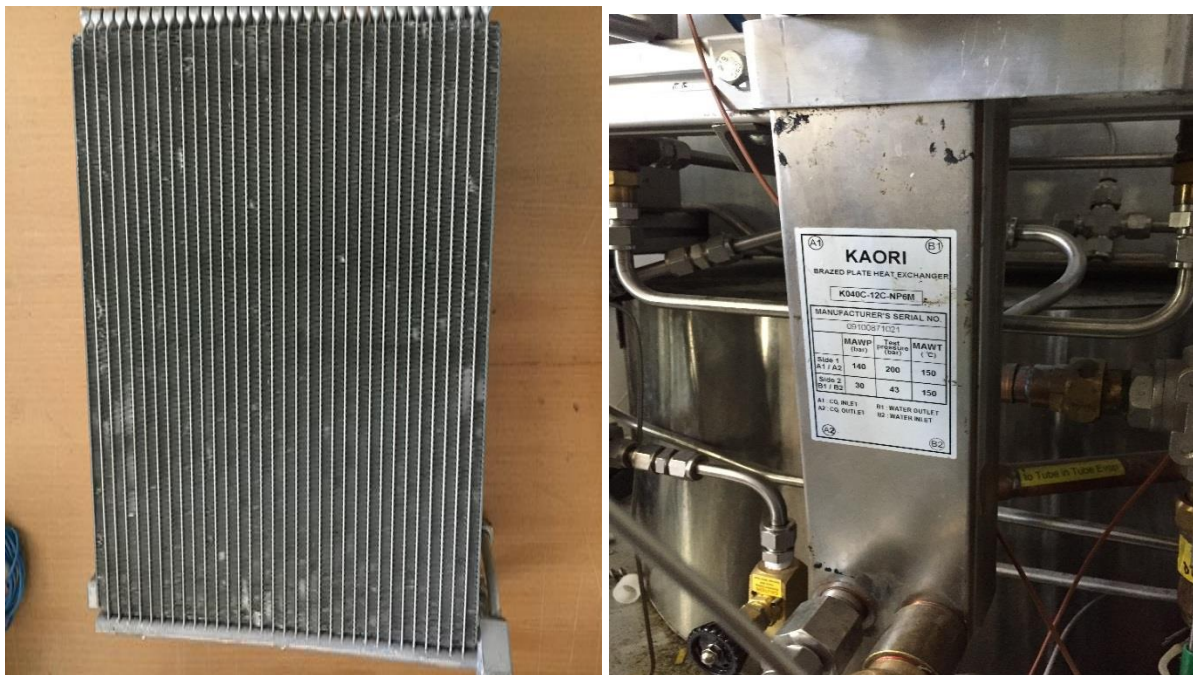


Figure 4.5: Air and glycol evaporators

Connecting tube

A tubing used for the conveying of CO₂ refrigerant is made of Copper. The copper tube that is also used for connecting the components of the heat pump systems to each other has an inner diameter of 8 mm. While the connection pipes for the secondary fluids, (glycol and water) were chosen to match the inlet and outlet dimensions of the brazed plate heat exchangers.

4.2 TEST PROCEDURE

The operation of the test rig components were monitored using a PID controlled program, LabVIEW run on a computer. The PID controls the compressor, glycol gas cooler, glycol evaporator and electric heaters. The signals from the positioned sensor nodes are collected by the sensors and logged in designated folder in excel sheets. The electric heaters are controlled to provide the required ambient temperature for the secondary fluids. The operation of the compressor is controlled by regulating the rpm. This is performed by selecting the percentage of the total rpm. PID also controls the fan speed of the air evaporator; this way the mass flow rate of the air is adjusted to match the preset operation parameters. The mass flow rate of the glycol in the glycol loop is also controlled by varying the percentage of the pump speed. Other system parameters are controlled manually; the mass flow rate of water into the water gas cooler and the intermediate heat exchanger for cooling the glycol out of the gas cooling process. The temperature of the two different evaporators when mixed at the suction of the compressor to ensure proper superheat, thereby adjusting the operation of the internal heat exchanger. An overview of the laboratory set up is shown in Figure 4.6 below.



Figure 4.6: A pictorial representation of the test facility

4.2.1 Start-up procedure

1. Check that portable CO₂ detector has enough battery. Switch it on and keep it in operation during tests.
2. Energize the circuit breakers in the electric cabinet, turn on, 'Hovedstrøm', 'styres', 'Hx2', 'Hx3', 'Fans and pumps
3. Check that the hoses for the cooling water disposal are well positioned at the exhaust sink in the basement
4. Open the two shut-off valves for the cooling water supply
5. Check and regulate, if needed, the position of the valve that controls the cooling water flow rate through the glycol to water heat exchanger
6. Check and regulate, if needed the position of the valve that controls the cooling water flow rate through the water-cooled gas cooler.
7. Run LabVIEW program (Gas cooler or Evaporator, dependent on requested specification).
8. Activate glycol pumps in both loops (evaporator and gas cooler) and fan in LabVIEW Front Panel by selecting percentage of the available rotational speed range

9. Activate electric heaters in the evaporator loops (air and glycol) in LabVIEW Front Panel (HX2 for air-supplied evaporator and HX3 for glycol-supplied evaporator) by either selecting percentage of the maximum electric power (in manual mode) or selecting the requested heat source temperature (in PID controlled mode). The Maximum allowable set point temperature in either air or glycol loop is 50°C.
10. Check every shut-off valve installed on the CO₂ side downstream the compressor outlet and verify the refrigerant circulation in the system. Open the manually operated expansion device (in parallel with the PI controlled).
11. Turn on compressor in LabVIEW Front Panel. Watch the discharge/suction pressure, avoiding excessive values on both sides (higher than 120 bar on the discharge and lower than 15 bar on suction).

4.2.2 During the experiment (Pressure and Temperature control)

1. Control continually the indication of analogue sensors/gauges
2. Control visually the oil level in the oil sight glass of the compressor. Actual level must be greater than the indicated minimum level.
3. Control the oil return mass flow rate from the receiver (minimum mas flow rate indicated by FT103 $\geq 30\text{g/min}$)
4. Provide enough superheating at the compressor suction (verify that reading from PT101 and TT101 results in minimum 5°C superheating).
5. Maintain appropriate liquid refrigerant level in the receiver (charge the system if needed).
6. Try to avoid compressor operation below 35%.
7. Control continually the parameters logged into the DAQ system by following profiles plotted in additional tags for mas flow rate meters, pressure cells and thermocouples.

4.2.3 End of experiment

Shut down procedure for the experimental campaign is highlighted below:

1. Start-up procedure in reverse order.

4.2.4 Test Matrix

The test matrix for the experimental campaign are basically constituted around the pressure and temperature. Hence, the experiments were conducted within the ranges highlighted in Table 4.4.

Table 4.4: Test matrix for experimental campaign

Parameters	Unit	Range
Gas cooler pressure	Bar	80-95
Gas cooler outlet temperature	°C	25-35
Evaporation temperature	°C	5-10
Air inlet temperature	°C	25-30
Air outlet temperature	°C	20-25
Glycol inlet temperature (evaporator)	°C	25-30
Glycol outlet temperature (evaporator)	°C	12-25

4.3 INSTRUMENTATION

In order to measure the operating parameters and performance of the test rig, proper instrumentation was needed. Parameters to be measured include the system pressures, temperatures, mass flow rates, compressor frequency. Other system parameters were calculated from these measured values.

4.3.1 Pressure

Endress + Hauser pressure transmitters were employed for the measurement of both the absolute pressure and differential pressure in the experimental set up. The system has in total number of 24 pressure sensors at different positions of the test rig. The transmitters are also designed with digital screen. The two most important pressure nodes and the corresponding tag names are listed in table 4.5 below:

Table 4.5: Pressure nodes

Sensor node (position)	Tag name
Compressor suction line	PT 101
Compressor discharge line	PT 102

4.3.2 Temperature

Thermocouples were used for the measurement of the temperatures at different points in the experiments. A tiny hole was bored into the connecting tubing and pipes, through which the thermocouples measured the temperature and transmits it to the logging system. Some of the most important sensor nodes are listed in table 4.6.

Table 4.6: Temperature nodes

Sensor node (position)	Tag name
Compressor suction line	TT 101
Compressor discharge line	TT 102
Oil separator outlet	TT 115
Glycol gas cooler outlet (CO2 side)	TT 104
Glycol gas cooler inlet (CO2 side)	TT 102
Water gas cooler inlet (CO2 side)	TT 217
Water gas cooler outlet (CO2 side)	TT 116
Air evaporator outlet (CO2 side)	TT 110
Air evaporator inlet (Air side)	TT 304- 307
Air evaporator outlet (Air side)	TT 310- 324
Glycol evaporator outlet (CO2 side)	TT 111
Mixing temperature at evaporator outlets (CO2)	TT 113

4.3.3 Mass flow rate

The mass flow rate in the experimental setup is measured using rheonik mass flow meters. The mass flow meter consist of sensor, transmitter and connection cable. The flow in the connecting tube is deflected and recorded by velocity sensors. The measured quantity that is equivalent to

mass flow rate is processed in the transmitter and conveyed to the logger. The measured flow rates are listed in Table 4.7.

Table 4.7: Mass flow rate nodes

Sensor node (position)	Tag name
Compressor discharge line	FT 102
Glycol evaporator	FT 105

4.4 UNCERTAINTY OF PARAMETERS

The uncertainty of the measurements taken helps ascertain how close the measured values are from the true value. It gives the level of confidence on which the measurements are based, while highlighting the accuracy and precision of the instrument. The uncertainty of measurements can be estimated in two ways:

1. Using the accuracy of the sensor as provided in the manufacturers reference
2. Estimating the uncertainty from the standard deviation of measured values for a measuring point within a specified time interval.

With uncertainty of individual parameters known, the uncertainty for derived parameters can be calculated as follows;

$$\Delta f(x, y) = \sqrt{\left(\frac{dy}{dx} \Delta x\right)^2 + \left(\frac{dy}{dx} \Delta y\right)^2} \quad \text{Equation 4.1}$$

If,

$$f(x, y, z) = x \pm y \pm z \quad \text{Equation 4.2}$$

$$\Delta f = \sqrt{(\Delta x)^2 + (\Delta y)^2 + (\Delta z)^2} \quad \text{Equation 4.3}$$

If,

$$f(x, y, z) = \frac{x+y}{z} \quad \text{Equation 4.4}$$

$$\Delta f = \sqrt{\left(\frac{\Delta x}{x}\right)^2 + \left(\frac{\Delta y}{y}\right)^2 + \left(\frac{\Delta z}{z}\right)^2} \quad \text{Equation 4.5}$$

If,

$$f(x) = x^y \quad \text{Equation 4.6}$$

$$\Delta f = f \cdot \left| y \cdot \frac{\Delta x}{x} \right| \quad \text{Equation 4.7}$$

4.4.1 Compressor:

The uncertainty for the work input into the compressor is evaluated from the energy balance for compressor highlighted in section (modelling). It is expressed as shown in equation 4.8. The uncertainties of the enthalpy are defined as a function of the suction and discharge pressures of the compressor.

$$\Delta W_{comp} = \sqrt{[(h_{co2,out} - h_{co2,in}) \cdot \Delta \dot{m}_{co2}]^2 + [\dot{m}_{co2} \cdot \Delta h_{co2,out}]^2 + [\dot{m}_{co2} \cdot \Delta h_{co2,in}]^2} \quad \text{Eqn 4.8}$$

4.4.2 Gas cooler:

Using the energy balance for the gas coolers capacity shown highlighted in section (modelling), the uncertainty is evaluated as;

$$\Delta Q_{gc} = \sqrt{[Cp_{co2} \cdot (T_{co2,in} - T_{co2,out}) \cdot \Delta \dot{m}_{co2}]^2 + 2[\dot{m}_{co2} \cdot Cp_{co2} \cdot \Delta T]^2} \quad \text{Equation 4.9}$$

Or

$$\Delta Q_{gc} = \sqrt{[(h_{co2,in} - h_{co2,out}) \cdot \Delta \dot{m}_{co2}]^2 + [\dot{m}_{co2} \cdot \Delta h_{co2,in}]^2 + [\dot{m}_{co2} \cdot \Delta h_{co2,out}]^2} \quad \text{Equation 4.10}$$

4.4.3 Evaporator

The uncertainty of the evaporators can be evaluated from the evaporator capacity using the energy equation for evaporators in section (modelling);

$$\Delta Q_{gc} = \sqrt{[Cp_{co2} \cdot (T_{co2,out} - T_{co2,in}) \cdot \Delta \dot{m}_{co2}]^2 + 2[\dot{m}_{co2} \cdot Cp_{co2} \cdot \Delta T]^2} \quad \text{Equation 4.11}$$

Or

$$\Delta Q_{gc} = \sqrt{[(h_{co2,out} - h_{co2,in}) \cdot \Delta \dot{m}_{co2}]^2 + [\dot{m}_{co2} \cdot \Delta h_{co2,out}]^2 + [\dot{m}_{co2} \cdot \Delta h_{co2,in}]^2} \quad \text{Equation 4.12}$$

4.4.4 Coefficient of performance

The uncertainties for both the performances of the evaporator and the gas cooler can be evaluated as;

$$\Delta COP_{cooling} = \sqrt{\left[\left(\frac{1}{Q_{evap}}\right) \cdot \Delta Q_{evap}\right]^2 + \left[\left(-\frac{Q_{evap}}{W_{comp}}\right) \cdot \Delta W_{comp}\right]^2} \quad \text{Equation 4.13}$$

$$\Delta COP_{heating} = \sqrt{\left[\left(\frac{1}{Q_{gc}}\right) \cdot \Delta Q_{gc}\right]^2 + \left[\left(-\frac{Q_{gc}}{W_{comp}}\right) \cdot \Delta W_{comp}\right]^2} \quad \text{Equation 4.14}$$

Due to insufficient data on the instrumentation components, the individual uncertainty of measured parameters were calculated using the second method. The uncertainties of a sample experiment is presented in the table 4.8 below. The gas cooler pressure of 90 bar and evaporation temperature of 10°C.

Table 4.8: Calculated uncertainty results

Parameter	Unit	Absolute Uncertainty
Pressure	Bar	± (0.084)
Temperature	°C	± (0.1)
Mass flow	kg/s	± (0.007)
Compressor	kW	± (0.34)
Water gas cooler	kW	± (0.48)
Glycol gas cooler	kW	± (0.88)
Air evaporator	kW	± (0.02)
Glycol evaporator	kW	± (0.13)
COP (glycol gas cooler)	-	± (0.9)
COP (air evaporator)	-	± (0.46)

CHAPTER 5. SIMULATIONS

For this study, modelling of the integrated CO₂ solar assisted heat pump for cooling, hot water heating and drying is carried out. This is to enable the analysis of the performance of the system and its individual components. The modelling of system components includes the compressor, air side evaporator, glycol side evaporator, expansion valve, internal heat exchanger, water gas cooler and glycol gas cooler. The model results enables to simulate how variables affects its system's performance. The COP of both the cooling and the heating process, the efficiency of the micro channel louvered heat exchanger, the heat transfer coefficients of the brazed plate heat exchangers and the efficiencies of the compressor were evaluated. The simulation results was used to both supplement and validate experimental results. Further system analysis can be estimated from the model.

To understand how the model procedure, a brief highlight is given. Since the primary aim of the design is for space cooling, the other applications such as hot water heating and drying are considered secondary, it was considered to first establish the cooling load to be met by the system at cooling demand peak.

5.1 Design Conditions for space cooling

Based on common knowledge of air conditioner operation, to create a good comfort zone, the relative indoor humidity should not be more 60%. The cooling load for the referenced parameter was modelled using Rhvac, which is an ACCA approved Manual J and Manual D computer program. Calculations are performed per ACCA Manual J 8th Edition, Version 2, and ACCA Manual D. The following parameters considered as reference values for the case study are listed in Table 5.1 below.

Table 5.1: Design parameters for space cooling

Parameter	Value	Unit
Reference City	Milan, Italy	-
Daily range	Medium	
Peak temperature	30.5	°C
Building volume		Above grade
Building area	80	m ²
Front door direction	North	-
No of occupants	4	

5.2 Energy consumption profiling

To be able to estimate the seasonal performance of the system for space cooling, the energy input for the operation of the heat pump should be accounted for the duration of the cooling load. This is evaluated using Pack Calculation Pro, a simulation tool for comparing the yearly energy consumption of the heat pumps. It was also used to estimate an hourly performance of the system.

A reference system was set up as a one stage transcritical and refrigerant and compressor is selected from a database. The suction side is set as a dimensioning capacity of the evaporator for the maximum value equivalent cooling load previously simulated using Rhvac. The ambient temperature at dimensioning capacity is also set accordingly; the evaporation temperature is also set. A constraint temperature was also set, a temperature below which the system doesn't run. The operating conditions are also set accordingly.

Before running the simulation, the reference city, monthly and weekly schedule were selected. This is controlled by ambient temperature and runs only when the temperature is above the set point. The monthly energy consumption (kWh) is calculated, a summary of the load fulfillment and other system results profiles are collected.

5.3 Heat pump modelling

Although the experimental set-up consisted of one or more components for the same function, they were first modelled as a single unit for energy balance analysis. The implication of this is such that, the energy balance of the heat rejecting side consisting of both the glycol cooled gas cooler and water cooled gas was carried out as a single unit. In the same vein, the energy balance of the air and glycol evaporators were carried out. This way, the COP of the cooling side and the heating side of the system were estimated. Thereafter, characteristics of individual components were evaluated. The calculations were made on excel spreadsheet and the thermodynamic properties of the fluids were extracted from RnLib and miniREFPROP. A few assumptions were made with regards to this modelling and they include:

- Negligible pressure drop in piping, evaporator and gas cooler
- Zero heat transfer with the environment with exceptions in the evaporator and gas cooler
- The state of the refrigerant leaving the evaporator and condenser was superheated vapor and subcooled liquid respectively. This is to allow a proper temperature approach between the ambient temperatures and the refrigerant flow.

a. Compressor model:

The performance of a compressor are defined by its isentropic efficiency and the volumetric efficiency. The model is also used to predict the power input, discharge temperature and mass flowrate in the compressor. Isentropic efficiency defines the amount of energy degeneration in a component under a steady state assumption. It is the ratio of the power needed for isentropic compression to the power to the power input from the compressor shaft.

Volumetric efficiency of the compressor is the ratio of the quantity of the refrigerant entering the compressor to the quantity of the refrigerant exiting the compressor. It is a function of both the clearance volume and the pressure ratio. Both isentropic and volumetric efficiencies are expressed in percentages. The under listed are the input and output parameters for the compressor model.

Table 5.2: Compressor model parameters

Input parameter	Output parameter
Suction pressure	Discharge temperature
Suction temperature	Mass flow rate
Discharge pressure	Power
Swept volume	

The isentropic and volumetric efficiency of the compressor are expressed in equations 5.1 and 5.2.

$$\eta_{is} = -0.26 + 0.7952 \left(\frac{P_d}{P_s}\right) - 0.2803 \left(\frac{P_d}{P_s}\right)^2 + 0.0414 \left(\frac{P_d}{P_s}\right)^3 - 0.0022 \left(\frac{P_d}{P_s}\right)^4 \quad \text{Equation 5.1}$$

$$\eta_v = 0.00650755 \left(\frac{P_d}{P_s}\right)^2 - 0.0094066 \left(\frac{P_d}{P_s}\right) + 0.93917957 \quad \text{Equation 5.2}$$

Where P_d, P_s are discharge and suction line discharge pressure respectively.

The mass flow rate and required power input by the compressor is expressed as follows;

$$\dot{m}_r = \rho_1 \eta_v V_s \frac{N}{60} \quad \text{Equation 5.3}$$

$$W_{comp} = \dot{m}_{CO_2} * (h_2 - h_1) \quad \text{Equation 5.4}$$

The enthalpy at the discharge line is expressed in equation xxx below. The discharge temperature is a function of this the enthalpy and the high side pressure and this is derived from the thermo-physical properties of the refrigerant using Rnlib, a spread sheet

$$h_2 = h_1 + \left(\frac{h_{2s} - h_1}{\eta_{is}}\right) \quad \text{Equation 5.5}$$

$$T_2 = f(h_2, p_2)$$

b. Evaporator

Two evaporators were modelled. The primary evaporator being a micro channel louvered exchanger is modelled as the air handling unit for space cooling. The secondary evaporator is modelled as the alternative heat exchanger projected to supply the low pressure side with extra heat. Since the cooling capacity is defined, the other parameters are highlighted in table 5.3.

Table 5.3: Evaporator model parameters

Input parameters	Output parameters
Refrigerant inlet temperature	Refrigerant outlet temperature
Refrigerant mass flow rate	Air outlet temperature
Air side cooling capacity	Overall heat transfer coefficients
Air mass flow rate	
Air inlet temperature	
Heat exchanger geometry	

The heat balance of both the air and glycol evaporator is expressed in equation 5.6

$$Q_{evap} = Q_{h,evap} = Q_{c,evap} \quad \text{Equation 5.6}$$

Where $Q_{h,evap}, Q_{c,evap}$ represents the capacity on the hot and cold side of the evaporator respectively.

The heat transfer capacity of the hot and cold side of the evaporators are expressed as

$$Q_{h,evap} = \dot{m}_{sec} \cdot C_{p,sec} (T_{sec,in} - T_{sec,out}) \quad \text{Equation 5.7}$$

$$Q_{c,evap} = \dot{m}_{CO_2} \cdot C_{p,CO_2} (T_{CO_2,out} - T_{CO_2,in}) \quad \text{Equation 5.8}$$

The overall heat transfer coefficient of the evaporator is derived from the U-A.LMTD relation:

$$Q_{evap} = U \cdot A \cdot LMTD \quad \text{Equation 5.9}$$

$$LMTD = \frac{\Delta T_2 - \Delta T_1}{\ln(\Delta T_2 / \Delta T_1)} \quad \text{Equation 5.10}$$

$$U = \frac{Q}{A \cdot LMTD} \quad \text{Equation 5.11}$$

The heat transfer coefficient of the micro channel louvered heat exchanger is evaluated using the NTU- ϵ (effectiveness method). Heat exchanger effectiveness is described as the ratio the actual heat transfer capacity to the maximum heat transfer capacity possible. This method takes into consideration the number of transfer units (NTU), the capacity ratio and effectiveness. The relation between effectiveness and the heat transfer capacities is shown in equation 5.12 below:

$$q = \epsilon \cdot q_{max} \quad \text{Equation 5.12}$$

Where q_{max} is maximum heat transfer obtainable between fluids per unit time. It takes into consideration the difference between the inlet of the hot side and cold side, where C_{min} depicts the smallest capacity rate of the calculated capacity rates of bot the hot and cold side while C_{max} is the larger of two rates.

$$q_{max} = C_{min} \cdot (t_{hi} - t_{ci}) \quad \text{Equation 5.13}$$

$$C_h = \dot{m}_h \cdot C_{p,h} \quad \text{Equation 5.14}$$

$$C_c = \dot{m}_c \cdot C_{p,c} \quad \text{Equation 5.15}$$

$$C_r = \frac{C_{min}}{C_{max}} \quad \text{Equation 5.16}$$

Expressing ϵ as a function of number of transfer units (NTU) and capacity ratio (C_r), with an orientation of the flow in the exchanger is counter-flow. The relation can be expressed using the equation 5.17.

$$\epsilon = \frac{1 - \exp[-N(1 - C_r)]}{1 - C_r \exp[-N(1 - C_r)]} \quad \text{Equation 5.17}$$

However, with change of state of fluid occurring in the evaporator, temperature of fluids is not considered in the calculation of the effectiveness of the heat exchanger which is expressed as:

$$\epsilon = 1 - \exp(-NTU) \quad \text{Equation 5.18}$$

$$\text{Where, } NTU = \frac{UA}{C_{min}} \quad \text{Equation 5.19}$$

c. Gas cooler

Since the primary aim of the gas cooler configuration in this study is to heat the secondary fluid for further application of hot water heating and clothe drying, the energy balance was performed as a single. The input parameters and output parameters are highlighted in table 5.4.

Table 5.4: Gas cooler model parameters

Input parameters	Output parameters
Refrigerant inlet temperature	Heat capacity of refrigerant
Secondary fluid inlet temperature	Heat capacity on the secondary fluid side
Refrigerant mass flow rate	Secondary fluid outlet temperature
Refrigerant outlet temperature	Mass flow rate of secondary fluid
Secondary fluid outlet temperature	

Heat balance of the gas cooler is expressed as:

$$Q_{gc} = Q_h = Q_c \quad \text{Equation 5.20}$$

Heat transfer capacity for both hot side and the cold side is expressed in equations 5.21 and 5.22.

$$Q_h = \dot{m}_{CO_2} c_p (T_{CO_2,in} - T_{CO_2,out}) \quad \text{Equation 5.21}$$

$$Q_c = \dot{m}_{sec} c_p (T_{sec,out} - T_{sec,in}) \quad \text{Equation 5.22}$$

Due to scarce literatures on heat transfers coefficients on CO₂ brazed plate heat exchangers, UA-LMTD method was utilized. The heat balance in both the water and glycol gas cooler are expressed as:

$$Q_{gc} = U \cdot A \cdot LMTD \quad \text{Equation 5.23}$$

$$LMTD = \frac{\Delta T_2 - \Delta T_1}{\ln(\Delta T_2 / \Delta T_1)} \quad \text{Equation 5.24}$$

The overall heat transfer coefficient can be expressed as:

$$U = \frac{Q}{A \cdot LMTD} \quad \text{Equation 5.25}$$

d. Expansion valve

The expansion valve, which is an isenthalpic process, is modelled as a function of state pressure and temperature. With the inlet properties of the expansion valve set by exit condition of the internal heat exchanger on the subcooling side and the exit properties of the valve set the inlet conditions of the evaporator.

$$h_{exp,in} = h_{sub,out}$$

$$h_{exp,out} = h_{evap,in}$$

$$h_{exp,in} = f(P_{in}, T_{in})$$

$$h_{exp,out} = f(P_{out}, T_{out})$$

CHAPTER 6. RESULTS AND DISCUSSIONS

6.1 RHVAC RESULTS

Setting the reference building conditions for the Rhvac simulation, which mainly hinges on the temperature and humidity profile of such location and climate. At a peak outdoor temperature of 32°C and indoor temperature of 20°C, resulted in a peak cooling load of 2.73 kWh. Other parameters, which contributes or influences the cooling loads, are the sources of heat gains. For the Milan climate, the contribution of each heat gain sources is shown in Figure 6.1.

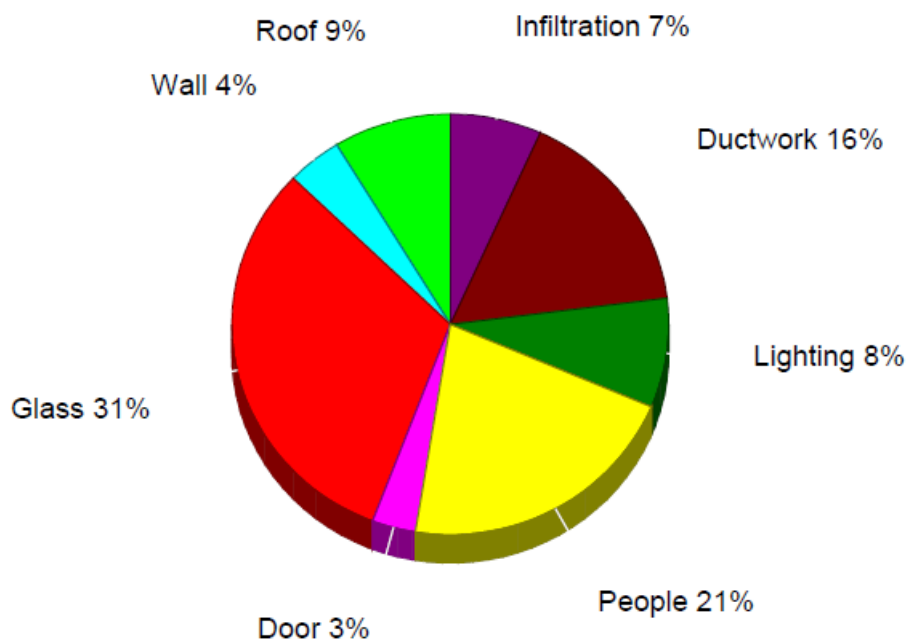


Figure 6.1: Heat gain sources

Heat gains through glass and people is shown to have stronger influence with 31% and 21% contribution respectively. The time of the day, building rotation hourly net gain with the direction the front door faces are also presented in Appendix 2.

Although, indoor conditions are set based on personal comfort, yet it is important to understand how this influences systems performances. Considering fluctuations in system parameters and climate conditions, the variation of cooling load with outdoor temperature at different required indoor temperature is simulated and the results presented as shown in Figure 6.2.

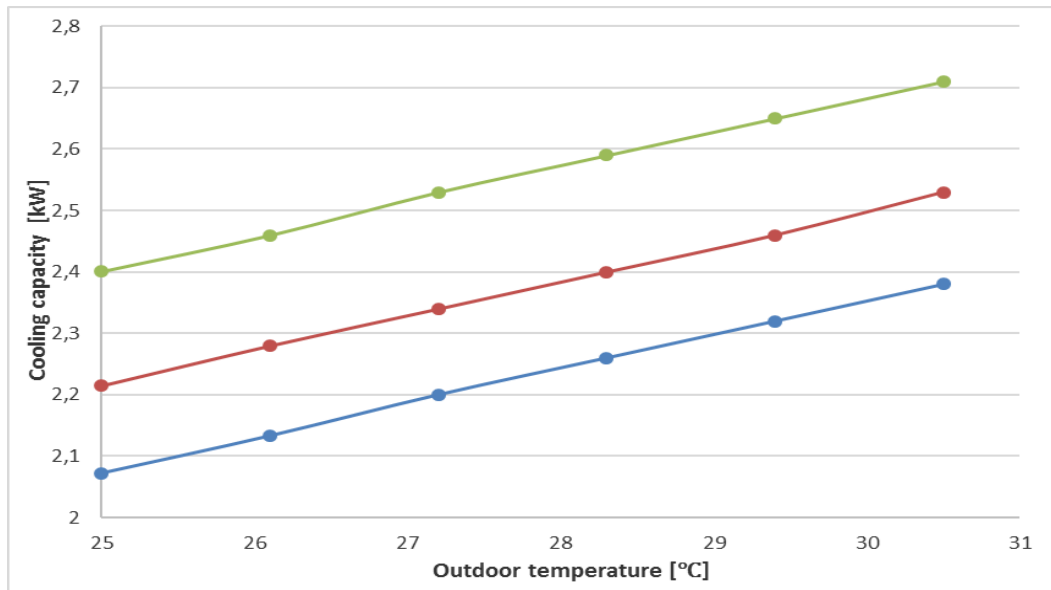


Figure 6.2: Variation of the required cooling capacity with outdoor temperature

Results shows that the cooling load for the reference unit increases with linearly with increasing outdoor temperature while it decreases with increasing indoor temperature. The peak cooling load of 2.73 kWh was achieved outdoor and indoor temperatures of 30.5°C and 20°C respectively. This decreases by about 8% with 2°C increase in indoor temperature at same outdoor temperature. At it set indoor temperature of 20°C and change in outdoor temperature from 29.5°C to 30.5°C, the cooling load increases by about 3%.

6.2 PACK CALCULATION PRO RESULTS

The one stage transcritical CO₂ heat pump system was selected with a Dorin CD 380H compressor model, which matches that for the experiment. The cooling capacity is also set to match the 2.7 kW cooling load demand. The capacity is dimensioned at the cooling capacity with a 10°C and a superheat of 20K. The minimum gas cooler temperature is set at a minimum of 30°C. The monthly schedule from April to September is defined as the cooling season, with a daily operation from 8:00 to 18:00 hours. The required peak cooling was observed to be in the month of June.

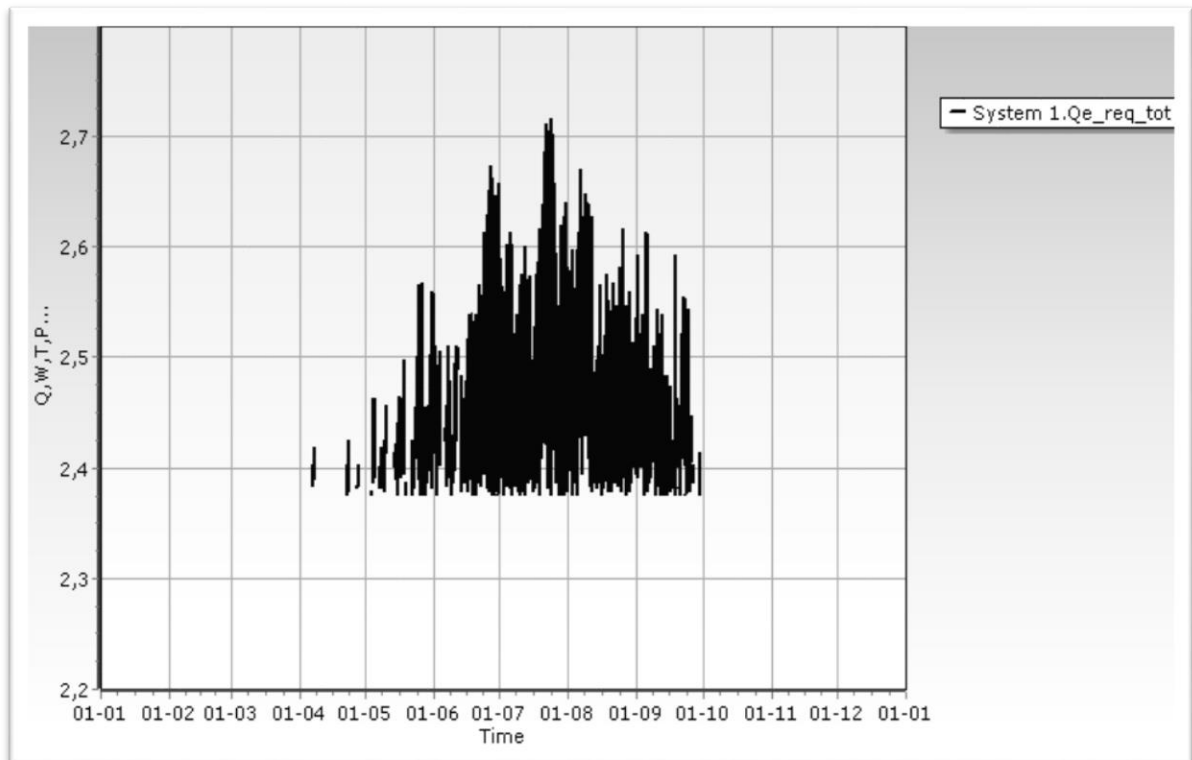


Figure 6.3: Cooling load profile for the year

This corresponds to five months of cooling season with high cooling demands within the median three months. The daily system performance for the peak month of July is plotted in Figure 6.4 below;

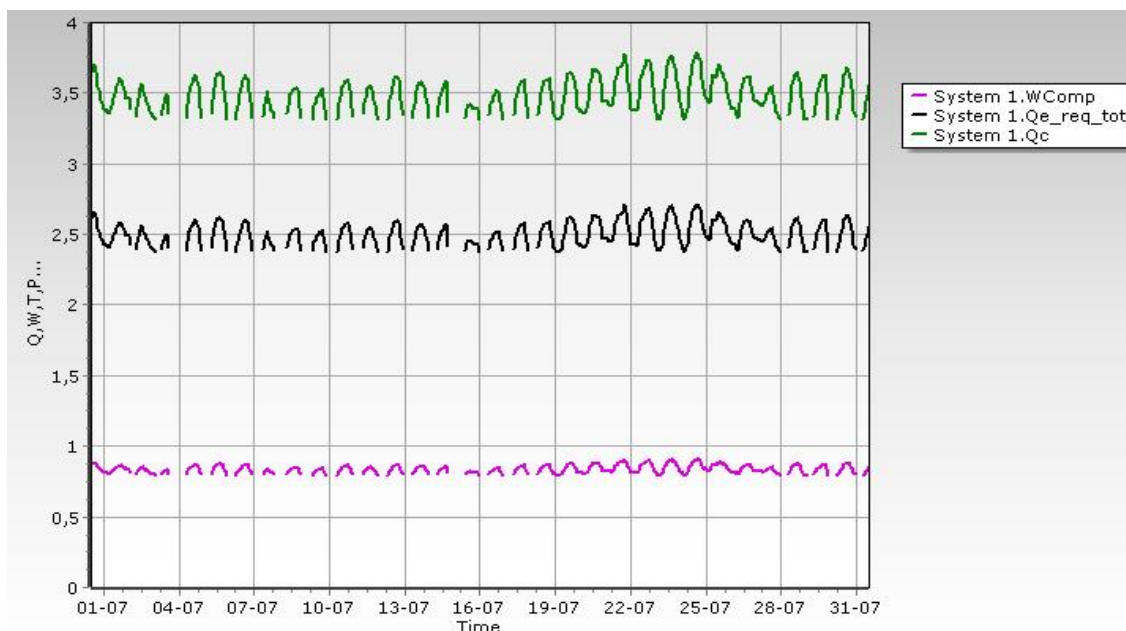


Figure 6.4: Cooling load profile in the peak month

The average cooling capacity of the evaporator is 2.5 kW while the heating capacity and the compressor work is 3.5 kW and 0.86 kW, which corresponds to the average outdoor temperature of 25°C of an outdoor temperature profile ranging between 15 to 32°C and average relative humidity of up to 95%. At gas cooler pressure of 87 bar, a daily profile of the heat

pump operation on an hourly basis was generated as shown in Figure 6.5. At peak cooling load of 2.73 kW, the energy input into the compressor was 0.92 kW.

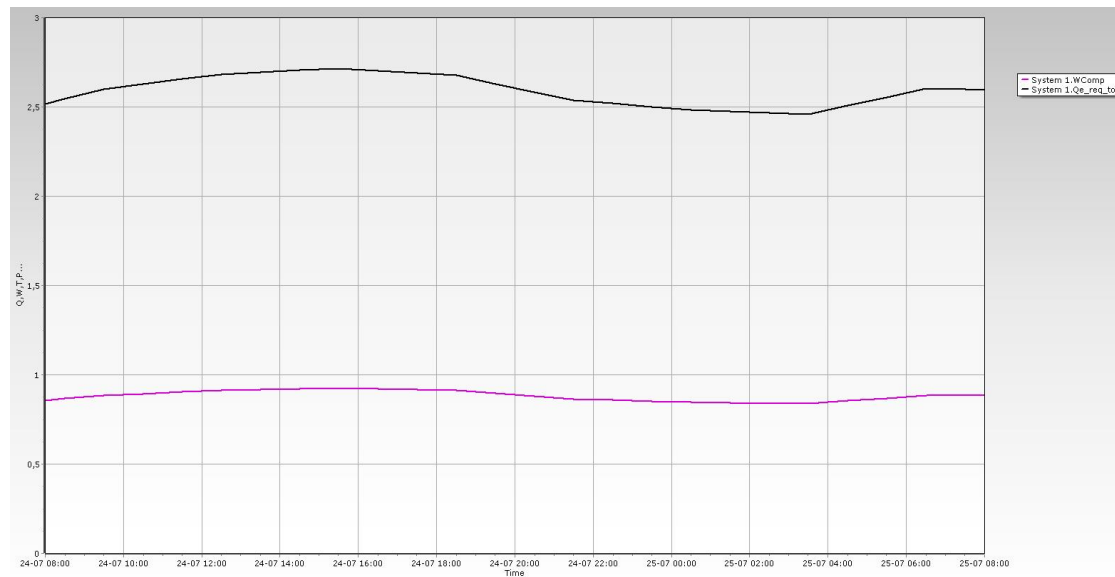


Figure 6.5: Daily profile of the cooling load

An average $COP_{cooling}$ of 1.79 was achieved for the cooling season. With a discharge line temperature of 83.7°C, $COP_{heating}$ of 3.8 was achieved on the high pressure side of the heat pump.

6.3 SIMULATION RESULTS

The result of the modelled process is presented in this section. The model is used to predict the operation of real heat pump process. The simulation considers two evaporation temperatures of 5.30°C, 10°C and gas cooler pressure ranging between 80 to 90 bar. The heat source inlet and outlet temperatures of 30°C and 20°C corresponding to 2.73 kW and temperature approach of 2 K between the inlet temperature of the heat sources and the refrigerant outlet temperature. The CO₂ outlet temperature of the gas cooler was assumed to be 30°C.

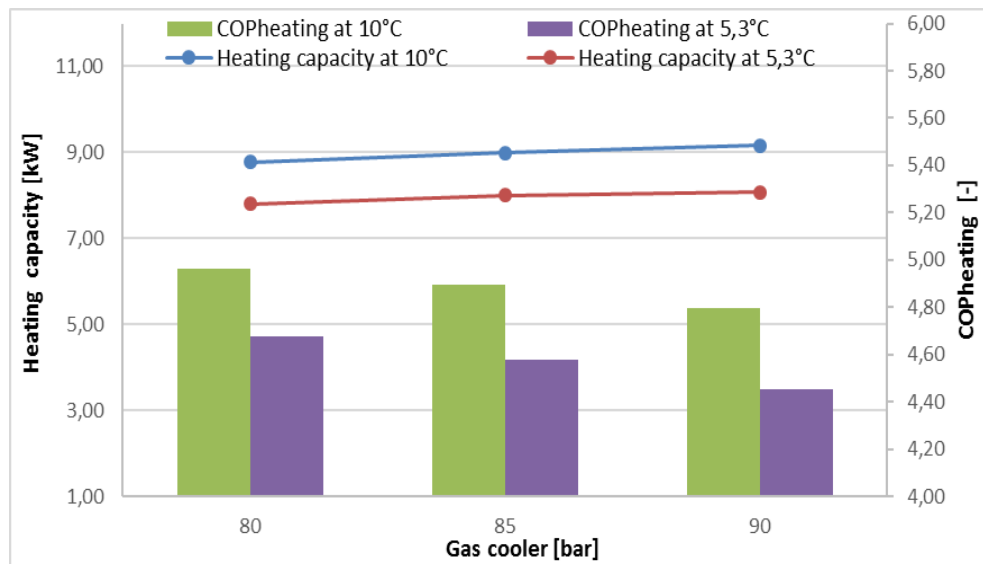


Figure 6.6: COPheating and heating capacity at air evaporator capacity of 2.73 kW

At fixed air evaporator capacity of 2.73 kW and same operating conditions as the glycol evaporator stated above. The results shown in Figure 6.6 demonstrates the performance of the heat rejecting process of the heat pump. The COPheating of the heat pump decreased while increasing the gas cooler pressure. However, the heating capacity and cooling capacity of the system increases with the gas cooler pressure due to increase in the specific enthalpy of evaporation. The performance of the system also favors a higher evaporation temperature. At 5°C, the COPheating is seen to decrease alongside an increasing gas cooler, however the COPcooling increases as the cooling capacity. The performance of the air evaporator depicts a declining trend in the COPcooling with increasing gas cooler pressure at same outlet conditions. As it, also evident from Figure 6.7 below, the system propagates better performance at lower evaporation temperature.

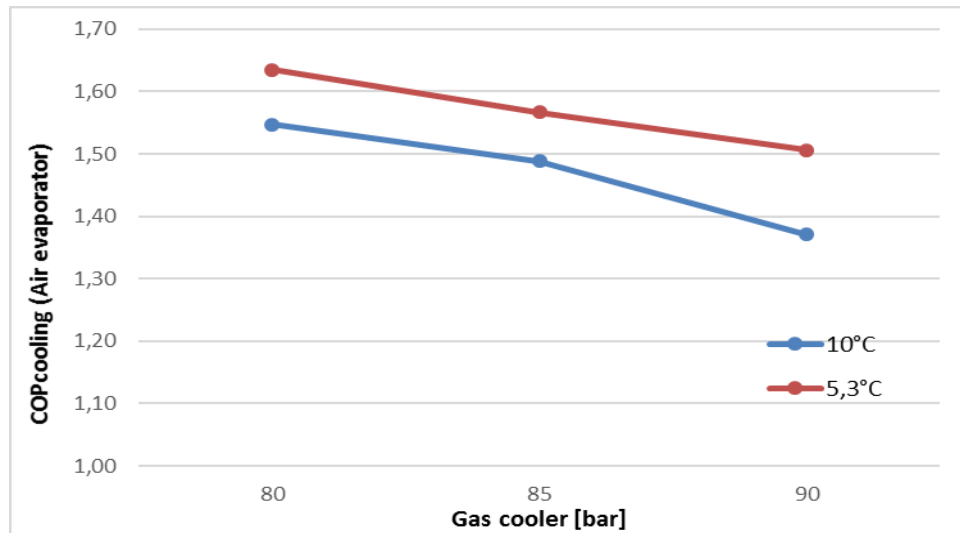


Figure 6.7: Variation of the COPcooling of the air evaporator

A trend similar to that of 2.73 kW air evaporator capacity is observed for the 2.73 kW air evaporator capacity with varying heating capacity, total cooling capacity of the evaporators as shown in Figure 6.8. With varying degrees of deviation, the higher capacity air evaporator (2.73 kW) had a better cooling performance than the lower capacity air evaporator (2.37 kW) did. While the lower capacity system showed a steeper slope in its COPcooling with respect to increasing gas cooler pressure, the higher capacity system however showed a lesser change in its COPcooling with respect to the change in gas cooler pressure.

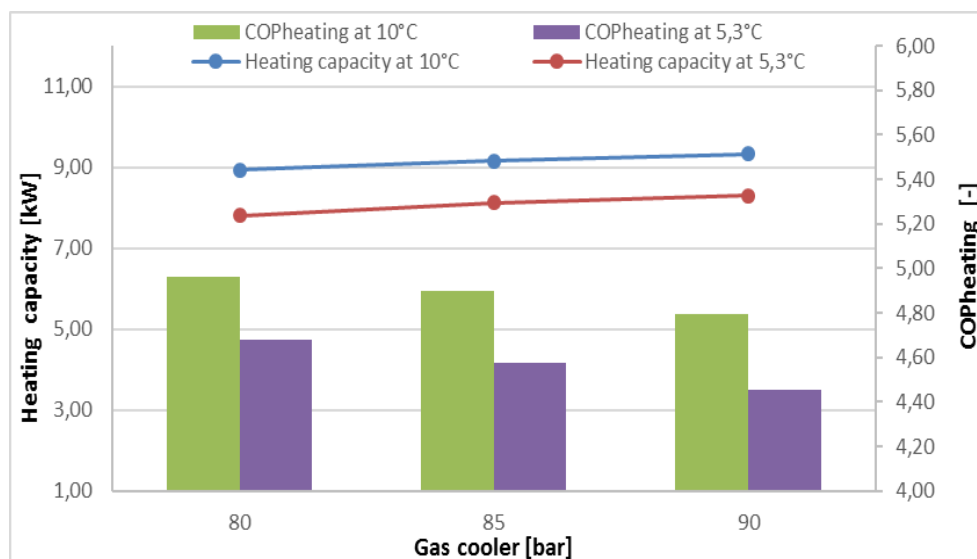


Figure 6.8: COPheating and heating capacity at air evaporator capacity of 2.37 kW

6.4 EXPERIMENTAL RESULTS

Experimental studies were conducted to validate theoretical analysis carried out and aims to represent an actual integrated operating unit. At varying air evaporator capacities within the range of 2.37 to 2.73 kW which represents outdoor and indoor conditions of the building, the air inlet and outlet temperatures of the evaporator side was set to match the building conditions. The results are presented in Appendix 3.

Three different conditions were run for the 2.37 kW cooling load with evaporation temperature varying between 5 to 10°C and the gas cooler within the range of 80-85 bar. The evaporation temperature has been substituted for their corresponding saturation pressure, which ranges between 40 to 45 bar and used for descriptive purpose. Hence, 84/45 implies a gas cooler pressure of 84 bar and evaporation temperature of 45 bar which represents the evaporation temperature of 10°C. The corresponding system performance results are evaluated as presented in Figure 6.9.

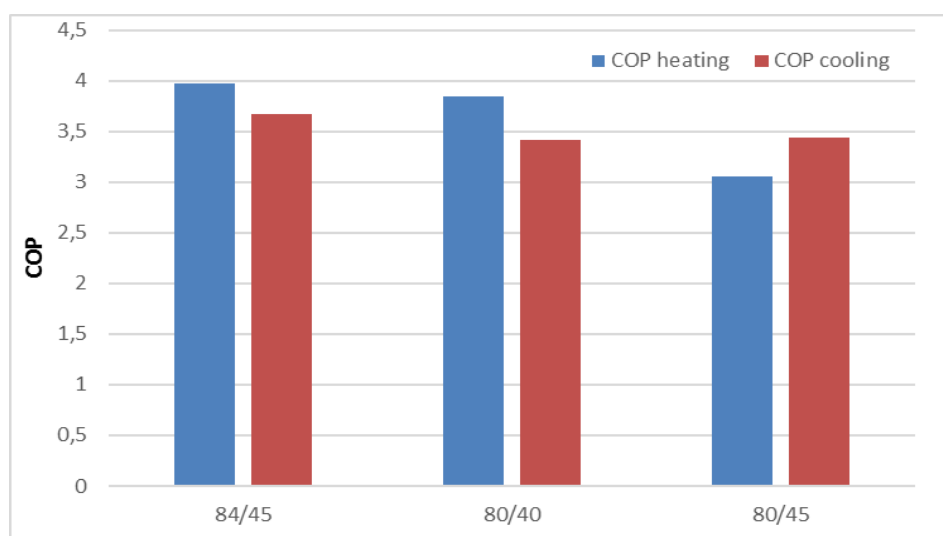


Figure 6.9: Cooling and heating performance at 2.37 kW air evaporator capacity

The highest COP for both the heating and cooling application was obtained at 84/45 with corresponding values of 3.97 and 3.67. Reducing the gas cooler pressure by 5 bar and the evaporation temperature by almost 50%, 80/40 operating conditions resulted in lower system COPs of 3.84 and 3.41 for the heating and cooling respectively. This represents a reduction of about 3 to 7% in respective COPs. This is to validate a previous assertion that increasing the evaporation temperature results in lower specific enthalpy of evaporation, while decreasing the gas cooler pressure results in decreasing specific enthalpy of condensation. The 80/45 condition however gave a different performance to that of both the 84/45 and 80/40 trend. The resulting COP_{cooling} of 3.44 was higher than 80/45 condition, it however, a reduction in the COP_{heating} of about 20% can be observed.

Subsequently, the impact of having a higher gas cooler pressure for the same evaporation temperature cannot be underestimated. For the same evaporation temperature, the 80/45 condition gave a COP_{cooling} about 6% lesser than that of the 84/45. This shows that increasing the gas cooler pressure for the same evaporation temperature at constant CO₂ gas cooler outlet temperature of 31°C has the potentials of increasing the cooling performance of the heat pump by about 6%. The corresponding COP_{cooling} from the air evaporator for space cooling are 1.18, 1.1, 1.08 for 84/45, 80/40 and 80/45 conditions respectively. The volumetric heating capacity is maximum at a higher gas cooler pressure of 85 bar due to large vapor density of the

refrigerant while a higher volumetric cooling capacity also results from high pressure of the evaporator.

Three different conditions were run for the 2.73 kW cooling load with evaporation temperature varying between 5 to 10°C and the gas cooler within the range of 80-90 bar. The air evaporator performance represents the required indoor and outdoor conditions of 20°C and 30°C respectively. The highest system performance is obtained from 90/45 operating conditions. The resulting heating and cooling COPs are 4.04 and 3.55 respectively. Decreasing the gas cooler pressure by 10 bar while keeping the evaporation temperature constant at 10°C resulted in about 13% and 7% decrease in COP. Other resulting system performance are highlighted in figure 6.10.

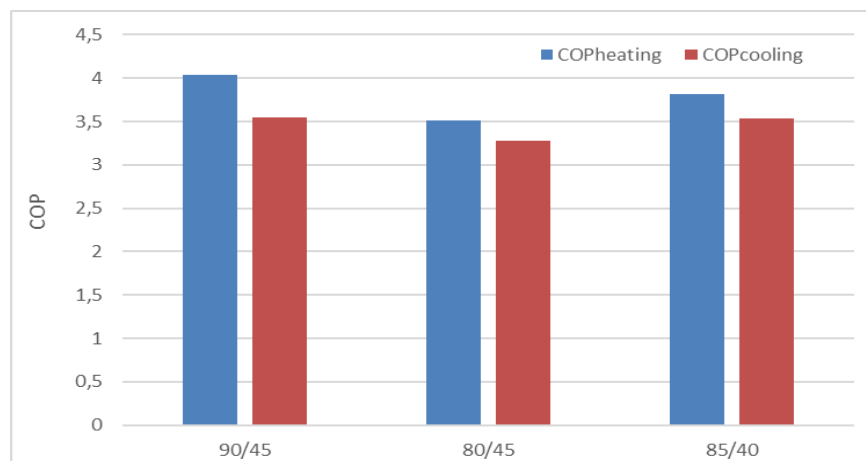


Figure 6.10: Cooling and heating performance at 2.73 kW air evaporator capacity

At a lower evaporation temperature of 5°C and gas cooler pressure of 85 bar, COPs of 3.81 and 3.54 for heating and cooling respectively. This implies that its heating performance is about 6% lesser than that of 90/45 while COPcooling remains relatively close. It however also had a better performance than 80/45 with COPs increasing by up to 7% for both heating and cooling. It can also be deduced from the result that the optimum gas cooler is between 85 and 90 bar, as they represent the region with the highest COPheating. The corresponding COPcooling from the air evaporator for space cooling are 1.37, 1.28, 1.34 for 90/45, 80/45 and 85/40 operating conditions respectively.

Comparing the performance of similar operating conditions for different cooling capacity is discussed as follows. At an air evaporator capacity of 2.73 kW, the 80/45 condition showed a better heating performance with about 15% to that of the 2.73 kW air evaporator capacity. While the 2.37 kW air evaporator capacity has a better, cooling performance than its counterpart does by about 5%.

Evaluating the Carnot COPs and Carnot efficiencies for the space cooling operation of the experiment, the results are highlighted in Table 6.2.

Table 6.2: Calculated Carnot efficiency

	Cooling capacity (kW)	T_{room} (°C)	T_{amb} (°C)	COP_{carnot}	COP_{actual}	η_{system} (%)
Operating condition						
84/45	2,37	22	28	49,2	1,18	2,40 %
80/40	2,37	22	28	49,2	1,11	2,26 %
80/45	2,37	22	28	49,2	1,08	2,20 %
90/45	2,73	20	30	29,3	1,37	4,67 %
80/45	2,73	20	30	29,3	1,28	4,37 %
85/40	2,73	20	30	29,3	1,34	4,57 %

The system efficiency compares the actual COP to the real COP of the system. It describes how close the performance of the system is to an ideal situation. It describes how much power is required for the real process to operate in an ideal situation.

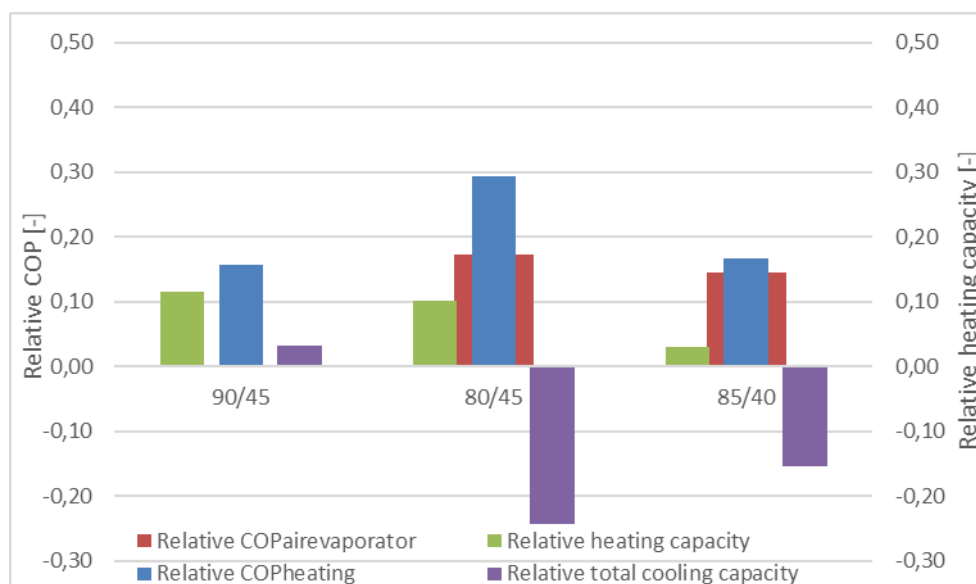


Figure 6.11: Relative comparison of simulated results to experimental results

Some results of the simulation was compared and expressed in terms of its relativity to the experimental results, the outcome of which is plotted in figure 6.11 above. The deviation of the experimental results from the simulation results for the COP of the air evaporator at capacity of 2.73 kW ranges from 0.01 up to 0.15. The COP_{heating} of the experiment relative to those of the simulation ranges had up to 0.3. The heating capacity of experiment was up to 0.12 relative to the simulated results. The experiment demonstrated better performance than the simulation. The predicted values from the simulation was within a maximum value of 0.25 relative to the experimental results. The largest deviation as can be seen from figure xxx above to occur at gas cooler pressure of 80 bar and evaporation temperature of 10°C.

6.4.1 Space cooling performance rating

The performance of the system with respect to the evaporator capacity is evaluated with varying operating conditions. At a reference cooling capacity of the air evaporator at 2.37 kW to meet the indoor and outdoor condition of 22°C and 28°C. Since these conditions were not

run in actual room set up, EER and SEER used for the comparative analysis are considered instantaneous and only apply for a single operating condition. At evaporation temperature of 10°C and gas cooler pressure 84 bar, an EER value of 4.04. Decreasing the gas cooler pressure to 80 bar at same evaporation temperature, an EER value of 3.69. Subsequently the SEER decreases from 4.61 to 4.22. The decrease by 5 bar in the gas cooler resulted in about 9% decreases in the values of the EER and SEER. At lower evaporation temperature of 5.30°C and gas cooler pressure of 80 bar resulted in EER and SEER values of 3.8 and 4.34 respectively. This depicts an increase of about 3%. This clearly shows the energy efficiency of the heat pump for space cooling purpose is highly dependent on the COP_{cooling}.

Comparing the performance of the experimental integrated CO₂ heat pump to that of a single transcritical space cooling simulated at peak load using Pack calculation pro, it is observed that higher SEER and EER values were obtained. From the simulation, for a 2.73kw cooling load with corresponding operating conditions of gas cooler pressure of 87 bar and evaporation temperature of 10°C, EER and SEER values of 10.11 and 11.7 are obtainable. The SEER is within the quoted values for SEER rating. The reason between the disparity between the results of the simulation and experiment is that the compressor work input value in the experiment does not account only for the mass flow rate of CO₂ through the air evaporator. By proportionally calculating the mass flow rate through the glycol and air evaporator, the corresponding compressor work input can be re-evaluated. The EER and SEER value for the space cooling is corrected to 12.6 and 14.5 respectively at evaporating temperature of 10°C.

6.4.2 Heat exchanger performance

The overall heat transfer coefficient (U) of some of the heat transfer components are calculated using the equations xxx highlighted in section xxx. The U-value of water gas cooler with complete instrumentations for the 2.73 kW air evaporator experiment is enumerated and represented in Figure 6.12 below:

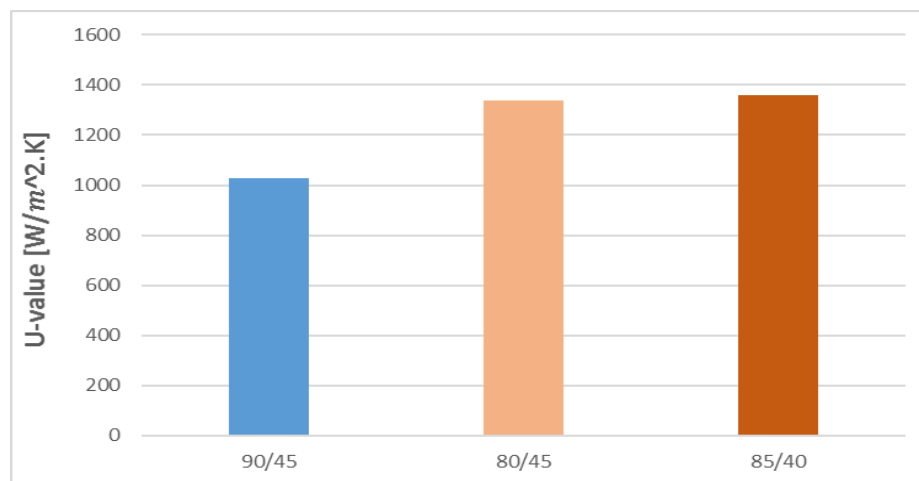


Figure 6.12: Overall heat transfer coefficients of experimental results

6.5 DRYING

The performance of the R744 is evaluated using the SMER and SEC and comparison with alternative refrigerants likewise was made. These parameters, SMER and SEC has been discussed in previous section. With specified reference values for the primary properties, other properties of the drying air is extracted for the air heating and moisture absorption process as shown in Table 5.2. The R744 driven heat pump dryer has demonstrated to be an effective system, which removes more moisture at low energy consumption. Its operation results in a dryer's efficiency of about 66% with potentials of removing about 3.14 kg/kWh while requiring low energy consumption of about 0.292 kWh/kg.

Table 6.3: Parameters for the drying process

Drying Air conditions							
T(air1)	20	R.H(air1)	0.90	H(air1)	55.66	X(air1)	0.015
T(air2)	60	R.H(air2)	0.11	H(air2)	96.94	X(air2)	0.015
T(air3)	35	R.H(air3)	0.55	H(air3)	89	X(air3)	0.021

Given the same conditions, the R744 cycle has the highest SMER of 3.42 kg/kWh, which is about 28% and 45% better performance when compared to R410a and R134a cycle. This implies that the R744 heat pump removes more moisture from the fabric for the same amount of energy input than R410a and R134a as shown in Figure 6.13. Even though the R744 has the lowest (\dot{m}_a/\dot{m}_r) value and lowest specific enthalpy of condensation it however has the lowest specific enthalpy of compression which depicts lesser energy consumption.

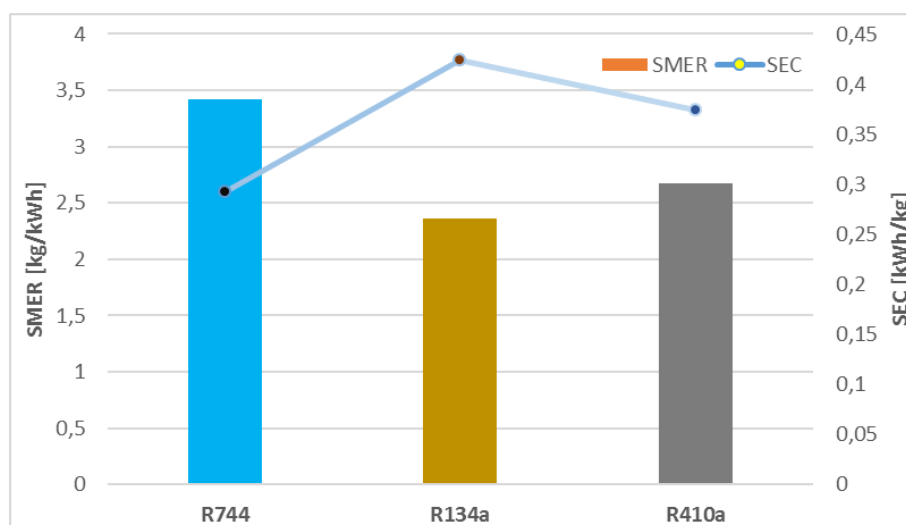


Figure 6.13: Comparison with alternative refrigerants for drying

Subsequently, the R744 system has the lowest SEC of 0.29 kWh/kg compared to R134a, which has a value of about 45% more. This implies that R744 requires lesser energy input into the system for the removal of moisture in the drying chamber. The R410a system also had a SEC value about 28% more than the R744 system which means it consumes 0.37 kWh energy per 1 kg of moisture removed from the cloth.

6.6 DISCUSSIONS

The influence of some of the parameters of the heat pumps on its performance is examined. The performance of alternative refrigerants in comparison to R744 is also discussed. The operation of drying process under varying condition, utilization of alternative fluids and system performance was also reviewed.

6.6.1 Influence of solar collector on heat pump performance

The influence of the solar collector on the performance of the heat pump system is analyzed. The solar collector can be used as either as a heat source for the evaporator, for preheating water for hot water production on the heat rejection side of the heat pump or both. Due to the available resources, the possible configuration was to use it as heat source of the evaporator. Irrespective of the method of application, it enhances the potential heating capacity of the heat pump system.

Comparing the performance of the pack pro simulation with the same air evaporator capacity, the heating capacity of up to 4 kW was achievable. Integrating the solar collector as an extra heat source to serve as the secondary evaporator increases the heating capacity potentials of the system to twice the capacity of when a single evaporator is used. The secondary evaporator also has the possibility of operating as a refrigeration. This way, the applicability of the heat pump is further expanded beyond its current scope of application and the energy efficiency of the system is further enhanced.

6.6.2 Impact of outlet temperature of gas cooler

The impact of the temperature of the refrigerant at the outlet of the gas cooler is examined. For an air evaporator capacity of 2.73 kW, two gas cooler outlet temperatures (30°C, 35°C) are considered. As shown in Figure 6.14, the heat pump had better performance at the lower outlet temperature. A high deviation up to 0.3 in COP_{heating} at 30°C relative to 35°C was predicted for a gas cooler pressure of 80 bar at an evaporation temperature of 10°C. This deviation decreases by about 67% when the gas cooler was increased to 90 bar. The heating capacity of the gas cooler also follows similar trend at relatively close deviation values. This seemingly will be the case for the cooling performance of the heat pump system. The overall performance of the heat pump system can also be observed to decrease at an evaporation temperature of 5°C.

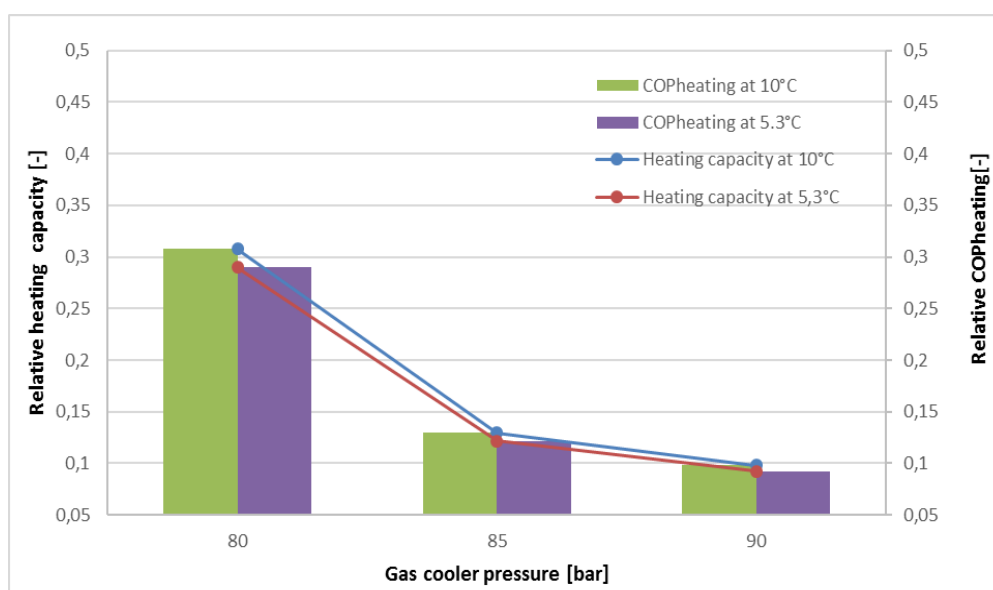


Figure 6.14: relative performance of the heat pump at different gas cooler exit temperatures

6.6.3 Comparison of CO₂ cycle to alternative refrigerants

The performance of the CO₂ cycle, which shall hitherto be referred to as R744 heat pump unit, was compared with systems using alternative refrigerants like R134a and R410a. The same temperature state points were considered for this comparison at fixed evaporator capacity of 2.37 kW. The operating pressures were adjusted accordingly for the alternative refrigerants. At varying operating conditions, the corresponding COPs for cooling and heating are presented in Figure 6.15 and 6.16 below.

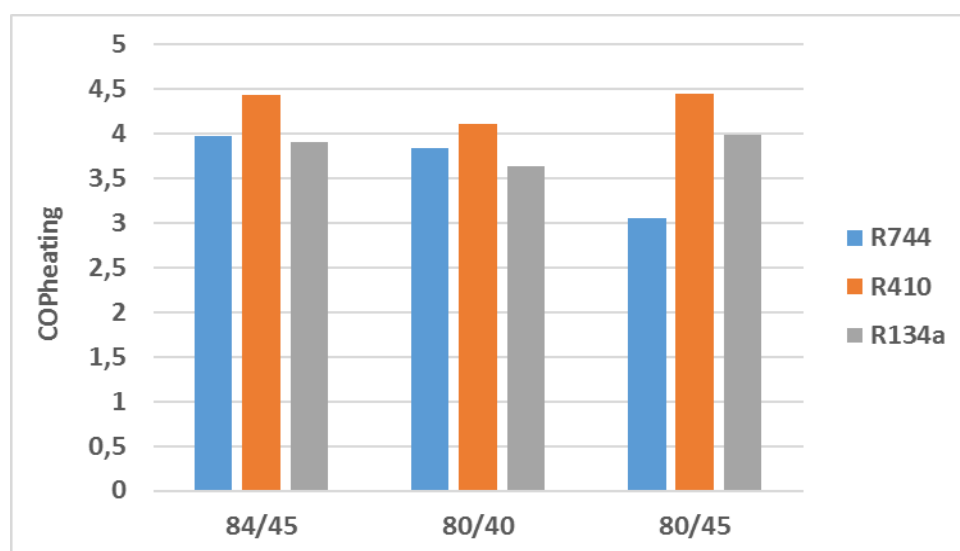


Figure 6.15: Comparison of heating performance with alternative refrigerants

At evaporation temperature of 10°C and high side pressure of 84 bar, R410 turned out to have the highest COP of 4.44, which is 11% and 13.8% better than that of R744 and R134a respectively. The same trend is observed at evaporation temperature of 5.30°C and high side pressure of 80 bar. This is due to large specific enthalpy of condensation value for the R410a at the same discharge temperature and this translates into lesser mass flow rate and compressor power requirement subsequently. However, same is not obtainable for R134a. At an evaporation temperature of 10°C and high side pressure of 80 bar, R744 performed badly against the two other refrigerants. This is due to low increase in the heating capacity relative to the increase in the compressor power input which is the other way round for R410a and R134a. An increase in evaporation temperature at same pressure leads to increase in the compressor power requirement. The performance of R410a can be attributed to its low molar mass and high vapor density and this translates into a high volumetric heating capacity. Even though R744 has a much lower molar mass, however its low vapor density compared to that of R410a, which results in a relatively lower volumetric heating capacity.

Comparing their performance on the evaporator side, both R744 and R410a showed similar cooling COP values while R134a showed a lower value at evaporation temperature of 10°C and high side pressure of 84 bar as shown in Figure xxx. At lower evaporation of 5.30°C and pressure of 80 bar, R744 cycle had a cooling COP about 3% and 22% more than that of R410a and R134a respectively and this is due to higher specific enthalpy of evaporation in R744 cycle compared to others. However, at evaporation temperature of 10°C and a lower high side pressure, R744 exhibited a slight increase in cooling COP compared to the previous operating condition. This resulted in R410a having a higher cooling COP while R134a also experienced

some increase in COP. This reduction can be attributed to the decrease in the specific enthalpy of evaporation with increasing evaporation temperature in trans-critical R744 cycle.

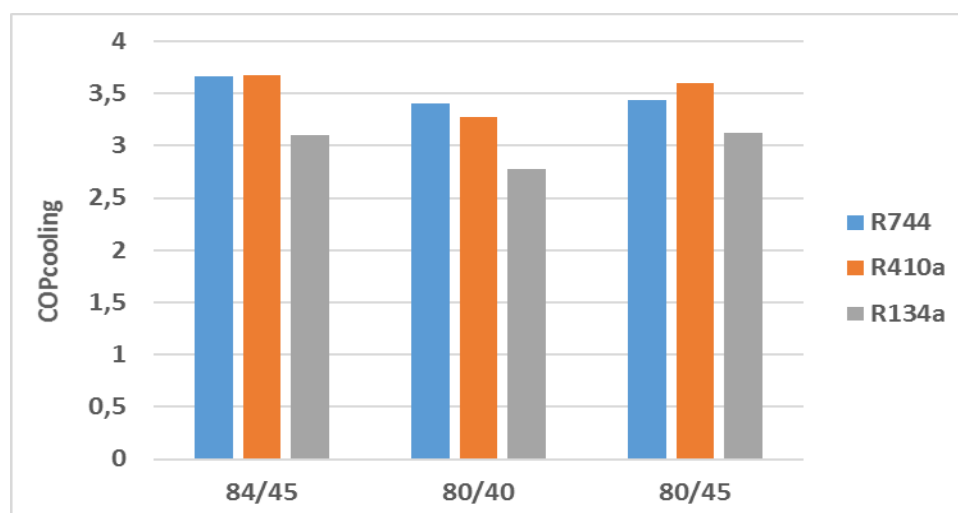


Figure 6.16: Comparison of heating performance with alternative refrigerants

Comparing the energy efficiency performance of the air evaporator for space cooling using the alternative refrigerants, R744 system had a high performance at an evaporation temperature of 10°C and gas cooler pressure of 84 bar. Although the R410a system has similar EER and SEC values of 12.6 and 14.5, same as that of the R744 system. However, the R134a system had low estimated EER and SEER values of 10.6 and 12.2 respectively. This is because of low COPcooling on the air evaporator side attributed to the relatively high compressor work input required. At cooling capacity of 2.73 kW, the heat pump systems has the potential for even higher EER and SEER ratings of about 13 and 15 respectively.

6.6.4 Lorentz efficiency

In a practical CO₂ heat pump, heat rejection and absorption occurs at gliding temperatures, hence it becomes appropriate to describe the performance of the system using Lorentz COP and efficiency as defined in section xxx. The corresponding Lorentz COP for both the heat rejection and absorption of some experimental results are evaluated as presented in Table 6.4.

Table 6.4: Calculated Lorentz COPs and efficiency

	Cooling Capacity [kW]	
	2.73	2.37
Temperature (T1)	28.75°C	30.05°C
Temperature (T2)	92.1°C	86°C
Temperature (T3)	31°C	31°C
Temperature (T4)	9.99°C	9.99°C
Lorentz COPcooling	7.08	7.75
Actual COPcooling	3.55	3.67
Lorentz efficiency (cooling)	0.5	0.47
Lorentz COPheating	8.07	8.75
Actual COPheating	4.04	3.97
Lorentz efficiency (heating)	0.5	0.45

6.6.5 Impact of air outlet temperature and relative humidity on dryer performance and efficiency

The performance of drying process of the heat pump can be influenced by the major system variables, which are temperature and relative humidity. The degree of influence will also be evaluated accordingly.

6.6.5.1 Effect of air temperature at dryer exit

The performance of a drying system can be impacted both positively and negatively by the temperature of the moist air exiting the drying chamber. This effect is considered for three exit temperatures, 30°C, 35°C and 40°C at fixed exit air relative humidity of 55%. These exit temperatures are hitherto labelled as System A, B and C respectively.

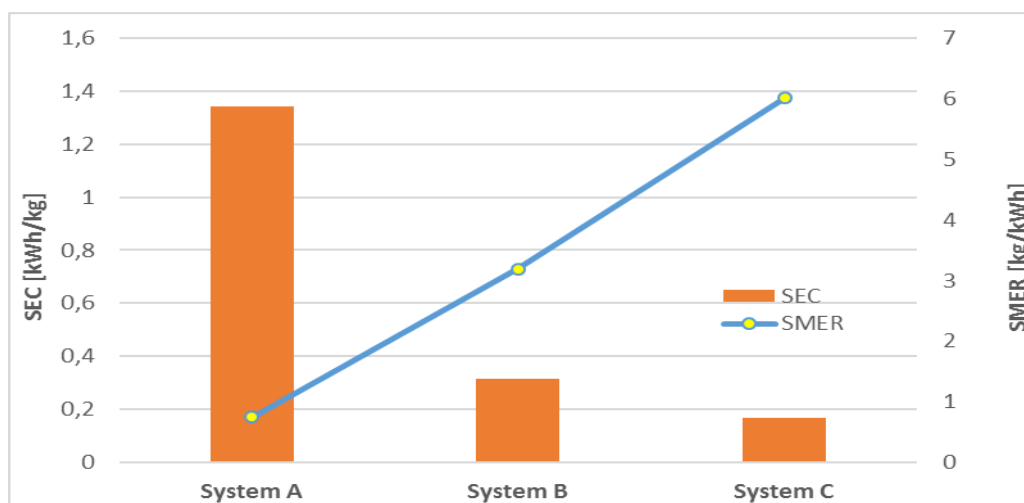


Figure 6.17: Variation of dryer exit temperature at fixed relative humidity

As shown in figure 6.17 above, System C has the highest SMER at 6.01 kg/kWh, which is about 47% and 88% higher than the Systems B and C respectively. It also has the lowest SEC accordingly thereby presenting the best system operation. The high performance attributed to System C is due to a very high enthalpy and relatively high moisture content at the exit conditions. Since its desirable to have high performance system, high exit temperature of the moist air will be most preferred.

6.6.5.2 Effect of relative humidity at the outlet of the dryer

Another parameter that influences the performance of the drying process is the relative humidity of the moist air at the exit of the dryer. At a fixed exit temperature of 35°C and relative humidity values of 45%, 55% and 80% are labelled as systems A, B and C representing the various operating conditions.

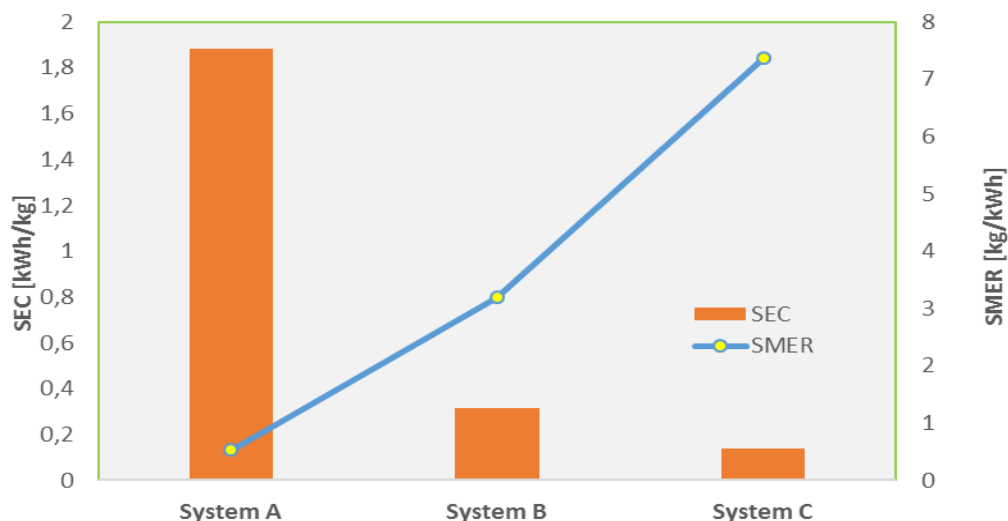


Figure 6.18: Variation of dryer exit humidity at fixed exit temperature

Figure 6.18 presents the performance of the different system are discussed as follows. The system C with the highest relative humidity gave the highest SMER and lowest SEC values of 7.36 kg/kWh and 0.14 kWh/kg, depicting a very effective performance which is 57% and 93% relative to systems B and A respectively. The results further implies that the influence of the relative humidity of exit air is as important as its exit temperature.

6.6.6 Integration of the dryer with the air evaporator

Integration of the dryer with the air evaporator is considered for a more compact and flexible design. The air at the exit of the drying chamber is utilized as the heat source for the air evaporator for space cooling. Considering the same operating demands and conditions highlighted in section 6.5, the exit air conditions for the dryer was adjusted to match the inlet conditions of the air evaporator. The exit temperature of the dryer without integration at 35°C is adjusted to 28°C, which is the inlet temperature of the air inflow into the evaporator and an inlet temperature of 22°C into the heat exchanger for heating. However, a constraint of relative humidity of maximum 60% is set for indoor comfort purpose.

The corresponding integrated system results in SMER and SEC values of 1.74 kg/kWh and 0.58 kWh/kg respectively which depicts a system performance 49% less effective than when integration is not considered. Henceforth for cooling load of 2.37 kW, a simultaneous operation of the heat pump system for both space cooling and drying without integration is the most preferred by performance.

CHAPTER 7. CONCLUSION AND FURTHER WORK

As shown in both the simulations and experimental results, there potentials of better heat pump performance with integrating of solar energy. The heating capacity of the system will increase with no negative impact on the overall performance of the heat pump. With the increase in the heating capacity, the range of application can widened to cover simultaneous water heating and drying purposes. Supplementary-cooling load can be generated from the solar collector for refrigeration purposes.

Integrating the exit flow of the dryer, as heat source for air evaporator will further increase the overall energy efficiency of integrated system. Although this was not possible at a low air evaporator capacity of 2.37 kW, its applicability at a higher capacity of 2.73 kW was established.

The CO₂ heat pump featured well among alternative refrigerants, with R410a having a relatively performance value to that of CO₂, R134a performed lesser.

For this study, only the series connection of the evaporators was considered, further studies should be carried out on alternative connections. The solar collector (glycol evaporator) was only integrated with the low pressure even though it has potential of improving the system even better when integrated with high pressure side. Experimental investigation should be carried out to justify this assumption.

The theoretical analysis of the dryer integration with the heat pump cycle looks quite promising. Implementation of a real solar collector should also be considered, to predict the efficiency of solar collectors and their impact on the overall performance. A complete test rig illustrated as figure 3.14 in section 3.6.2 should considered for construction. This will be a big step in the right direction in the research and development of prospective domestic solar assisted CO₂ integrated heat pumps.

NOMENCLATURE

Abbreviations

CO ₂	Carbon dioxide
HFC	Hydrofluorocarbon
R744	Carbon dioxide
ODP	ozone depletion potential
GWP	global warming potentials
COP	coefficient of performance
IHE	intermediate heat exchanger
SMER	Specific moisture content
SEC	Specific energy consumption
SEER	Seasonal energy efficiency

Symbols

h	Specific enthalpy (kJ kg ⁻¹)
\dot{m}	Mass flow rate (kg s ⁻¹)
s	Specific entropy (kJ kg ⁻¹ K ⁻¹)
T	Temperature (°C)
v	Velocity (m s ⁻¹)
V	Volumetric flow rate (m ³ s ⁻¹)
w	Specific compression work (kJ kg ⁻¹)
W	Power (kW)
ΔP	pressure drop (kPa)
ΔT	Temperature difference (K)
η	Component efficiency (-)
Π_s	suction pressure ratio (-)
ρ	Density (kg m ⁻³)
Φ_m	mass entrainment ratio (-)

Subscripts

in	inlet
out	outlet
is	isentropic
evap	evaporator
comp	compressor
sep	separator
liq	liquid
sat	saturation

References

- Bantle, M., Kvalsvik, K.H. and Tolstorebrov, I., 2016. Performance simulation of a Heat Pump Drying System using R744 as refrigerant. In *Proceedings of the 12th IIR Gustav Lorentzen Conference on Natural Refrigerants GL2016, 21-24 August 2016, Edinburgh, UK*.
- Ceylan, I., Aktaş, M. and Doğan, H., 2007. Energy and exergy analysis of timber dryer assisted heat pump. *Applied Thermal Engineering*, 27(1), pp.216-222.
- Klöcker, K., Schmidt, E.L. and Steimle, F., 2001. Carbon dioxide as a working fluid in drying heat pumps. *International journal of refrigeration*, 24(1), pp.100-107.
- Sarkar, J., Bhattacharyya, S. and Gopal, M.R., 2006. Transcritical CO₂ heat pump dryer: Part 1. Mathematical model and simulation. *Drying technology*, 24(12), pp.1583-1591.
- Klöcker, K., Schmidt, E.L. and Steimle, F., 2002. A drying heat pump using carbon dioxide as working fluid. *Drying technology*, 20(8), pp.1659-1671.
- Lorentzen, G., 1994. Revival of carbon dioxide as a refrigerant. *International journal of refrigeration*, 17(5), pp.292-301.
- Nekså, P., Rekstad, H., Zakeri, G.R. and Schiefloe, P.A., 1998. CO₂-heat pump water heater: characteristics, system design and experimental results. *International Journal of refrigeration*, 21(3), pp.172-179.
- Stene, J., 2007. Integrated CO₂ heat pump systems for space heating and hot water heating in low-energy houses and passive houses. *International Energy Agency (IEA) Heat Pump Programme–Annex*, 32.
- Gestore dei Servizi Energetici 2015. Assessment of the National potential for high-efficiency cogeneration and efficient district heating. https://ec.europa.eu/energy/sites/ener/files/documents/cz_report_eed_art_141_en.pdf
- Lapillonne, B., Pollier, K. and Samci, N., 2014. Energy efficiency trends for households in the EU. *Enerdata*. Retrieved June, 22, p.2015.
- Communication from the Commission to the European Parliament, the Council, the European Economic and Social Committee and the Committee of the Regions on an EU Strategy for Heating and Cooling. <https://ec.europa.eu/transparency/regdoc/rep/1/2016/EN/1-2016-51-EN-F1-1.PDF>
- Sarbu, I. and Sebarchievici, C., 2014. General review of ground-source heat pump systems for heating and cooling of buildings. *Energy and buildings*, 70, pp.441-454.
- Barber, E.M. and Provey, J., 2010. *Convert your home to solar energy*. Taunton Press.
- Sukhatme, K. and Sukhatme, S.P., 1996. *Solar energy: principles of thermal collection and storage*. Tata McGraw-Hill Education.
- Bakari, R., Minja, R.J. and Njau, K.N., 2014. Effect of glass thickness on performance of flat plate solar collectors for fruits drying. *Journal of Energy*, 2014.

Islam, M.R. and Sumathy, K., 2013. Carbon dioxide driven solar-assisted heat pump water heating System: A theoretical analysis. *Int. Res. J. Env. Sciences*, 2(10), pp.77-92.

Desai, N.B. and Bandyopadhyay, S., 2016. Line-focusing concentrating solar collector-based power plants: a review. *Clean Technologies and Environmental Policy*, 1(19), pp.9-35.

Francipane, A., Pumo, D., Viola, F., Noto, L.V. and Noto, M.T., Long term analysis of small desalination plant for potable water supply of tourist areas (in Sicily). Available online: https://www.researchgate.net/publication/257116870_Long_term_analysis_of_small_desalination_plant_for_potable_water_supply_of_tourist_areas_in_Sicily (accessed on 3 August 2016).

Samdarshi, S.K. and Mullick, S.C., 1990. Analysis of the top heat loss factor of flat plate solar collectors with single and double glazing. *International Journal of Energy Research*, 14(9), pp.975-990.

Struckmann, F., 2008. Analysis of a flat-plate solar collector. *Heat and Mass Transport, Project Report, 2008MVK160*.

Agbo, S.N. and Okoroigwe, E.C., 2007. Analysis of thermal losses in the flat-plate collector of a Thermosyphon Solar water Heater. *Research journal of physics*, 1(1), pp.35-41.

Xu, G., Zhang, X. and Deng, S., 2006. A simulation study on the operating performance of a solar–air source heat pump water heater. *Applied Thermal Engineering*, 26(11), pp.1257-1265.

Hadorn, J.C., 2012. IEA solar and heat pump systems Solar heating and cooling Task 44 & heat pump programme Annex 38. *Energy Procedia*, 30, pp.125-133.

Cooling, A.H.H., 2008. Systems and equipment. *SI edition, US: American Society of Heating Refrigerating and Air-Conditioning Engineers (ASHRAE), Atlanta, GA*.

<https://www.homepower.com/articles/solar-water-heating/domestic-hot-water/heat-pump-water-heaters/page/0/2?v=print>

Cecchinato, L., Corradi, M., Fornasieri, E. and Zamboni, L., 2005. Carbon dioxide as refrigerant for tap water heat pumps: a comparison with the traditional solution. *International Journal of Refrigeration*, 28(8), pp.1250-1258.

Morrison G, Anderson T, Behnia M. Seasonal performance rating of heat pump water heaters. *Solar Energy* 2004;76:147–52.

Kim, M., Kim, M.S. and Chung, J.D., 2004. Transient thermal behavior of a water heater system driven by a heat pump. *International journal of refrigeration*, 27(4), pp.415-421.

Chen, Y. and Gu, J., 2005. The optimum high pressure for CO₂ transcritical refrigeration systems with internal heat exchangers. *International Journal of Refrigeration*, 28(8), pp.1238-1249.

Sarkar, J., Bhattacharyya, S. and Gopal, M.R., 2006. Simulation of a transcritical CO₂ heat pump cycle for simultaneous cooling and heating applications. *International Journal of Refrigeration*, 29(5), pp.735-743.

- Yokoyama, R., Shimizu, T., Ito, K. and Takemura, K., 2007. Influence of ambient temperatures on performance of a CO₂ heat pump water heating system. *Energy*, 32(4), pp.388-398.
- Laipradit, P., Tiansuwan, J., Kiatsiriroat, T. and Aye, L., 2008. Theoretical performance analysis of heat pump water heaters using carbon dioxide as refrigerant. *International Journal of Energy Research*, 32(4), pp.356-366.
- Qi, P.C., He, Y.L., Wang, X.L. and Meng, X.Z., 2013. Experimental investigation of the optimal heat rejection pressure for a transcritical CO₂ heat pump water heater. *Applied Thermal Engineering*, 56(1), pp.120-125.
- Daghigh, R., Ruslan, M.H., Sulaiman, M.Y. and Sopian, K., 2010. Review of solar assisted heat pump drying systems for agricultural and marine products. *Renewable and Sustainable Energy Reviews*, 14(9), pp.2564-2579.
- Klöcker, K., Schmidt, E.L. and Steimle, F., 2001. Carbon dioxide as a working fluid in drying heat pumps. *International journal of refrigeration*, 24(1), pp.100-107.
- Conde, M.R., 1997. Energy conservation with tumbler drying in laundries. *Applied thermal engineering*, 17(12), pp.1163-1172.
- Colak, N. and Hepbasli, A., 2009. A review of heat-pump drying (HPD): Part 2—Applications and performance assessments. *Energy Conversion and Management*
- Klöcker, K., Schmidt, E.L. and Steimle, F., 2002. A drying heat pump using carbon dioxide as working fluid. *Drying technology*, 20(8), pp.1659-1671.
- Braun, J.E., Bansal, P.K. and Groll, E.A., 2002. Energy efficiency analysis of air cycle heat pump dryers. *International Journal of Refrigeration*, 25(7), pp.954-965.
- Ameen, A. and Bari, S., 2004. Investigation into the effectiveness of heat pump assisted clothes dryer for humid tropics. *Energy conversion and Management*, 45(9), pp.1397-1405.
- Ambarita, H., Nasution, D.M., Gunawan, S. and Nasution, A.H., 2017, March. Performance and Characteristics of Heat Pump Clothes Drier. In *IOP Conference Series: Materials Science and Engineering* (Vol. 180, No. 1, p. 012027). IOP Publishing.
- Deng, S. and Han, H., 2004. An experimental study on clothes drying using rejected heat (CDURH) with split-type residential air conditioners. *Applied thermal engineering*, 24(17), pp.2789-2800.
- Bansal, P., Islam, S. and Sharma, K., 2010. A novel design of a household clothes tumbler dryer. *Applied Thermal Engineering*, 30(4), pp.277-285.
- Bansal, P., Sharma, K. and Islam, S., 2010. Thermal analysis of a new concept in a household clothes tumbler dryer. *Applied Energy*, 87(5), pp.1562-1571.
- Deans, J., 2001. The modelling of a domestic tumbler dryer. *Applied Thermal Engineering*, 21(9), pp.977-990.
- Bengtsson, P., Berghel, J. and Renström, R., 2014. Performance study of a closed-type heat pump tumble dryer using a simulation model and an experimental set-up. *Drying technology*, 32(8), pp.891-901.

Yamankaradeniz, N., Sokmen, F.K., Coskun, S., Kaynakli, O. and Pastakkaya, B., 2016. Performance analysis of a re-circulating heat pump dryer. *Thermal Science*, 20(1), pp.267-277.

Dudley, K.F., Paige, L.E. and Dunshee, K.B., Electric Power Research Institute, Inc., 1991. *Controllable variable speed heat pump for combined water heating and space cooling*. U.S. Patent 5,050,394.

Harmon, S. and You, Y., Quantum Energy Technologies Pty Limited, 2007. *Energy efficient heat pump systems for water heating and air conditioning*. U.S. Patent 7,155,922.

Richter, M.R., Song, S.M., Yin, J.M., Kim, M.H., Bullard, C.W. and Hrnjak, P.S., 2003. Experimental results of transcritical CO₂ heat pump for residential application. *Energy*, 28(10), pp.1005-1019.

Ji, J., Chow, T.T., Pei, G., Dong, J. and He, W., 2003. Domestic air-conditioner and integrated water heater for subtropical climate. *Applied Thermal Engineering*, 23(5), pp.581-592.

Techarungpaisan, P., Theerakulpisut, S. and Priprem, S., 2007. Modeling of a split type air conditioner with integrated water heater. *Energy Conversion and Management*, 48(4), pp.1222-1237.

Byrne, P., Miriel, J. and Lenat, Y., 2009. Design and simulation of a heat pump for simultaneous heating and cooling using HFC or CO₂ as a working fluid. *International Journal of Refrigeration*, 32(7), pp.1711-1723.

Belman-Flores, J.M., Pérez-García, V., Ituna-Yudonago, J.F., Rodríguez-Muñoz, J.L. and Ramírez-Minguela, J.D.J., 2014. General aspects of carbon dioxide as a refrigerant. *Journal of Energy in Southern Africa*, 25(2), pp.96-106.

<https://hub.globalccsinstitute.com/publications/hazard-analysis-offshore-carbon-capture-platforms-and-offshore-pipelines/21-properties-co2>

Taylor, C.R., 2002. Carbon dioxide-based refrigerant systems. *ASHRAE journal*, 44(9), p.22.

Nekså, P., Walnum, H.T. and Hafner, A., 2010. CO₂-a refrigerant from the past with prospects of being one of the main refrigerants in the future. In *9th IIR Gustav Lorentzen conference* (pp. 2-14).

Lorentzen, G. and Pettersen, J., 1993. A new, efficient and environmentally benign system for car air-conditioning. *International Journal of Refrigeration*, 16(1), pp.4-12.

Prapainnop, R. and Suen, K.O., 2012. Effects of refrigerant properties on refrigerant performance comparison: A review. *International Journal of Engineering and Research and Applications*, 2, pp.486-493.

Kim, M.H., Pettersen, J. and Bullard, C.W., 2004. Fundamental process and system design issues in CO₂ vapor compression systems. *Progress in energy and combustion science*, 30(2), pp.119-174.

Working Document on a Draft COMMISSION DELEGATED REGULATION (EU) No [...] of [...] supplementing Directive 2010/30/EU of the European Parliament and of the Council with regard to energy labelling of water heaters, hot water storage tanks and packages of water heater and solar-only system. Given date: February 2nd 2012.


Appendix 1. Tapping Profile of Hot water

h	M				L				XL			
	Q_{tap}	f	T_m	T_p	Q_{tap}	f	T_m	T_p	Q_{tap}	f	T_m	T_p
	kWh	l/mn	°C	°C	kWh	l/min	°C	°C	kWh	l/min	°C	°C
07:00	0,105	3	25		0,105	3	25		0,105	3	25	
07:05	1,4	6	40		1,4	6	40					
07:15									1,82	6	40	
07:26									0,105	3	25	
07:30	0,105	3	25		0,105	3	25					
07:45					0,105	3	25		4,42	10	10	40
08:01	0,105	3	25						0,105	3	25	
08:05					3,605	10	10	40				
08:15	0,105	3	25						0,105	3	25	
08:25					0,105	3	25					
08:30	0,105	3	25		0,105	3	25		0,105	3	25	
08:45	0,105	3	25		0,105	3	25		0,105	3	25	
09:00	0,105	3	25		0,105	3	25		0,105	3	25	
09:30	0,105	3	25		0,105	3	25		0,105	3	25	
10:00									0,105	3	25	
10:30	0,105	3	10	40	0,105	3	10	40	0,105	3	10	40
11:00									0,105	3	25	
11:30	0,105	3	25		0,105	3	25		0,105	3	25	
11:45	0,105	3	25		0,105	3	25		0,105	3	25	
12:00												
12:30												
12:45	0,315	4	10	55	0,315	4	10	55	0,735	4	10	55
14:30	0,105	3	25		0,105	3	25		0,105	3	25	
15:00									0,105	3	25	
15:30	0,105	3	25		0,105	3	25		0,105	3	25	
16:00									0,105	3	25	
16:30	0,105	3	25		0,105	3	25		0,105	3	25	
17:00									0,105	3	25	
18:00	0,105	3	25		0,105	3	25		0,105	3	25	
18:15	0,105	3	40		0,105	3	40		0,105	3	40	
18:30	0,105	3	40		0,105	3	40		0,105	3	40	
19:00	0,105	3	25		0,105	3	25		0,105	3	25	
19:30												
20:00												
20:30	0,735	4	10	55	0,735	4	10	55	0,735	4	10	55
20:45												
20:46									4,42	10	10	40
21:00					3,605	10	10	40				
21:15	0,105	3	25						0,105	3	25	
21:30	1,4	6	40		0,105	3	25		4,42	10	10	40
21:30												
21:45												
Q_{ref}	5,845				11,655				19,07			

h	XXL				3XL				4XL			
	Q_{tap}	f	T_m	T_p	Q_{tap}	f	T_m	T_p	Q_{tap}	f	T_m	T_p
	kWh	l/min	°C	°C	kWh	l/min	°C	°C	kWh	l/min	°C	°C
07:00	0,105	3	25		11,2	48	40		22,4	96	40	
07:05												
07:15	1,82	6	40									
07:26	0,105	3	25									
07:30												
07:45	6,24	16	10	40								
08:01	0,105	3	25		5,04	24	25		10,08	48	25	
08:05												
08:15	0,105	3	25									
08:25												
08:30	0,105	3	25									
08:45	0,105	3	25									
09:00	0,105	3	25		1,68	24	25		3,36	48	25	
09:30	0,105	3	25									
10:00	0,105	3	25									
10:30	0,105	3	10	40	0,84	24	10	40	1,68	48	10	40
11:00	0,105	3	25									
11:30	0,105	3	25									
11:45	0,105	3	25		1,68	24	25		3,36	48	25	
12:00												
12:30												
12:45	0,735	4	10	55	2,52	32	10	55	5,04	64	10	55
14:30	0,105	3	25									
15:00	0,105	3	25									
15:30	0,105	3	25		2,52	24	25		5,04	48	25	
16:00	0,105	3	25									
16:30	0,105	3	25									
17:00	0,105	3	25									
18:00	0,105	3	25									
18:15	0,105	3	40									
18:30	0,105	3	40		3,36	24	25		6,72	48	25	
19:00	0,105	3	25									
19:30												
20:00												
20:30	0,735	4	10	55	5,88	32	10	55	11,76	64	10	55
20:45												
20:46	6,24	16	10	40								
21:00												
21:15	0,105	3	25									
21:30	6,24	16	10	40	12,04	48	40		24,08	96	40	
21:30												
21:45												
Q_{ref}	24,53				46,76				93,52			

Source: Working Document on a Draft COMMISSION DELEGATED REGULATION (EU) No [...] of [...] supplementing Directive 2010/30/EU of the European Parliament and of the Council with regard to energy labelling of water heaters, hot water storage tanks and packages of water heater and solar-only system. Given date: February 2nd 2012.

Appendix 2. RHVAC simulation result

Rhvac - Residential & Light Commercial HVAC Loads		Elite Software Development, Inc.				
Elite Software Development College Station, TX 77845		Thesis Page 2				
						
Project Report						
General Project Information						
Project Title:	Thesis					
Designed By:	Oluwafemi					
Project Date:	21.03.2017					
Client Name:	NTNU					
Client Address:	Trondheim					
Company Name:	Ept					
Design Data						
Reference City:	Milan, Italy					
Building Orientation:	Front door faces North					
Daily Temperature Range:	Medium					
Latitude:	45 Degrees					
Elevation:	337 ft.					
Altitude Factor:	0,988					
	<u>Outdoor Dry Bulb</u>	<u>Outdoor Wet Bulb</u>	<u>Outdoor Rel.Hum</u>	<u>Indoor Rel.Hum</u>	<u>Indoor Dry Bulb</u>	<u>Grains Difference</u>
Winter:	25	23,3	n/a	n/a	70	n/a
Summer:	87	72	49%	50%	75	30
Check Figures						
Total Building Supply CFM:	305		CFM Per Square ft.:	0,782		
Square ft. of Room Area:	390		Square ft. Per Ton:	576		
Volume (ft ³) (Above Grade):	3 120					
Volume (ft ³) (Total):	3 120					
Building Loads						
Total Heating Required Including Ventilation Air:	8 614 Btuh	8,614 MBH				
Total Sensible Gain:	8 821 Btuh	84 %				
Total Latent Gain:	1 306 Btuh	16 %				
Total Cooling Required Including Ventilation Air:	8 127 Btuh	0,68 Tons (Based On Sensible + Latent)				
Notes						
Rhvac is an ACCA approved Manual J and Manual D computer program.						
Calculations are performed per ACCA Manual J 8th Edition, Version 2, and ACCA Manual D.						
All computed results are estimates as building use and weather may vary.						
Be sure to select a unit that meets both sensible and latent loads according to the manufacturer's performance data at your design conditions.						



Miscellaneous Report

System 1 Major Input Data	Outdoor Dry Bulb	Outdoor Wet Bulb	Outdoor Rel.Hum	Indoor Rel.Hum	Indoor Dry Bulb	Grains Difference
Winter:	25	23,3	80%	n/a	70	n/a
Summer:	87	72	49%	50%	75	29,87

Duct Sizing Inputs

	Main Trunk	Runouts
Calculate:	Ja	Ja
Use Schedule:	Ja	Ja
Roughness Factor:	0,00300	0,01000
Pressure Drop:	0,1000 in.wg./100 ft.	0,1000 in.wg./100 ft.
Minimum Velocity:	650 ft./min	450 ft./min
Maximum Velocity:	900 ft./min	750 ft./min
Minimum Height:	0 in.	0 in.
Maximum Height:	0 in.	0 in.

Outside Air Data

	Winter	Summer
Infiltration Specified:	0,610 AC/hr 32 CFM	0,320 AC/hr 17 CFM
Infiltration Actual:	0,610 AC/hr	0,320 AC/hr
Above Grade Volume:	X 3,120 Cu.ft. 1 903 Cu.ft./hr X 0,0167	X 3,120 Cu.ft. 998 Cu.ft./hr X 0,0167
Total Building Infiltration:	32 CFM	17 CFM
Total Building Ventilation:	0 CFM	0 CFM

---System 1---

Infiltration & Ventilation Sensible Gain Multiplier:	13,04	= (1.10 X 0,988 X 12,00 Summer Temp. Difference)
Infiltration & Ventilation Latent Gain Multiplier:	20,07	= (0.68 X 0,988 X 29,87 Grains Difference)
Infiltration & Ventilation Sensible Loss Multiplier:	48,90	= (1.10 X 0,988 X 45,00 Winter Temp. Difference)
Winter Infiltration Specified:	0,610 AC/hr (32 CFM), Construction: Average	
Summer Infiltration Specified:	0,320 AC/hr (17 CFM), Construction: Average	

Duct Load Factor Scenarios for System 1

No.	Type	Description	Location	Attic Ceiling	Duct Leakage	Duct Insulation	Surface Area	From [T]MDD
1	Supply		Attic	16B	0,12	6	105	No
1	Return		Attic	16B	0,12	6	20	No



Duct Size Preview

Room or Duct Name	Source	Minimum Velocity	Maximum Velocity	Rough. Factor	Design L/100	SP Loss	Duct Velocity	Duct Length	Htg Flow	Clg Flow	Act. Flow	Duct Size
System 1												
Supply Runouts												
Zone 1												
1-Living Room	Built-In	450	750	0,01	0,1		481,0		46	131	131	2--5
2-Bedroom 1	Built-In	450	750	0,01	0,1		636,4		34	87	87	1--5
3-Bedroom 2	Built-In	450	750	0,01	0,1		636,4		34	87	87	1--5
Other Ducts in System 1												
Supply Main Trunk	Built-In	650	900	0,003	0,1		686,1		113	305	305	8x8

Summary

System 1

Heating Flow: 113

Cooling Flow: 305



Total Building Summary Loads

Component Description	Area Quan	Sen Loss	Lat Gain	Sen Gain	Total Gain
2B-w-o: Glazing-Double pane low-e (e = 0.60), fixed sash, wood frame, u-value 0,54, SHGC 0,66	44	1 070	0	2 556	2 556
11G: Door-Wood - Panel	21	510	0	261	261
12C-2bw: Wall-Frame, R-13 insulation in 2 x 4 stud cavity, R-2 board insulation, brick finish, wood studs	487	1 776	0	330	330
16C-19: Roof/Ceiling-Under Attic with Insulation on Attic Floor (also use for Knee Walls and Partition Ceilings), Vented Attic, No Radiant Barrier, White or Light Color Shingles, Any Wood Shake, Light Metal, Tar and Gravel or Membrane, R-19 insulation	390	861	0	708	708
22B-5rh: Floor-Slab on grade, Vertical board insulation covers slab edge and extends straight down to 3' below grade, any floor cover, R-5 insulation, radiant, heavy moist soil	69	2 845	0	0	0
Subtotals for structure:		7 062	0	3 855	3 855
People:	4		800	920	1 720
Equipment:			0	0	0
Lighting:	200			682	682
Ductwork:		0	173	1 147	1 320
Infiltration: Winter CFM: 32, Summer CFM: 17		1 552	333	217	550
Ventilation: Winter CFM: 0, Summer CFM: 0		0	0	0	0
Total Building Load Totals:		8 614	1 306	6 821	8 127

Check Figures

Total Building Supply CFM:	305	CFM Per Square ft.:	0,782
Square ft. of Room Area:	390	Square ft. Per Ton:	576
Volume (ft ³) (Above Grade):	3 120		
Volume (ft ³) (Total):	3 120		

Building Loads

Total Heating Required Including Ventilation Air:	8 614 Btuh	8,614 MBH
Total Sensible Gain:	6 821 Btuh	84 %
Total Latent Gain:	1 306 Btuh	16 %
Total Cooling Required Including Ventilation Air:	8 127 Btuh	0,68 Tons (Based On Sensible + Latent)

Notes

Rhvac is an ACCA approved Manual J and Manual D computer program.

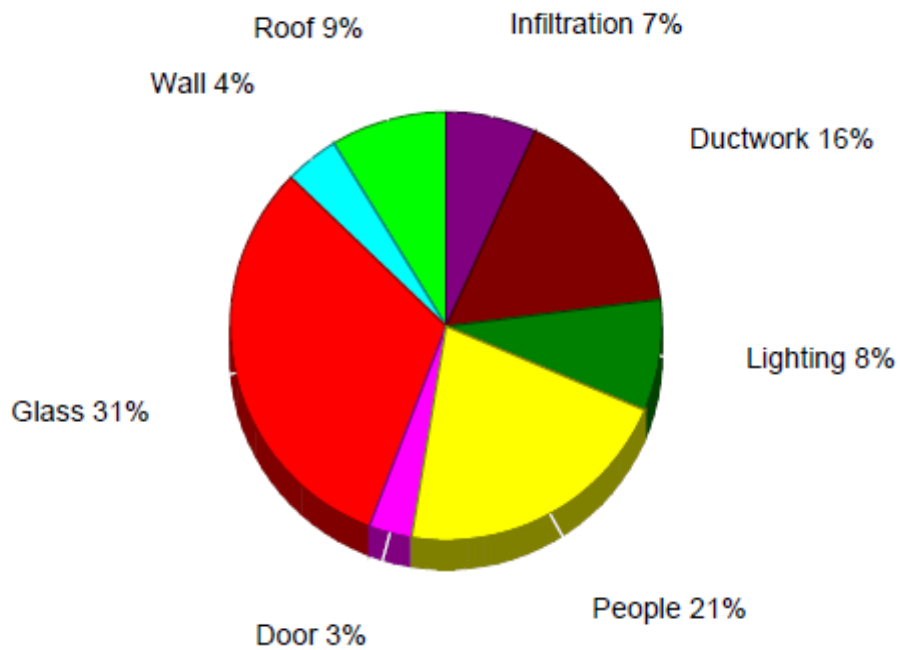
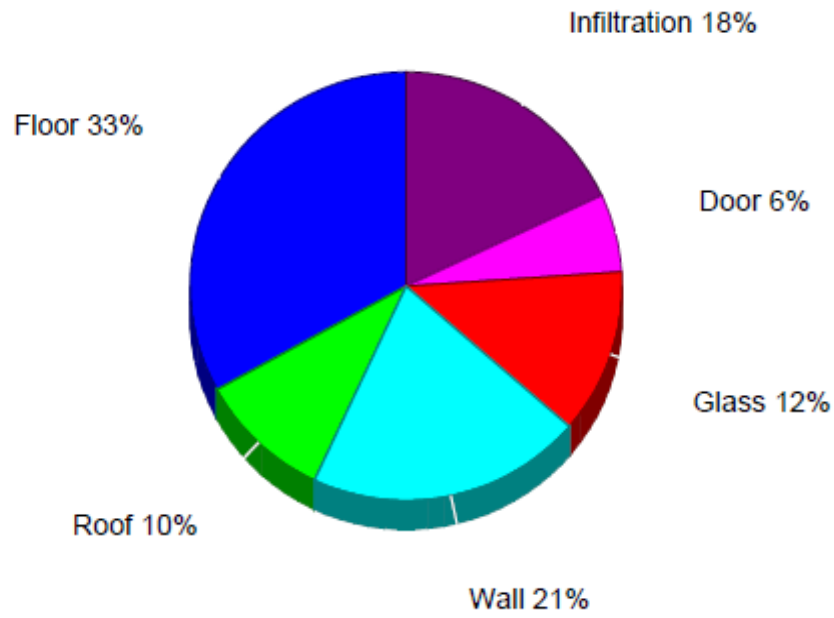
Calculations are performed per ACCA Manual J 8th Edition, Version 2, and ACCA Manual D.

All computed results are estimates as building use and weather may vary.

Be sure to select a unit that meets both sensible and latent loads according to the manufacturer's performance data at your design conditions.



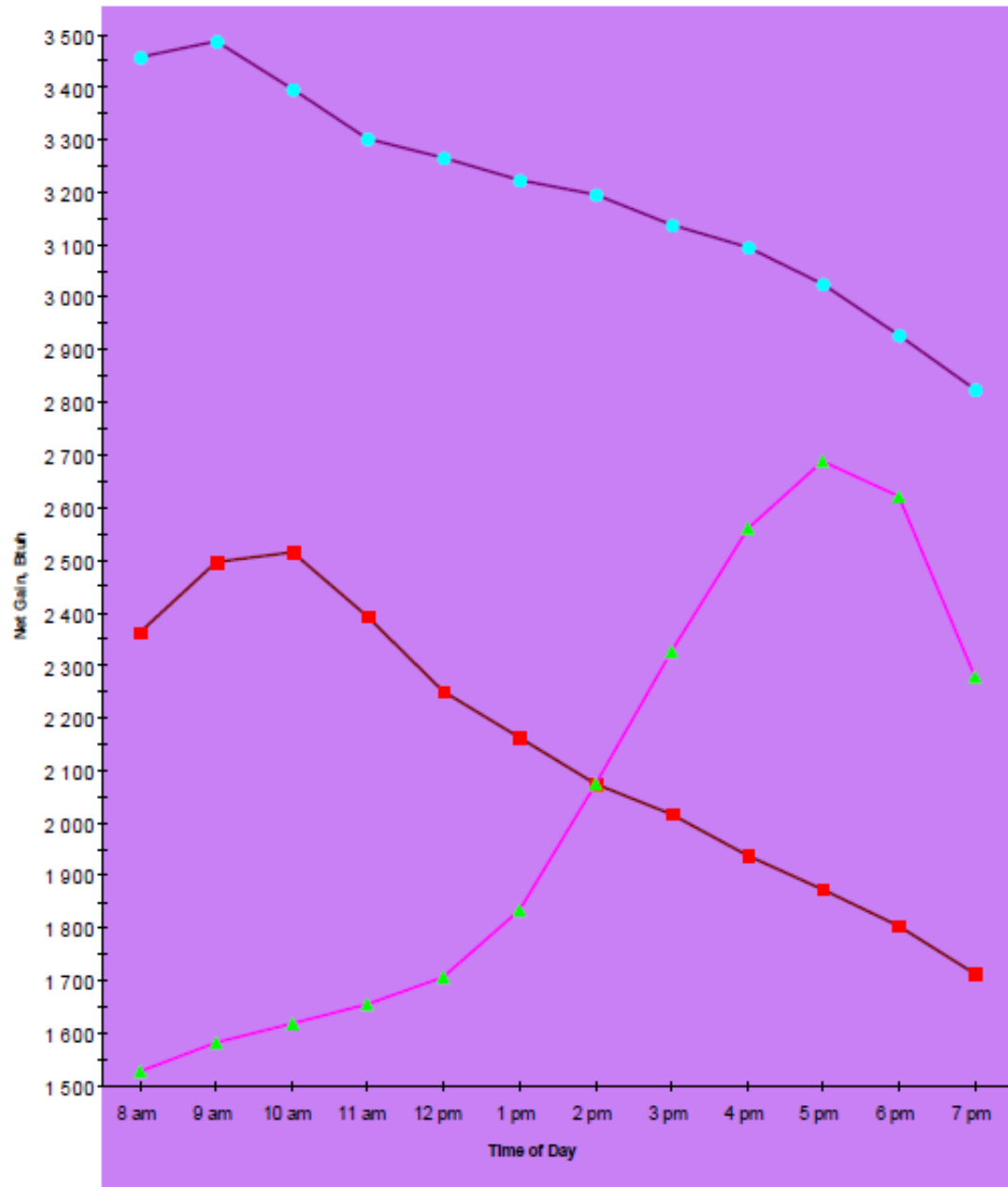
Building Pie Chart





System 1 - Hourly Room Net Gain


System 1 Hourly Room Net Gain



- Living Room (27%)
- Bedroom 1 (37%)
- ▲— Bedroom 2 (37%)

Note: Glass gain as a percent of net gain is shown in parenthesis. Although floor, roof, wall and door gains also vary throughout the day, for this graph and in Manual J glass gains are the only ones that fluctuate.

R HVAC - Residential & Light Commercial HVAC Loads					Elite Software Development, Inc.				
Elite Software Development College Station, TX 77845					Thesis Page 19				



Building Rotation Report

All rotation degree values in this report are clockwise with respect to the project's original orientation.
 Building orientation as entered (zero degrees rotation): Front door faces North

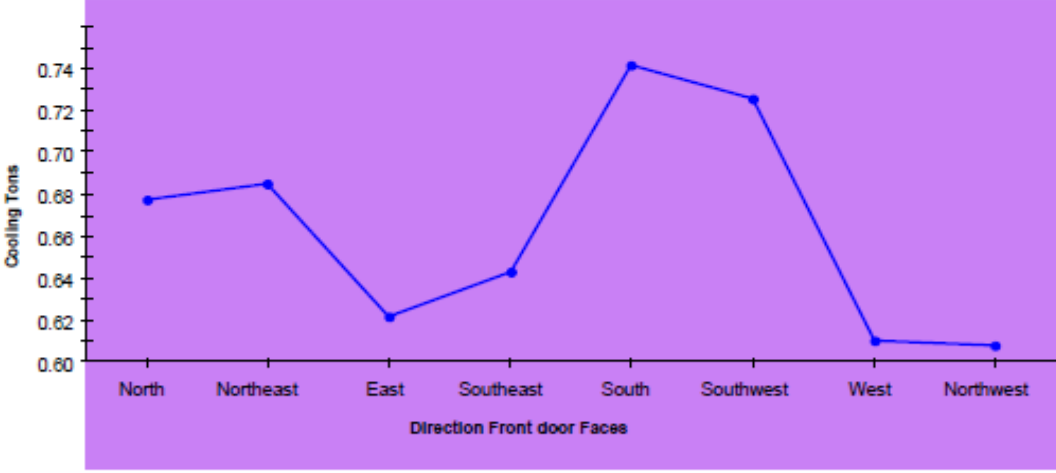
Individual Rooms										
Rm. No.	Room Name	0° Rot. CFM	45° Rot. CFM	90° Rot. CFM	135° Rot. CFM	180° Rot. CFM	225° Rot. CFM	270° Rot. CFM	315° Rot. CFM	High Duct Size
System 1:										
Zone 1:										
1	Living Room	131	155	150	126	156	*188	139	106	2-5
2	Bedroom 1	87	82	68	85	*92	78	58	76	1-6
3	Bedroom 2	87	73	56	75	*92	88	71	85	1-6

* Indicates highest CFM of all rotations.

Whole Building						
Rotation Degrees	Front door Faces	Supply CFM	Sensible Gain	Latent Gain	Net Tons	
0°	North	305	6 821	1 306	0,68	
45°	Northeast	309	6 917	1 305	0,69	
90°	East	274	6 151	1 305	0,62	
135°	Southeast	286	6 412	*1 306	0,64	
180°	South	*341	*7 595	1 305	*0,74	
225°	Southwest	332	7 405	1 305	0,73	
270°	West	268	6 016	1 305	0,61	
315°	Northwest	267	5 990	1 305	0,61	

* Indicates highest value of all rotations.

Building Rotation Tonnage



Direction	Net Tons
North	0.68
Northeast	0.69
East	0.62
Southeast	0.64
South	0.74
Southwest	0.73
West	0.61
Northwest	0.61

Appendix 3: TEST RESULTS

SET CONDITIONS	Unit	Value
----------------	------	-------

Air Evaporator Capacity	kW	2.37
Air temperature, inlet of evaporator	°C	28.12
Air evaporator, outlet of evaporator	°C	22.03
Air flow rate	Kg/s	0.4
Glycol temperature, inlet of evaporator	°C	28.01
Evaporating temperature	°C	10
High side pressure	Bar	85
HEAT PUMP PERFORMANCE		
Air Evaporator		
CO2 inlet temperature	°C	9.99
CO2 outlet temperature	°C	27.69
Evaporator superheat	K	17.70
Mass flow rate of the CO2	Kg/s	0,0138
Glycol Evaporator		
CO2 inlet temperature	°C	9.99
CO2 outlet temperature	°C	26.91
Evaporator superheat	K	16.92
Mass flow rate of the CO2	Kg/s	0.293
Suction heat exchanger		
CO2 inlet temperature	°C	26.21
CO2 outlet temperature	°C	30.05
Superheat	K	3.84
Mass flow rate of the CO2	Kg/s	0.432
Compressor		
Suction pressure	bar	45
Discharge line pressure	bar	84
CO2 inlet temperature	°C	30.05
CO2 outlet temperature	°C	92.90
CO2 temperature outlet of oil separator	°C	85.97
Mass flow rate of the CO2	Kg/s	0.0432
Glycol gas cooler		
High side Pressure	bar	85
CO2 inlet temperature	°C	85.97
CO2 outlet temperature	°C	44.01
Water Gas cooler		
CO2 inlet temperature	°C	39.80
CO2 inlet temperature	°C	31,23
Water inlet temperature	°C	12
Test No: 2		
SET CONDITIONS		
Air Evaporator Capacity	Unit kW	Value 2.37

Air temperature, inlet of evaporator	°C	27.93
Air evaporator, outlet of evaporator	°C	22.22
Air flow rate	Kg/s	0.416
Glycol temperature, inlet of evaporator	°C	28
Evaporating temperature	°C	5.31
High side pressure	Bar	80
HEAT PUMP PERFORMANCE		
Air Evaporator		
CO2 inlet temperature	°C	5.37
CO2 outlet temperature	°C	26.16
Evaporator superheat	K	20.79
Mass flow rate of the CO2	Kg/s	0.135
Glycol Evaporator		
CO2 inlet temperature	°C	5.37
CO2 outlet temperature	°C	26.97
Evaporator superheat	K	21.6
Mass flow rate of the CO2	Kg/s	0.277
Suction heat exchanger		
CO2 inlet temperature	°C	25.89
CO2 outlet temperature	°C	27.97
Superheat	K	2.08
Mass flow rate of the CO2	Kg/s	0.412
Compressor		
Suction pressure	bar	40
Discharge line pressure	bar	80
CO2 inlet temperature	°C	27.97
CO2 outlet temperature	°C	97.70
CO2 temperature outlet of oil separator	°C	90.37
Mass flow rate of the CO2	Kg/s	0.412
Glycol gas cooler		
High side Pressure	bar	80
CO2 inlet temperature	°C	90.37
CO2 outlet temperature	°C	37.94
Water Gas cooler		
CO2 inlet temperature	°C	35.88
CO2 inlet temperature	°C	30.50
Water inlet temperature	°C	11.88
Test No: 3		
SET CONDITIONS		
Air Evaporator Capacity	Unit kW	Value 2.37

Air temperature, inlet of evaporator	°C	28.78
Air evaporator, outlet of evaporator	°C	22.14
Air flow rate	Kg/s	0.36
Glycol temperature, inlet of evaporator	°C	27.9
Evaporating temperature	°C	10.05
High side pressure	Bar	80
HEAT PUMP PERFORMANCE		
Air Evaporator		
CO2 inlet temperature	°C	10.05
CO2 outlet temperature	°C	21.8
Evaporator superheat	K	11.75
Mass flow rate of the CO2	Kg/s	0.015
Glycol Evaporator		
CO2 inlet temperature	°C	10.05
CO2 outlet temperature	°C	25.03
Evaporator superheat	K	14.97
Mass flow rate of the CO2	Kg/s	0.0317
Suction heat exchanger		
CO2 inlet temperature	°C	23.44
CO2 outlet temperature	°C	28.90
Superheat	K	5.46
Mass flow rate of the CO2	Kg/s	0.0467
Compressor		
Suction pressure	bar	45
Discharge line pressure	bar	80
CO2 inlet temperature	°C	28.9
CO2 outlet temperature	°C	89.5
CO2 temperature outlet of oil separator	°C	83.7
Mass flow rate of the CO2	Kg/s	0.0467
Glycol gas cooler		
High side Pressure	bar	80
CO2 inlet temperature	°C	83.7
CO2 outlet temperature	°C	38.45
Water Gas cooler		
CO2 inlet temperature	°C	34.43
CO2 inlet temperature	°C	31.2
Water inlet temperature	°C	12
Test No: 4		
SET CONDITIONS	Unit	Value
Air Evaporator Capacity	kW	2.75

Air temperature, inlet of evaporator	°C	30
Air evaporator, outlet of evaporator	°C	20.1
Air flow rate	Kg/s	0.27
Glycol temperature, inlet of evaporator	°C	30
Evaporating temperature	°C	9.99
High side pressure	Bar	90
HEAT PUMP PERFORMANCE		
Air Evaporator		
CO2 inlet temperature	°C	9.99
CO2 outlet temperature	°C	29.63
Evaporator superheat	K	19.64
Mass flow rate of the CO2	Kg/s	0.0153
Glycol Evaporator		
CO2 inlet temperature	°C	9.99
CO2 outlet temperature	°C	21.39
Evaporator superheat	K	11.4
Mass flow rate of the CO2	Kg/s	0.0263
Suction heat exchanger		
CO2 inlet temperature	°C	26.3
CO2 outlet temperature	°C	28.75
Superheat	K	2.45
Mass flow rate of the CO2	Kg/s	0.0417
Compressor		
Suction pressure	bar	45
Discharge line pressure	bar	90
CO2 inlet temperature	°C	28.75
CO2 outlet temperature	°C	96.23
CO2 temperature outlet of oil separator	°C	92.07
Mass flow rate of the CO2	Kg/s	0.0417
Glycol gas cooler		
High side Pressure	bar	90
CO2 inlet temperature	°C	92.07
CO2 outlet temperature	°C	42.83
Water Gas cooler		
CO2 inlet temperature	°C	40.48
CO2 inlet temperature	°C	31.03
Water inlet temperature	°C	12

Test No: 5		
SET CONDITIONS	Unit	Value

Air Evaporator Capacity	kW	2.77
Air temperature, inlet of evaporator	°C	30
Air evaporator, outlet of evaporator	°C	20
Air flow rate	Kg/s	0.28
Glycol temperature, inlet of evaporator	°C	22.22
Evaporating temperature	°C	9.99
High side pressure	Bar	80
HEAT PUMP PERFORMANCE		
Air Evaporator		
CO2 inlet temperature	°C	9.99
CO2 outlet temperature	°C	29.01
Evaporator superheat	K	19.02
Mass flow rate of the CO2	Kg/s	0.016
Glycol Evaporator		
CO2 inlet temperature	°C	9.99
CO2 outlet temperature	°C	12.22
Evaporator superheat	K	2.23
Mass flow rate of the CO2	Kg/s	0.032
Suction heat exchanger		
CO2 inlet temperature	°C	17
CO2 outlet temperature	°C	21.88
Superheat	K	4.88
Mass flow rate of the CO2	Kg/s	0.0475
Compressor		
Suction pressure	bar	45
Discharge line pressure	bar	80
CO2 inlet temperature	°C	21.88
CO2 outlet temperature	°C	82.06
CO2 temperature outlet of oil separator	°C	75.88
Mass flow rate of the CO2	Kg/s	0.0475
Glycol gas cooler		
High side Pressure	bar	80
CO2 inlet temperature	°C	75.88
CO2 outlet temperature	°C	41.85
Water Gas cooler		
CO2 inlet temperature	°C	36.85
CO2 inlet temperature	°C	30.43
Water inlet temperature	°C	12
Test No: 6		
SET CONDITIONS	Unit	Value

Air Evaporator Capacity	kW	2.73
Air temperature, inlet of evaporator	°C	20.09
Air evaporator, outlet of evaporator	°C	30.1
Air flow rate	Kg/s	0.273
Glycol temperature, inlet of evaporator	°C	22
Evaporating temperature	°C	5.30
High side pressure	Bar	85
HEAT PUMP PERFORMANCE		
Air Evaporator		
CO2 inlet temperature	°C	5.30
CO2 outlet temperature	°C	28.79
Evaporator superheat	K	23.49
Mass flow rate of the CO2	Kg/s	0.015
Glycol Evaporator		
CO2 inlet temperature	°C	5.3
CO2 outlet temperature	°C	16.56
Evaporator superheat	K	11.26
Mass flow rate of the CO2	Kg/s	0.027
Suction heat exchanger		
CO2 inlet temperature	°C	18.27
CO2 outlet temperature	°C	25.01
Superheat	K	6,74
Mass flow rate of the CO2	Kg/s	0.0423
Compressor		
Suction pressure	bar	40
Discharge line pressure	bar	85
CO2 inlet temperature	°C	25.01
CO2 outlet temperature	°C	95.12
CO2 temperature outlet of oil separator	°C	87.87
Mass flow rate of the CO2	Kg/s	0.0423
Glycol gas cooler		
High side Pressure	bar	85
CO2 inlet temperature	°C	87.87
CO2 outlet temperature	°C	45.20
Water Gas cooler		
CO2 inlet temperature	°C	40.4
CO2 inlet temperature	°C	30.2
Water inlet temperature	°C	12



CO₂ Solar Assisted Heat Pump System for Water heating, Drying and Cooling

Oluwafemi Nana

ABSTRACT

Improvising the solar collector with a glycol evaporator, additional heat was absorbed into the system, thereby increasing the heating capacity of the heat pump. The cooling load reference for the air evaporator ranges from 2.37 to 2.73 kW. A single transcritical heat pump was simulated in Pack calculation to predict the behavior of the system with only the air evaporator. Depending on the amount of heat supplied from glycol, a heat increase of twice the it's initial capacity was recorded.

The system parameters were varied to predict their influence on system performance. At 2.37 kW cooling load, the highest COP of 3.97 and 3.67 for heating and cooling at an evaporation temperature of 10°C with a high side pressure of 84 bar. At a cooling load of 2.73 kW, the highest obtainable COP for heating and Cooling were 4.04 and 3.55 respectively at an evaporation temperature of 10°C and high side pressure of 90 bar. The seasonal energy efficiency ratio (SEER) rating of the air evaporator was also performed. The performance of the system for drying applications was also carried out with a potential drying efficiency of 66% calculated. It was further discovered that integrating the dryer with the air evaporator at 2.73 kW cooling capacity, the drying efficiency increased to about 75%.

Keywords – CO₂ solar assisted heat pumps, solar collector, drying, space cooling, and performance indicators.

1. INTRODUCTION

CO₂ heat pumps have been highlighted as the solution for present and future heat pump and refrigeration challenges associated with other heat pump systems. With emphasis on a greener world, which has led to the re-emergence of natural working fluids, previous studies has shown CO₂ heat pump systems to possess better system performance, safety, availability and with huge potentials. One of such potentials is the recovery and utilization of waste heat/energy in a heat pump systems with aim of improving system efficiency while also proving to be a useful application. The integrated systems typically consist of two or more different process cycles. The integration is such that it which comprises of a primary refrigeration cycle and another cycle which can be used for secondary applications. The secondary application can either be in a single, dual or multiple mode.

During the CO₂ heat pump process, a lot of heat accompanies the compression of the working fluid. This heat is removed from during gas cooling or condensation and is considered a waste. This waste heat can be harnessed. When harnessed, this recovered heat is put into useful work such as space heating, hot water heating, drying and other applications. This supplement the primary work being done and hence better energy efficiency of system is achieved. This will not only enhance the

system performance, but also will lead to decrease in total energy demand, which hitherto has been supplemented by the successful conversion of the waste heat.

Previous studies have shown the potentials of reducing energy demand. One of such secondary processes that employs heat pumps for alternative applications is drying. Sequel to the use of heat pump systems, different drying processes such as sun drying, direct resistance heaters e.t.c. These applications have shown to either not to be so effective or costly. The sun drying process is highly dependent on the amount of solar radiation available, time of the day, location. Since this not equally distributed, it raises the question of efficiency. The direct resistance on the other is an energy intensive process and it is also costly. Bantle et. al (2016), reported a 70% reduction in energy demand from the simulation of a CO₂ heat pump system for drying applications. Ceylan et. al (2006), conducted an energy and exergy analysis timber dryer assisted heat pump. The study reported the potency of drying integrated heat pump, as initial moisture content of the poplar and pine timbers with 1.28 kg water/kg dry matter and 0.6 kg water/kg dry matter respectively was reduced to 0.15 kg water/kg. KloÈcker et. al (2001) designed a drying heat pump with a 12kw capacity and experimentally recorded 65% energy savings compared to Passat type 132E direct heating mode. Sarkar et. al. (2006), modelled a transcritical CO₂ heat pump dryer and validated with experimental results while also establishing the important operating parameters such as dryer

efficiency, recirculation air ratio, air mass flowrate and ambient temperature. KloËcker et. al (2002), established a relationship that showed that the energy saving potential increases with the Carnot efficiency of heat pump dryer.

Lorentzen 1994, introduced a novel approach of hot tap water heating. He proposed a transcritical Co₂ process simultaneous refrigeration and hot tap water production. This employs the sensible cooling for gas cooling and simultaneously hot water heating. Neskå et al. (1998), proposed that the application of CO₂ heat pump systems can reduce primary energy consumption with more than 75% compared to electrical heating. Stene 2007, highlighted the potential of CO₂ heat pump systems for domestic hot water sighting the annual heating demand for domestic hot water (DHW) typically constitutes 50 to 85% of the total annual heating demand in the residence. Combining space cooling with water heating is a technology that most adaptable to geographical regions where the annual cooling load is large. For such regions, having a system that primarily cools residential building and also provides or supplement the hot water demand by residence is important. Heat pumps system that achieves this by using the heat rejected to provide this secondary application. Not only does it helps cuts energy cost but more importantly, it aids energy conservation and enhances better energy efficiency of the system.

2. THEORETICAL ANALYSIS

Transcritical cycle

Lorentzen introduced the application of CO₂ for air conditioning, which was utilized car. The lorentzen cycle has some distinct components from the conventional cycle, which include the positioning of the receiver after the evaporator and the introduction of intermediate heat exchanger for superheating and sub-cooling.

The positioning of the receiver enables the sufficient supply of CO₂ while also mitigating against the flooding of the compressor, which could result in liquid slugging by retaining the liquid fraction of the refrigerant at the exit of the evaporator. It also helps to moderate refrigerant supply depending on the variations in the system's capacity or operations. The intermediate heat exchanger is able to sub-cool the refrigerant at gas cooler and reduce the large expansion loss associated with CO₂ systems. The superheating at the suction line of the

compressor ensures complete vaporization of the refrigerant. Sub-cooling and superheating increases the cooling capacity. During sub-cooling, the state of the refrigerant is shifted from point b to c as seen on the p-h diagram in Figure 3.3. The liquid fraction of the refrigerant also increases at the evaporator inlet which enhances better evaporator performance. On this superheating side, this is achieved by shifting the state of the refrigerant, which is saturated or flooded at point e to superheated state f. Even though superheating decreases the density of the refrigerant and could influence the cooling effect negatively, it is however increases the discharge temperature of the compressor. The higher the discharge temperature of the refrigerant, the higher the potentials of matching it with high hot water return temperatures demand. The enthalpy difference between the evaporator outlet to compressor suction is equal to the amount of enthalpy difference for sub-cooling in the internal heat exchanger.

In a transcritical cycle, an evaporator still serves the heat absorption function, but heat rejection occurs through sensible cooling in gas cooler and not through condensation at high pressure within the supercritical region. The pressure ratio is higher in transcritical cycle compared to subcritical cycle and this is due to its high pressure and is often accompanied with large expansion loss. The superheated vapor is compressed to deliver high temperature. Energy consumption in transcritical systems is relatively low in cold climates or season, while efficiency is reduced in hot climates or season. The distinctions between the processes in transcritical Lorentz cycle and conventional cycles are highlighted in Table 2.1

Table 2.1: Comparison of Lorentz cycle to a conventional heat pump cycle

Lorentz cycle	Conventional
Irreversible non-adiabatic compression	Isentropic compression
Non-isobaric, non-isothermal heat rejection	Isobaric heat rejection
Non isenthalpic expansion	Isenthalpic expansion
Non-isobaric, non-isothermal heat absorption	Isobaric heat absorption

For a transcritical process, while heat absorption takes place at constant evaporation temperature, the heat rejection takes place at gliding temperature. Hence, the performance of the cycle is

better defined by Lorentz coefficient of performance ($COP_{lorentz}$) as proposed by Neska. It expressed using the state points as shown below:

$$COP_{lorentz,heating} = \frac{T_2 - T_3}{(T_2 - T_3) - (T_0) * \ln(T_2/T_3)} \quad \text{Eq 2.1}$$

$$COP_{lorentz,cooling} = \frac{(T_0) * \ln(T_2/T_3)}{(T_2 - T_3) - (T_0) * \ln(T_2/T_3)} \quad \text{Eq 2.2}$$

Where,

$$T_0 = \left(\frac{T_1 - T_4}{\ln(T_1/T_4)} \right) \quad \text{Eq 2.3}$$

$$\eta_{lorentz} = \frac{COP_{actual}}{COP_{lorentz}} \quad \text{Eq 2.4}$$

Air drying cycle

The air-drying cycle is different cycle from the heat pump cycle. Even though integrated to be known as heat pump dryer, unlike the conventional heat pump cycle, it takes into consideration the humidity alongside the temperature. Air-drying process for clothe typically operates at standard atmospheric pressure which is relatively constant throughout the process. The air-drying cycle under review utilizes a closed loop circulation. Even though the air circulation and heat absorption is similar for both CO₂ and HFCs heat pumps, however its performance is influenced by that of the heat pump cycle. The air-drying cycle is often represented in psychrometric and mollier diagrams, shown in Figure 2.1 below.

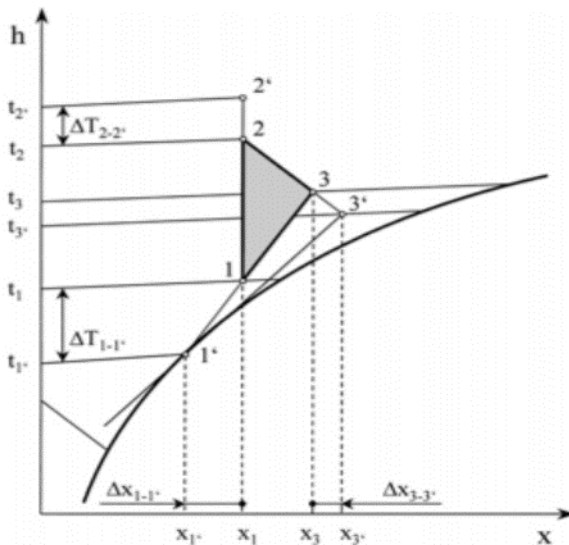


Figure 2.1: A h-x diagram of the drying process ((Klocker et al, 2000))

There are three main processes involved in the air drying cycle namely;

- Process 1-2 : heating of the air in condenser or gas cooler, as it the case for CO₂ heat pumps
- Process 2-3: adiabatic humidification of the drying air by cloth moisture in the drying chamber
- Process 3-1: dehumidification and condensation of absorbed moisture from the drying air.

Performance Indicators

Coefficient of performance of a heat pump is a parameter that indicates the efficiency of a heat pump. It evaluates the amount power required to generate the cooling/heating capacity from the system. It is the basics for most comparisons of different heat pump's performance. The $COP_{cooling}$ is the ratio of the cooling effect generated by the evaporator to the amount of power input from the compressor while the $COP_{heating}$ is the ratio of the useful heat generated from the gas cooler to the compressor power input. It is expressed as follows:

$$COP_{cooling} = \frac{Q_{evap}}{W_{comp}} \quad \text{Eq 2.5}$$

$$COP_{heating} = \frac{Q_{gc}}{W_{comp}} \quad \text{Eq 2.6}$$

To determine the energy efficiency of a space-cooling heat pump, a terminology known as Seasonal energy efficiency ratio (SEER) is defined. SEER is the ratio of the total cooling load provided by the heat pump in a cooling season to the total energy input within the same season. A high SEER depicts a high efficiency. The instantaneous energy efficiency of the system can also be established by energy efficiency ratio (EER) which is defined as the ratio cooling capacity of the system to the energy input into the system. While SEER covers different temperature ranges, EER covers an individual indoor and outdoor temperature. SEER and EER can be related to the COP of a system using the following equations 2.7 and 2.8.

$$SEER = \frac{EER}{0.87} \quad \text{Eq 2.8}$$

$$EER = 3.413 \times COP \quad \text{Eq 2.9}$$

3. SYSTEM DESIGN

The system design for the Solar assisted integrated CO₂ heat pumps first considered the alternative integration of the solar insolation to a heat pump system. Different ways by which this can be achieved includes solar energy as power source, energy source for heat pump evaporator, and heat source for water heating.

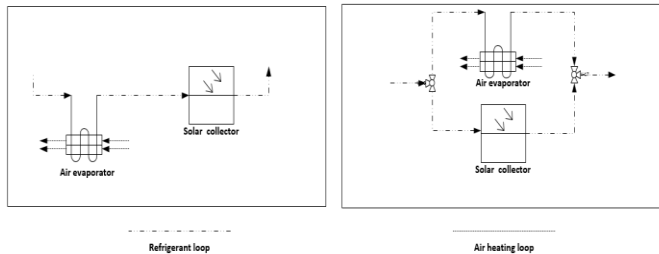


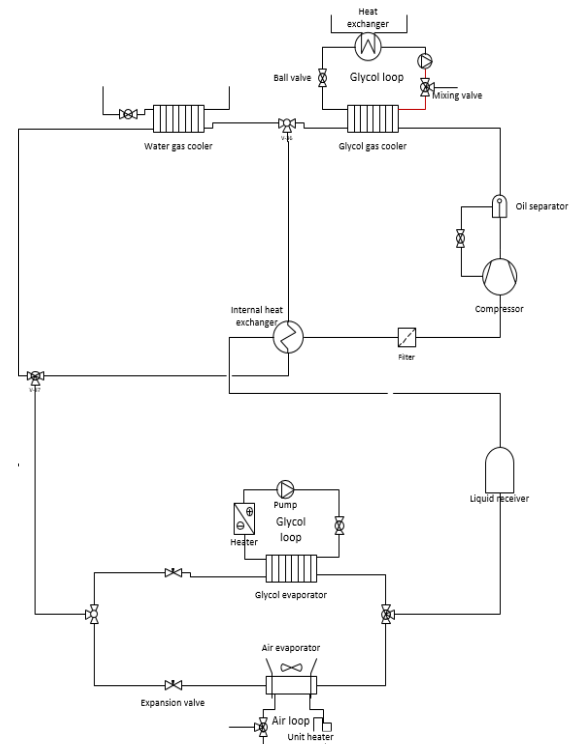
FIGURE 3.1: SOLAR COLLECTOR INTEGRATION

The solar could be integrated on the high pressure side of the heat pump to directly supplement the heating capacity of the gas cooler or integrated on the low pressure side as a secondary evaporator to increase the heating capacity of the gas cooler. Based on available resources, the preferred design option was to integrate the solar collector with the low pressure side of the heat pump. This way, water heating, space cooling and drying applications can be achieved.

There are different possible configurations to achieve this, either through parallel or series connection to the air evaporator. However, the series configuration is considered for this study. Due to the fact that, the operation of each evaporator can be controlled individually and it's not dependent on one another.

4. TEST FACILITY

The experimental facility used for this study was a previously constructed test rig for ejector experiments. The rig was modified to meet the configuration options discussed previous section. The ejectors were replaced with two expansion valves, one needle valve and a pneumatic valve. The pneumatic valve was not easy to control so it was set on the PID to operate at pressure above the operating high side pressure and this makes it in active. The rest of the components were kept as they are and a simplified process flow is presented in Figure 4.1.



The rig consist of five loops: the main refrigerant closed loop, the glycol loop evaporator, closed air loop, open water gas cooler flow and glycol gas cooler loop. The serial connection of the gas coolers enables for easy control of the gas cooler outlet temperature. The evaporators (air and glycol) was connected in parallel to stimulate the ambient conditions and the capacities of the evaporator.

The test rig consist of the following primary components;

- Semi hermetic reciprocating compressor
- Brazed plate heat exchangers
 - Glycol gas cooler
 - Water gas cooler
 - Glycol evaporator
- Micro channel louvered air evaporator
- Intermediate heat exchanger
- Throttling valves
- Low pressure receiver
- Electric heaters
- Fans
- Safety valves

Compressor Unit.

The compressor utilized for this experimental process is a dorin CD 380H model of CD200 semi hermetic compressor series. It has a heating capacity of 11kW at evaporation temperature of 10°C, gas

cooler out temperature of 35°C at gas cooler pressure of 90 bar. The specifications of the compressor are given in the table below;

Table 4.1: Compressor specifications

Number of Cylinders	2	
Bore	28	Mm
Stroke	28	Mm
Displacement @ 50 Hz	3,00	
Displacement @ 60 Hz	3,60	
Suction valve (socket welding)	10	
Suction valve (butt welding)	14	
Discharge valve (socket welding)	10	
Discharge valve (butt welding)	14	
Oil charge	1,3	
Net weight	77	

Gas cooler (Braze Plate Heat exchangers)

Three of the heat exchangers used in this setup are from Kaori, manufacturer of brazed plate heat exchangers. Their specialized K040C series CO₂ heat exchanger is a perfect fit for this experimental setup, both as gas cooler and evaporator. The K040C series which is characterized by 60-70% lower pressure drop and 10% better heat capacity than multiple tube heat exchangers, is about 1/3rd the space and weight of multiple tubes heat exchangers. A sample of the Kaori brazed plate heat exchanger is shown in Figure 4.2 below:



Figure 4.2 gas cooler

Evaporators

The evaporators were connected in parallel, this to allow for variation of refrigeration load. For this experiment, the glycol evaporator represents the solar collector. The heat that is sourced from the glycol evaporator represents the useful heat the solar evaporator contributes to the system. The rest of the heat is from the air source evaporator. The amount of heat contributed through the air source evaporator is determined by the required cooling capacity for the air conditioning. In a multiple evaporator system, individual evaporators are better controlled with fluctuations in loads. With a parallel configuration, the low side pressure is maintained and it is easier to control individual evaporators unlike series configuration there is alternation of the pressure level and the evaporating temperature likewise. The air evaporator used in this experimental campaign is a micro channel louvered heat exchanger

Test Matrix

The test matrix for the experimental campaign are basically constituted around the pressure and temperature. Hence, the experiments were conducted within the ranges highlighted in Table 4.2.

Table 4.2 Test matrix for experimental campaign

Parameters	Unit	Range
Gas cooler pressure	Bar	80-95
Gas cooler outlet temperature	°C	25-35
Evaporation temperature	°C	5-10
Air inlet temperature	°C	25-30
Air outlet temperature	°C	20-25
Glycol inlet temperature (evaporator)	°C	25-30
Glycol outlet temperature (evaporator)	°C	12-25

5. EXPERIMENTAL RESULTS

At varying air evaporator capacities within the range of 2.37 to 2.73 kW which represents outdoor and indoor conditions of the building, the air inlet and outlet temperatures of the evaporator side was set to match the building conditions.

Three different conditions were run for the 2.37 kW cooling load with evaporation temperature varying between 5 to 10°C and the gas cooler within the range of 80-85 bar. The evaporation temperature has been substituted for their corresponding saturation pressure, which ranges between 40 to 45 bar and used for descriptive purpose. Hence, 84/45 implies a gas cooler pressure of 84 bar and evaporation temperature of 45 bar which represents the evaporation temperature of 10 °C . The corresponding system performance results are evaluated as presented in Figure 5.1.

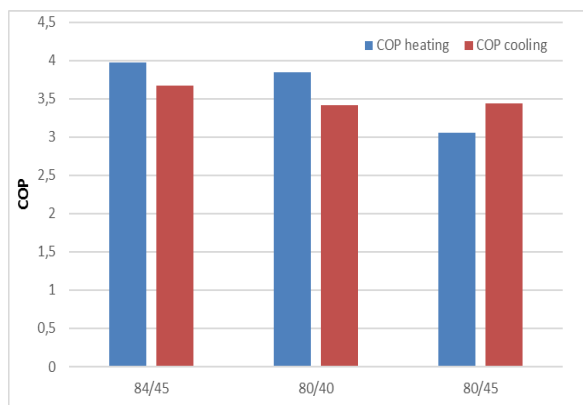


Figure 5.1: Cooling and heating performance at 2.37 kW air evaporator capacity

The highest COP for both the heating and cooling application was obtained at 84/45 with corresponding values of 3.97 and 3.67. Reducing the gas cooler pressure by 5 bar and the evaporation temperature by almost 50%, 80/40 operating conditions resulted in lower system COPs of 3.84 and 3.41 for the heating and cooling respectively. This represents a reduction of about 3 to 7% in respective COPs. This is to validate a previous assertion that increasing the evaporation temperature results in lower specific enthalpy of evaporation, while decreasing the gas cooler pressure results in decreasing specific enthalpy of condensation. The 80/45 condition however gave a different performance to that of both the 84/45 and 80/40 trend. The resulting COPcooling of 3.44 was higher than 80/45 condition, it however, a reduction in the COPheating of about 20% can be observed.

Subsequently, the impact of having a higher gas cooler pressure for the same evaporation temperature cannot be underestimated. For the same evaporation temperature, the 80/45 condition gave a COPcooling about 6% lesser than that of the 84/45. This shows that increasing the gas cooler pressure for the same

evaporation temperature at constant CO₂ gas cooler outlet temperature of 31 °C has the potentials of increasing the cooling performance of the heat pump by about 6%. The corresponding COPcooling from the air evaporator for space cooling are 1.18, 1.1, 1.08 for 84/45, 80/40 and 80/45 conditions respectively. The volumetric heating capacity is maximum at a higher gas cooler pressure of 85 bar due to large vapor density of the refrigerant while a higher volumetric cooling capacity also results from high pressure of the evaporator.

Three different conditions were run for the 2.73 kW cooling load with evaporation temperature varying between 5 to 10°C and the gas cooler within the range of 80-90 bar. The air evaporator performance represents the required indoor and outdoor conditions of 20°C and 30°C respectively. The highest system performance is obtained from 90/45 operating conditions. The resulting heating and cooling COPs are 4.04 and 3.55 respectively. Decreasing the gas cooler pressure by 10 bar while keeping the evaporation temperature constant at 10°C resulted in about 13% and 7% decrease in COP. Other resulting system performance are highlighted in figure 5.2.

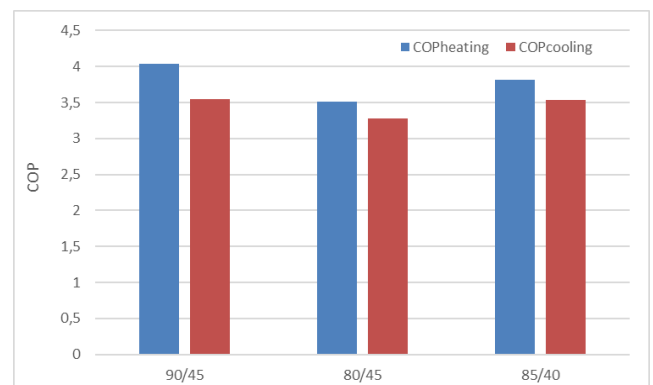


Figure 5.2: Cooling and heating performance at 2.73 kW air evaporator capacity

At a lower evaporation temperature of 5°C and gas cooler pressure of 85 bar, COPs of 3.81 and 3.54 for heating and cooling respectively. This implies that its heating performance is about 6% lesser than that of 90/45 while COPcooling remains relatively close. It however also had a better performance than 80/45 with COPs increasing by up to 7% for both heating and cooling. It can also be deduced from the result that the optimum gas cooler is between 85 and 90 bar, as they represent the region with the highest COPheating. The corresponding COPcooling from

the air evaporator for space cooling are 1.37, 1.28, 1.34 for 90/45, 80/45 and 85/40 operating conditions respectively.

Comparing the performance of similar operating conditions for different cooling capacity is discussed as follows. At an air evaporator capacity of 2.73 kW, the 80/45 condition showed a better heating performance with about 15% to that of the 2.73 kW air evaporator capacity. While the 2.37 kW air evaporator capacity has a better, cooling performance than its counterpart does by about 5%.

Evaluating the Carnot COPs and Carnot efficiencies for the space cooling operation of the experiment, the results are highlighted in Table 5.1.

Table 6.2: Calculated Carnot efficiency

Operating condition	Cooling capacity	T_{room}	T_{amb}	COP_{carnot}	COP_{actual}	η_{system}
	(kW)	(°C)	(°C)			(%)
84/45	2,37	22	28	49,2	1,18	2,40 %
80/40	2,37	22	28	49,2	1,11	2,26 %
80/45	2,37	22	28	49,2	1,08	2,20 %
90/45	2,73	20	30	29,3	1,37	4,67 %
80/45	2,73	20	30	29,3	1,28	4,37 %
85/40	2,73	20	30	29,3	1,34	4,57 %

The system efficiency compares the actual COP to the real COP of the system. It describes how close the performance of the system is to an ideal situation. It describes how much power is required for the real process to operate in an ideal situation.

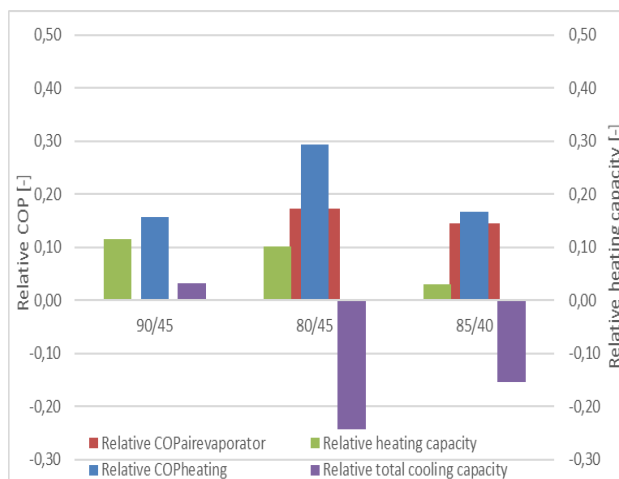


Figure 5.3: Relative comparison of simulated results to experimental results

Some results of the simulation was compared and expressed in terms of its relativity to the experimental results, the outcome of which is plotted in figure 5.3 above. The deviation of the experimental results from the simulation results for the COP of the air evaporator at capacity of 2.73 kW ranges from 0.01 up to 0.15. The COP_{heating} of the experiment relative to those of the simulation ranges had up to 0.3. The heating capacity of experiment was up to 0.12 relative to the simulated results. The experiment demonstrated better performance than the simulation. The predicted values from the simulation was within a maximum value of 0.25 relative to the experimental results. The largest deviation as can be seen from figure xxx above to occur at gas cooler pressure of 80 bar and evaporation temperature of 10°C.

Space cooling performance rating

The performance of the system with respect to the evaporator capacity is evaluated with varying operating conditions. At a reference cooling capacity of the air evaporator at 2.37 kW to meet the indoor and outdoor condition of 22°C and 28°C. Since these conditions were not run in actual room set up, EER and SEER used for the comparative analysis are considered instantaneous and only apply for a single operating condition. At evaporation temperature of 10°C and gas cooler pressure 84 bar, an EER value of 4.04. Decreasing the gas cooler pressure to 80 bar at same evaporation temperature, an EER value of 3.69. Subsequently the SEER decreases from 4.61 to 4.22. The decrease by 5 bar in the gas cooler resulted in about 9% decreases in the values of the EER and SEER. At lower evaporation temperature of 5.30°C and gas cooler pressure of 80 bar resulted in EER and SEER values of 3.8 and 4.34 respectively. This depicts an increase of about 3%. This clearly shows the energy efficiency of the heat pump for space cooling purpose is highly dependent on the COP_{cooling}.

By proportionally calculating the mass flow rate through the glycol and air evaporator, the corresponding compressor work input can be re-evaluated. The EER and SEER value for the space cooling is corrected to 12.6 and 14.5 respectively at evaporating temperature of 10°C.

6.4.2 Heat exchanger performance

The overall heat transfer coefficient (U) of some of the heat transfer components are calculated using the equations xxx highlighted in section xxx. The U -value of water gas cooler with complete instrumentations for the 2.73 kW air evaporator experiment is enumerated and represented in Figure 5.4 below:

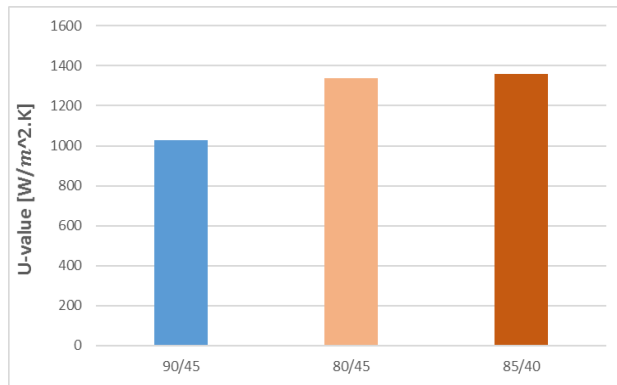


Figure 5.4: Overall heat transfer coefficients of experimental results.

Drying

The performance of the R744 is evaluated using the SMER and SEC and comparison with alternative refrigerants likewise was made. These parameters, SMER and SEC has been discussed in previous section. With specified reference values for the primary properties, other properties of the drying air is extracted for the air heating and moisture absorption process as shown in Table 5.2. The R744 driven heat pump dryer has demonstrated to be an effective system, which removes more moisture at low energy consumption. Its operation results in a dryer's efficiency of about 66% with potentials of removing about 3.14 kg/kWh while requiring low energy consumption of about 0.292 kWh/kg.

Given the same conditions, the R744 cycle has the highest SMER of 3.42 kg/kWh, which is about 28% and 45% better performance when compared to R410a and R134a cycle. This implies that the R744 heat pump removes more moisture from the fabric for the same amount of energy input than R410a and R134a as shown in Figure 6.13. Even though the R744 has the lowest (\dot{m}_a/\dot{m}_r) value and lowest specific enthalpy of condensation it however has the lowest specific enthalpy of compression which depicts lesser energy consumption.

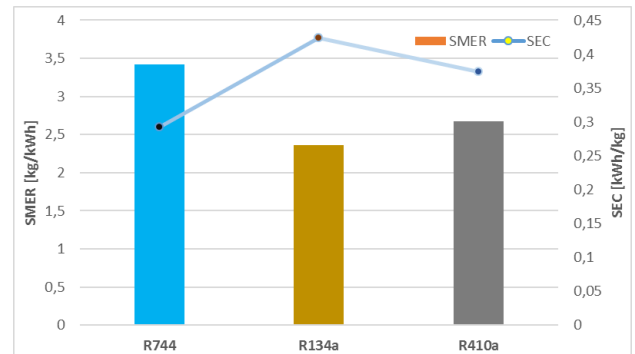


Figure 6.13: Comparison with alternative refrigerants for drying

Subsequently, the R744 system has the lowest SEC of 0.29 kWh/kg compared to R134a, which has a value of about 45% more. This implies that R744 requires lesser energy input into the system for the removal of moisture in the drying chamber. The R410a system also had a SEC value about 28% more than the R744 system which means it consumes 0.37 kWh energy per 1 kg of moisture removed from the cloth.

6. CONCLUSION

As shown in both the simulations and experimental results, there potentials of better heat pump performance with integrating of solar energy. The heating capacity of the system will increase with no negative impact on the overall performance of the heat pump. With the increase in the heating capacity, the range of application can widened to cover simultaneous water heating and drying purposes. Supplementary-cooling load can be generated from the solar collector for refrigeration purposes. Integrating the exit flow of the dryer, as heat source for air evaporator will further increase the overall energy efficiency of integrated system. Although this was not possible at a low air evaporator capacity of 2.37 kW, its applicability at a higher capacity of 2.73 kW was established.

The CO₂ heat pump featured well among alternative refrigerants, with R410a having a relatively performance value to that of CO₂, R134a performed lesser.



REFERENCES

Bantle, M., Kvalsvik, K.H. and Tolstorebrov, I., 2016. Performance simulation of a Heat Pump Drying System using R744 as refrigerant. In *Proceedings of the 12th IIR Gustav Lorentzen Conference on Natural Refrigerants GL2016, 21-24 August 2016, Edinburgh, UK.*

Ceylan, I., Aktaş, M. and Doğan, H., 2007. Energy and exergy analysis of timber dryer assisted heat pump. *Applied Thermal Engineering*, 27(1), pp.216-222.

Klöcker, K., Schmidt, E.L. and Steimle, F., 2001. Carbon dioxide as a working fluid in drying heat pumps. *International journal of refrigeration*, 24(1), pp.100-107.

Sarkar, J., Bhattacharyya, S. and Gopal, M.R., 2006. Transcritical CO₂ heat pump dryer: Part 1. Mathematical model and simulation. *Drying technology*, 24(12), pp.1583-1591.

Klöcker, K., Schmidt, E.L. and Steimle, F., 2002. A drying heat pump using carbon dioxide as working fluid. *Drying technology*, 20(8), pp.1659-1671.

Lorentzen, G., 1994. Revival of carbon dioxide as a refrigerant. *International journal of refrigeration*, 17(5), pp.292-301.

Nekså, P., Rekstad, H., Zakeri, G.R. and Schiefloe, P.A., 1998. CO₂-heat pump water heater: characteristics, system design and experimental results. *International Journal of refrigeration*, 21(3), pp.172-179.

Stene, J., 2007. Integrated CO₂ heat pump systems for space heating and hot water heating in low-energy houses and passive houses. *International Energy Agency (IEA) Heat Pump Programme—Annex, 32.*